Old Dominion University
ODU Digital Commons

Mathematics & Statistics Theses & Dissertations   Mathematics & Statistics

Spring 2014

Analyzing Cholera Dynamics in Homogeneous and Heterogeneous Environments

Drew Posny
Old Dominion University

Follow this and additional works at: https://digitalcommons.odu.edu/mathstat_etds

 Part of the Applied Mathematics Commons

ANALYZING CHOLERA DYNAMICS IN

HOMOGENEOUS AND HETEROGENEOUS

ENVIRONMENTS

by

Drew Posny
B.S. May 2009, University of North Carolina, Chapel Hill
M.S. May 2012, Old Dominion University

A Dissertation Submitted to the Faculty of
Old Dominion University in Partial Fulfillment of the
Requirements for the Degree of

DOCTOR OF PHILOSOPHY

COMPUTATIONAL AND APPLIED MATHEMATICS

OLD DOMINION UNIVERSITY
May 2014

Approved by:

_____
Jin Wang (Director)

_____
Fred Dobbs (Member)

_____
Sookyung Joo (Member)

_____
Richard Noren (Member)

ABSTRACT

ANALYZING CHOLERA DYNAMICS IN HOMOGENEOUS AND HETEROGENEOUS ENVIRONMENTS

Drew Posny
Old Dominion University, 2014
Director: Dr. Jin Wang

Cholera continues to be a serious public health concern in developing countries and the global increase in the number of reported outbreaks suggests that activities to control the diseases and surveillance programs to identify or predict the occurrence of the next outbreaks are not adequate. Mathematical models play a critical role in predicting and understanding disease mechanisms, and have long provided basic insights in the possible ways to control infectious diseases. This dissertation is concerned with mathematical modeling and analysis of cholera dynamics. First, we study an autonomous model in a homogeneous environment with added controls that involves both direct and indirect transmission pathways. We conduct a careful equilibrium analysis and, in particular, investigate the threshold dynamics of this model. Next, we propose a general multi-group model for cholera dynamics that incorporates spatial heterogeneity and dispersal. Under biologically feasible conditions, we show that the basic reproduction number $\mathcal{R}_0$ remains a sharp threshold for cholera dynamics in multi-group settings. We verify the analysis by numerical simulation results. Then, we propose a deterministic compartmental model for cholera dynamics in time-periodic environments. The model incorporates seasonal variation into a general formulation for the incidence (or, force of infection) and the pathogen concentration. The basic reproduction number of the periodic model is derived, based on which a careful analysis is conducted on the epidemic and endemic dynamics of cholera. Several specific examples are presented to demonstrate this general model, and numerical simulation results are used to validate the analytical prediction. Finally, we extend the general multi-group cholera model to a periodic environment.

ACKNOWLEDGEMENTS

I am deeply appreciative of many individuals who have supported my work and offered encouragement throughout the entire process of this dissertation.

Above all, I would like to thank my advisor Dr. Jin Wang for his never-ending guidance and support throughout my graduate studies and developing this dissertation. I am extremely grateful to have had the opportunity to work as his student. Without his help, this dissertation would not have been possible. I would like to extend my thanks to Dr. Fred Dobbs, Dr. Sookyung Joo and Dr. Richard Noren for serving on my dissertation committee. Each has my deepest gratitude for their time, advice and critiques.

I greatly appreciate the entire faculty and staff of the Department of Mathematics and Statistics. I would like to thank the Department of Mathematics and Statistics for providing me with financial support. My sincerest appreciations are offered to Barbara Jeffrey, Sheila Hegwood and Miriam Venable for making my life easier. The author gratefully acknowledges the support of the Modeling and Simulation Scholarship Program.

Special thanks go to my family, friends and colleagues. You guys are nuts.

This dissertation is dedicated to Cheddar.

TABLE OF CONTENTS

LIST OF TABLES

Table   Page

LIST OF FIGURES

CHAPTER 1

INTRODUCTION

Cholera is a severe intestinal infectious disease caused by ingesting food or water contaminated with the bacterium *Vibrio cholerae*. Symptoms of cholera infection include profuse watery diarrhea that rapidly causes dehydration, hypovolemic shock, and acidosis and can lead to death if appropriate treatment is not promptly given [60,70]. The World Health Organization estimates that there are 3 to 5 million cases of cholera infection and 100,000 to 120,000 deaths due to cholera each year. Recent years witnessed an increasing number of cholera outbreaks worldwide, including one of the largest cholera epidemics in modern history that took place in Haiti from 2010-2012 with more than 530,000 reported cases and over 7,000 deaths [70]. Major cholera outbreaks also include those in Sierra Leone (2012), Ghana (2011), Nigeria (2010), Vietnam (2009), Zimbabwe (2008), and India (2007), among others. Thus, cholera remains a serious public health concern in the developing world where poverty and poor sanitation and hygiene are prevalent.

Consequently, provision of clean water and proper sanitation facilities are the critical weapons in reducing the impact of cholera [15,70]. However, water and sanitation investments, which are the key for long-term cholera prevention and control, are usually not possible in emergency epidemic settings or not available in developing countries. These epidemics have increased in frequency, severity, and duration, implying that current knowledge in cholera dynamics and public health guidelines to control the disease are not adequate.

Cholera dynamics are subject to complex disease transmission pathways. The transmission of cholera involves both direct (human-to-human) and indirect (environment-to-human) routes, due to the multiple interactions between the human host, the pathogen, and the environment [51]. Both symptomatic and asymptomatic individuals shed the bacteria back into the environment, further fueling the pathogen concentration and persistence of the disease. Direct transmission of cholera through human-human contact is usually not expected because the infectious dose (ID) is high [60,68]. Here, we define direct human-to-human transmission as cholera transmission not involving the aquatic environment, i.e, cholera transmission through

other fecal to oral pathways of hyperinfectious vibrios such as ingesting food or water contaminated by a food handler. A recent cholera outbreak in Zimbabwe, a land-locked country in Africa, underscores such a direct human-to-human transmission pathway [47]. Indirect transmission of cholera arises from exposure to untreated water and sewage.

Mathematical modeling, simulation and analysis is a key approach to gain insight into the complex transmission dynamics of cholera. SIR and SIRS epidemiological models are commonly used to study the dynamics of infectious diseases. The total population is divided into homogeneous subpopulations, or compartments, based on the stage of the disease. In general, individuals are classified into three distinct compartments: susceptible (S), infected (I), and recovered (R). The susceptible compartment consists of individuals who could potentially become infected with the disease. Individuals who are currently infected (symptomatic and asymptomatic) with the disease are classified as infected. Lastly, individuals who have recovered and can no longer transmit the disease are classified as recovered. These epidemiological models describe the movement of individuals between S, I and R. In an SIR model, once an infectious individual enters the recovered compartment, the individual develops immunity and no longer transmits the disease. However, in an SIRS model, individuals are susceptible, then infected, then recovered, and finally lose immunity and become susceptible again. Frequently incorporated amongst proposed mathematical models studying cholera dynamics is an incidence function, which determines the rate of new infection. The incidence function incorporates transmission routes such as contact rates with the pathogen in untreated water (indirect transmission) and among human hosts (direct transmission).

Since cholera is a waterborne infectious disease, many mathematical cholera models extend the classical SIR framework by adding an environment component, denoted by B, that tracks the concentration of toxigenic cholera vibrios in water. The pathogen has a critical relationship with the aquatic environment. In the absence of an infected individual excreting the bacteria back into the environment, the pathogen can continue to persist and potentially infect others. That is, the aquatic environment may serve as a reservoir of toxigenic *V. cholerae* allowing the bacteria to survive for long periods of time [15, 68]. Biofilms provide protection to the bacteria from stresses in the environment, allowing for survival and persistence [60]. Hence, it is important

to understand the significance of the aquatic reservoir and its effects on cholera dynamics. A number of mathematical cholera models have been proposed and analyzed in recent years [2,7,13,15,28,31,43,47,61–63,65]; among these, several models have been driven by the ongoing outbreaks in Haiti [2,7,13,63].

In particular, Codeço [15] published a model that incorporated the environmental component into a regular SIR epidemiological model, building on the previous work in [10]. The environment component allows for the introduction of a function used to describe the rate of change for the pathogen in the environment. Codeço's model illustrated the pathogen concentration as $eI - \beta B$, where e is the human contribution to the pathogen concentration and β is the net death rate of vibrios. A saturation incidence given by $\lambda(B) = a\frac{B}{K+B}$ was used to model the infection from the environment, where a is the rate of exposure to the contaminated environment and K is the half saturation concentration of environmental vibrios. This model excluded the human-to-human transmission pathway.

On the other hand, Mukandavire et al. [47] proposed a new model incorporating both direct and indirect cholera transmission to study the 2008-2009 cholera outbreaks in Zimbabwe. This model considered human-to-human transmission defined in the context of infection by hyperinfectious vibrios [28,45,46,51]. The incidence term was modeled as $\beta_e \frac{B}{\kappa+B} + \beta_h I$ where β_e and β_h are rates of exposure to environmental and hyperinfectious vibrios, respectively. The results in [47] elucidates the importance of human-to-human transmission in shaping cholera epidemics in non-riverine and estuarine environments such as Zimbabwe.

Similarly, Tien and Earn [62] proposed a model with both environment-to-human and human-to-human transmission pathways; however, no saturation effect was considered. The bilinear incidence function was given by $b_W W + b_I I$, where W is the pathogen concentration in the environment, and b_W and b_I are defined in the same role as β_e and β_h, respectively. Moreover, Wang and Liao [65] recently proposed a deterministic cholera model that incorporates general nonlinear incidence factors and pathogen functions and that can unify many of the existing cholera models. These studies have certainly produced many useful results and have improved our understanding of cholera dynamics. For reference, we have listed details of these cholera models (Codeço, Mukandavire et al., Tien and Earn, and Wang and Liao) in Appendix A.

A major limitation of these cholera models and other current quantitative studies

(e.g., [28,57]) on cholera transmission and control is that spatial heterogeneity and dispersal are not sufficiently addressed, resulting in poor understanding of the spread of cholera infection. Mukandavire *et al.* [47] estimated basic reproduction numbers for the 10 provinces in Zimbabwe. The results were highly heterogeneous, showing that the underlying transmission pattern varied widely throughout the country. Similarly, in the work of Tuite *et al.* [63], very different basic reproduction numbers were established for the 10 administrative departments of Haiti. Although relatively simple mathematical models were used in these studies, they did imply that spatial heterogeneity takes an essential role in cholera transmission and the design of control strategies. Consequently, the effects of dispersal and movement among different spatial regions, including the communication of human populations and dispersal of vibrios, are critical in shaping the global epidemics and endemics of cholera.

One of the most successful approaches to investigate spatial heterogeneity and dispersal in mathematical epidemiology is multi-group modeling. In multi-group modeling, the entire population is divided into $n \geq 2$ distinct groups, with each group containing S, I, R, and B compartments. Thus, disease transmission occurs both within the same group and between different groups, reflecting the movement of human hosts and the pathogen from one spatial region to another. In this study, we will use the multi-group modeling approach to investigate the spatial dynamics of cholera transmission.

Another critical limitation of these cholera models (e.g., [15,28,47,57,62,65]), however, is that they all assume that the model parameters are constant in time, meaning that the disease contact rate, recovery rate, pathogen growth rate, etc., all take fixed values independent of time. From the mathematical point of view, such an assumption has the advantage of simplifying the models and analysis, and facilitating the use of some well known theory in autonomous dynamical systems. Yet seasonal environmental and climatic factors could significantly affect cholera dynamics. For example, temperature, salinity, rainfall and plankton influence the transmission of cholera in regions of the world where the human population relies on untreated water as a source of drinking water [17]. These seasonal and environmental variations represent another kind of heterogeneous environment for the disease dynamics that is defined in terms of time.

In many endemic places, cholera is a seasonal disease and infection peaks often occur annually in the rainy or monsoon season [21,30,53,60,68], further illustrating

the concept of a potential reservoir of toxigenic cholera vibrios in endemic regions. Such observations underline the limitation of current cholera models and imply that mathematical insight on cholera seasonality has largely lagged behind. It is thus important for mathematical cholera studies to incorporate these seasonal factors to gain deeper quantitative understanding of the short and long term evolution of cholera dynamics, and to better predict and prevent future cholera outbreaks. We will take a solid step in this work to investigate seasonal dynamics of cholera transmission. In particular, we will analyze the threshold properties of cholera dynamics in a periodic environment.

This dissertation is organized into five chapters. Following this introductory Chapter 1, in Chapter 2 we modify an autonomous cholera model to incorporate added control measures. This model is based on the essential assumption of a homogeneous environment; no spatial variations or seasonal oscillations are involved. Although unrealistic in some sense, this simplified, autonomous model allows us to conduct a careful analysis on the interaction between the disease control measures and the multiple transmission pathways of cholera, results of which would provide useful insight into the design of effective control strategies against cholera outbreaks. In particular, we determine the basic reproduction number $\mathcal{R}_0$ and conduct an equilibrium analysis for the epidemic and endemic dynamics of the system. In Chapter 3, we construct a general multi-group modeling framework for cholera with biologically reasonable assumptions to study spatial heterogeneity in cholera dynamics. We derive the basic reproduction number and analyze the global stability of the equilibria. We present numerical simulation results to validate our analysis. In Chapter 4, we construct a generalized cholera model in a periodic environment that represents seasonal variations. We again derive the basic reproduction number and study the global stability of the disease-free equilibrium. We further analyze the existence and uniform persistence of an endemic periodic solution and briefly study several specific cholera models. Then, we extend the general multi-group model to a periodic environment. Finally, in Chapter 5, we draw some conclusions and present future work.

CHAPTER 2

AUTONOMOUS CHOLERA MODEL

Mathematical modeling of cholera dynamics and conducting realistic numerical simulations based off historical data offers useful insight for public health administration. Cholera models can be utilized to establish potentially the most effective control measures needed during a cholera outbreak or for long-term cholera prevention. For example, appropriate sanitation facilities, safe water and medical treatment are critical in reducing the impact of cholera [70]. Thus, from modeling and simulation, public health guidelines can be improved. We will start our investigation by considering a simplified scenario where all human hosts are homogeneously mixed and all disease transmission rates are fixed, without complications from spatial and temporal variations. Our first goal is then to study the effects of different public health controls on cholera dynamics in such a homogeneous environment.

To that end, we modify the model of Mukandavire *et al.* [47] (original model presented in Appendix A) by adding three disease control measures: vaccination, treatment, and water sanitation, and by introducing a new class of vaccinated people to the SIR epidemiological model. Thus, our model classifies the human population, denoted by N, into the susceptibles (S), the vaccinated (V), the infected or infectives (I), and the recovered (R). We assume that individuals are born and die at an average rate μ. The concentration of vibrios in contaminated water is denoted by B. We, thus, have the following system of differential equations describing the cholera dynamics with added controls:

$$\frac{dS}{dt} = \mu N - (1 - \rho)\left[\beta_e \frac{B}{\kappa + B} + \beta_h I\right]S - (\phi(t) + \mu)S, \tag{1}$$

$$\frac{dV}{dt} = \phi(t)S - \sigma(1 - \rho)\left[\beta_e \frac{B}{\kappa + B} + \beta_h I\right]V - \mu V. \tag{2}$$

$$\frac{dI}{dt} = (1 - \rho)\left[\beta_e \frac{B}{\kappa + B} + \beta_h I\right](S + \sigma V) - (\tau(t) + \gamma + \mu)I, \tag{3}$$

$$\frac{dB}{dt} = \xi I - (\delta + \nu(t))B, \tag{4}$$

together with

$$\frac{dR}{dt} = (\tau(t) + \gamma)I - \mu R. \tag{5}$$

Susceptible individuals acquire cholera infection either by ingesting environmental vibrios from contaminated aquatic reservoirs or through human-to-human transmission, at rates $\lambda_e = (1 - \rho)\beta_e \dfrac{B}{\kappa + B}$ and $\lambda_h = (1 - \rho)\beta_h I$, respectively, with the subscripts e and h denoting environment-to-human and human-to-human transmissions. Here, κ is the pathogen concentration that yields 50% chance of infection cholera, and $\rho = \epsilon_1 p$ is the sanitation-induced preventability to cholera infection which is a product of the sanitation efficacy ϵ_1 and compliance p. We further assume that susceptible individuals are vaccinated at a rate $\phi(t)$, where t is the time variable, with a vaccine that has a degree of protection $\sigma = (1 - \epsilon_2)$, where ϵ_2 is the vaccine efficacy. Infected individuals are treated at a rate $\tau(t)$ and some recover naturally at a rate γ into the recovered class. Infected individuals contribute to *V. cholerae* in the aquatic environment at a rate ξ and vibrios have a net death rate δ in the environment. In addition, water sanitation leads to the death of vibrios at a rate $\nu(t)$.

In general, $\phi(t)$, $\tau(t)$ and $\nu(t)$ are functions of t, representing non-uniform and time-dependent controls. For the special case when the rates of all the three controls are positive constants, i.e.,

$$\phi(t) = \phi > 0, \qquad \tau(t) = \tau > 0, \qquad \text{and} \qquad \nu(t) = \nu > 0, \tag{6}$$

the model (1) - (4) is reduced to an autonomous system, that is, a system of ordinary differential equations of the form

$$\frac{dX}{dt} = F(X),$$

where $X = (S, V, I, R, B)^T$ and the right hand side does not explicitly depend on time. Therefore, any parameters incorporated into an autonomous epidemiological model are constant and independent of time. In this regard, once an infected individual enters a susceptible community, disease transmission occurs and control measures are put into place immediately at a constant rate. This simplifies the mathematical model and allows us to conduct a careful equilibrium analysis on both the disease-free and endemic equilibria. However, in most epidemic and endemic settings, control measures are difficult to implement at the onset of an outbreak and at a constant rate.

Since the total population N is fixed and $N = S + V + I + R$, we will not need equation (5) in our model analysis. It is clear to see that in this case, the feasible

region of the system (1) - (4) is

$$\Gamma = \left\{ (S, V, I, B) \,\middle|\, S \geq 0, \ V \geq 0, \ I \geq 0, \ 0 \leq S + V + I \leq N, \ 0 \leq B \leq \frac{\xi N}{\delta + \nu} \right\} \quad (7)$$

which is positively invariant for the flow of the system (1) - (4).

In the absence of infection (i.e., no infected individuals nor toxigenic bacteria in the water, $I = B = 0$), the disease-free equilibrium (DFE) of the system (1) - (4) is given by

$$X_0 = (S_0, V_0, I_0, B_0) = \left(\frac{\mu N}{\phi + \mu}, \ \frac{\phi N}{\phi + \mu}, \ 0, \ 0 \right) . \quad (8)$$

2.1 STABILITY ANALYSIS OF DISEASE-FREE EQUILIBRIUM

The basic reproduction number, denoted $\mathcal{R}_0$, is a fundamental concept in epidemiology. It is defined as the expected number of secondary infections that occur when a typical infective individual is introduced into a completely susceptible population [64, 66]. Therefore, the basic reproduction number defines a key biological threshold behavior for numerous epidemic models [66]. If $\mathcal{R}_0 < 1$, then the infectious disease will die out, whereas the infectious disease will spread and persist in a population if $\mathcal{R}_0 > 1$. This theoretical principle has been extensively applied to measure the effectiveness of vaccination strategy and antibiotic treatment, to estimate likelihood of eradicating a disease, and to guide public health administrators to properly scale their efforts [29]. Hence, it is crucial to determine an accurate estimate of $\mathcal{R}_0$ for any infectious disease. There are several ways to obtain the basic reproduction number for an infectious disease. One approach in determining $\mathcal{R}_0$ is based on the next-generation matrix theory [64, 66].

Let $x = (x_1, \ldots, x_n)^T$ where each x_i is the number of individuals in each compartment. The compartments are sorted so that the first m compartments correspond to the infected compartments and $(x_m, \ldots, x_n)$ correspond to the uninfected compartments. The set of all disease free states is defined by $X_s = \{x \geq 0 : x_i = 0, \ i = 1, \ldots, m\}$. Let $\mathcal{F}_i(x)$ be the rate of appearance of new infections in the ith compartment, $\mathcal{V}_i^+(x)$ be the rate of transfer of individuals into the ith compartment by other means, and $\mathcal{V}_i^-(x)$ be the rate of transfer of individuals out of the ith compartment. Then, a disease transmission model can be represented by

$$\frac{dx_i}{dt} = f_i(x) = \mathcal{F}_i(x) - \mathcal{V}_i(x), \qquad i = 1, \ldots, n \quad (9)$$

where $\mathcal{V}_i = \mathcal{V}_i^- - \mathcal{V}_i^+$ and $\mathcal{F}_i$, $\mathcal{V}_i^-$ and $\mathcal{V}_i^+$ are all assumed to be continuously differentiable at least twice in each variable.

Lemma 1. *[64] If x_0 is a disease-free equilibrium of (9) and the following assumptions are satisfied*

(A1) if $x \geq 0$, then $\mathcal{F}_i$, $\mathcal{V}_i^+$, $\mathcal{V}_i^- \geq 0$ for $i = 1, \ldots n$.

(A2) if $x_i = 0$ then $\mathcal{V}_i^- = 0$. In particular, if $x \in X_s$ then $\mathcal{V}_i^- = 0$ for $i = 1, \ldots, m$.

(A3) $\mathcal{F}_i = 0$ if $i > m$.

(A4) if $x \in X_s$ then $\mathcal{F}_i(x) = 0$ and $\mathcal{V}_i^+(x) = 0$ for $i = 1, \ldots, m$.

(A5) if $\mathcal{F}(x)$ is set to zero, then all eigenvalues of $Df(x_0)$ have negative real parts.

then the derivatives $D\mathcal{F}(x_0)$ and $D\mathcal{V}(x_0)$ are partitioned as

$$D\mathcal{F}(x_0) = \begin{pmatrix} F & 0 \\ 0 & 0 \end{pmatrix}, \qquad D\mathcal{V}(x_0) = \begin{pmatrix} V & 0 \\ J_3 & J_4 \end{pmatrix},$$

where F and V are the $m \times m$ matrices defined by

$$F = \left[\frac{\partial \mathcal{F}_i}{\partial x_j}(x_0) \right] \qquad \text{and} \qquad V = \left[\frac{\partial \mathcal{V}_i}{\partial x_j}(x_0) \right] \qquad i \leq i, \ j \leq m.$$

Further, F is nonnegative, V is a nonsingular M-matrix and all eigenvalues of J_4 have positive real parts.

Following [18] and [64], we define FV^{-1} as the next-generation matrix for the mathematical model and set the basic reproduction number as

$$\mathcal{R}_0 = \rho(FV^{-1}) \tag{10}$$

where $\rho(A)$ denotes the spectral radius of a matrix A.

Let $x = (I, B, S, V)^T$. Thus, the first two entries of x are directly related to infection. Our main interest lies in determining the matrices F and V in order to explicitly define $\mathcal{R}_0$. Hence, we consider the compartmentalized infectious subsystem:

$$\begin{bmatrix} dI/dt \\ dB/dt \end{bmatrix} = \begin{bmatrix} (1-\rho)\left(\beta_e \frac{B}{\kappa+B} + \beta_h I\right)(S + \sigma V) \\ 0 \end{bmatrix} - \begin{bmatrix} (\tau + \gamma + \mu)I \\ (\delta + \nu)B - \xi I \end{bmatrix} = \mathcal{F} - \mathcal{V} \tag{11}$$

where $\mathcal{F}$ denotes the rate of appearance of new infections and $\mathcal{V}$ denotes the rate of transfer of individuals into or out of each infected compartment. The Jacobian matrices evaluated at the disease-free equilibrium (8) are given by

$$F = D\mathcal{F}(X_0) = \begin{bmatrix} (1-\rho)\beta_h \left(\frac{\mu+\sigma\phi}{\phi+\mu}\right) N & (1-\rho)\frac{\beta_e}{\kappa}\left(\frac{\mu+\sigma\phi}{\phi+\mu}\right) N \\ 0 & 0 \end{bmatrix},$$ (12)

and

$$V = D\mathcal{V}(X_0) = \begin{bmatrix} (\tau+\gamma+\mu) & 0 \\ -\xi & (\delta+\nu) \end{bmatrix}.$$ (13)

Therefore, the next-generation matrix for the model (1) - (4) is

$$FV^{-1} = \begin{bmatrix} \frac{(1-\rho)}{\tau+\gamma+\mu}\left\{\beta_h + \frac{\beta_e\xi}{\kappa(\delta+\nu)}\right\}\left(\frac{\mu+\sigma\phi}{\phi+\mu}\right) N & (1-\rho)\frac{\beta_e}{\kappa(\delta+\nu)}\left(\frac{\mu+\sigma\phi}{\phi+\mu}\right) N \\ 0 & 0 \end{bmatrix}.$$ (14)

Furthermore, the basic reproduction number is defined by

$$\begin{aligned} \mathcal{R}_0(\phi,\nu,\tau) &= \rho(FV^{-1}) \\ &= \frac{(1-\rho)}{\tau+\gamma+\mu}\left\{\beta_h + \frac{\beta_e\xi}{\kappa(\delta+\nu)}\right\}\left(\frac{\mu+\sigma\phi}{\phi+\mu}\right) N \\ &= \frac{(1-\rho)}{\kappa(\delta+\nu)(\tau+\gamma+\mu)}\left(\frac{\mu+\sigma\phi}{\phi+\mu}\right)[\xi\beta_e + \kappa(\delta+\nu)\beta_h] N. \end{aligned}$$ (15)

Next, we will show that if $\mathcal{R}_0 < 1$, the disease-free equilibrium is locally and globally asymptotically stable, and if $\mathcal{R}_0 > 1$, the disease-free equilibrium is unstable. We make note of the following definition.

Definition 2. *An equilibrium point u^* of $\dot{u} = f(u)$ is:*

- *stable if for every $\epsilon > 0$, there is a $\delta > 0$ such that $|u^* - u(t)| < \epsilon$ for all $t > 0$ for any solution $u(t)$ with $|u^* - u(0)| < \delta$.*

- *locally asymptotically stable if u^* is stable and if there is a $\delta > 0$ such that $|u(t) - u^*| \to 0$ as $t \to \infty$ for any solution $u(t)$ with $|u^* - u(0)| \leq \delta$.*

- *globally asymptotically stable if u^* is stable and $|u(t) - u^*| \to 0$ as $t \to \infty$ for all solutions $u(t)$.*

- *unstable if it is not stable.*

Thus, when $\mathcal{R}_0 < 1$, local stability of the disease-free equilibrium implies that a small influx of infections will not lead to an outbreak, whereas global stability implies that disease will be eradicated (converge to the disease-free equilibrium) independent of the initial sizes of the sub-populations.

Furthermore, from [64], we immediately have the following theorem.

Theorem 3. *Let $\mathcal{R}_0$ be defined as in equation* (15). *The disease-free equilibrium (8) is locally asymptotically stable when $\mathcal{R}_0 < 1$, and unstable when $\mathcal{R}_0 > 1$.*

We mention that the basic reproduction number for the original model in [47] is given by

$$\widetilde{\mathcal{R}}_0 = \frac{N}{\delta\kappa(\gamma + \mu)}\Big[\xi\beta_e + \delta\kappa\beta_h\Big].$$ (16)

Comparing the expressions in (15) and (16), we note that

$$\mathcal{R}_0 < \widetilde{\mathcal{R}}_0$$ (17)

for all $\phi > 0$, $\tau > 0$ and $\nu > 0$, due to the effects of disease controls.

Theorem 3 states that if the strengths of the (constant) controls are strong enough to reduce the basic reproduction number below 1, then cholera will be eradicated. Otherwise, a cholera epidemic would occur, though with a lower infection level than that without controls owing to the reduced value of the reproduction number.

Indeed, the disease-free equilibrium is also globally asymptotically stable when $\mathcal{R}_0 < 1$. We prove this by using the following global stability result established in [11].

Theorem 4. *Consider a model system written in the form*

$$\frac{dX_1}{dt} = F(X_1, X_2) \qquad and \qquad \frac{dX_2}{dt} = G(X_1, X_2)$$

with $G(X_1, 0) = 0$, where $X_1 \in \mathbb{R}^m$ denotes (its components) the number of uninfected individuals and $X_2 \in \mathbb{R}^n$ denotes (its components) the number of infected individuals; $X_0 = (X_1^E, 0)$ denotes the disease-free equilibrium of the system. And assume,

1. *For $\frac{dX_1}{dt} = F(X_1, 0)$, X_1^E is globally asymptotically stable;*

2. *$G(X_1, X_2) = AX_2 - \hat{G}(X_1, X_2)$, $\hat{G}(X_1, X_2) \geq 0$ for $(X_1 X_2) \in \Omega$, where the Jacobian $A = \frac{\partial G}{\partial X_2}(X_1^F, 0)$ is an M-matrix (the off-diagonal elements of A are nonnegative) and Ω is the region where the model makes biological sense.*

Then the disease-free equilibrium $X_0 = (X_1^E, 0)$ is globally asymptotically stable provided that $\mathcal{R}_0 < 1$.

Let $X_1 = [S, \ V]^T$ and $X_2 = [I, \ B]^T$. That is, for our model (1) - (4) we have

$$\frac{d}{dt}\begin{bmatrix} S \\ V \end{bmatrix} = F(X_1, X_2) \quad \text{and} \quad \frac{d}{dt}\begin{bmatrix} I \\ B \end{bmatrix} = G(X_1, X_2)$$

with $G(X_1, 0) = 0$. Applying Theorem 4, we obtain

$$F(X_1, 0) = \begin{bmatrix} \frac{dS}{dt} \\ \frac{dV}{dt} \end{bmatrix}_{(X_1,0)} = \begin{bmatrix} \mu N - (\phi + \mu)S \\ \phi S - \mu V \end{bmatrix}. \tag{18}$$

It follows from solving these differential equations that $S(t) = \frac{\mu N}{\phi + \mu} + C_1 e^{-(\phi+\mu)t}$ and $V(t) = \frac{\phi N}{\phi + \mu} + C_2 e^{-\mu t} + C_3 e^{-(\phi+\mu)t}$ for some constants C_1, C_2 and C_3. Hence, $S(t) \to \frac{\mu N}{\phi + \mu}$ and $V(t) \to \frac{\phi N}{\phi + \mu}$ as $t \to \infty$, showing that X_1^E is globally asymptotically stable and condition 1 holds.

Now, consider

$$G(X_1, X_2) = AX_2 - \hat{G}(X_1, X_2), \tag{19}$$

where $A = \frac{\partial G}{\partial X_2}(X_1^E, 0)$. Specifically,

$$A = \begin{bmatrix} (1 - \rho)\beta_h(S + \sigma V) - (\tau + \gamma + \mu) & (1 - \rho)\beta_e(S + \sigma V)\frac{\kappa}{(\kappa + B)^2} \\ \xi & -(\delta + \nu) \end{bmatrix}_{(X_1^E, 0)} $$
$$= \begin{bmatrix} (1 - \rho)\beta_h\frac{(\mu + \sigma\phi)N}{\phi + \mu} - (\tau + \gamma + \mu) & (1 - \rho)\beta_e\frac{(\mu + \sigma\phi)N}{\kappa(\phi + \mu)} \\ \xi & -(\delta + \nu) \end{bmatrix}, \tag{20}$$

where the off-diagonal elements are obviously nonnegative. Substituting into equation (19) gives,

$$\hat{G}(X_1, X_2) = \begin{bmatrix} (1 - \rho)\beta_e\frac{(\mu + \sigma\phi)B^2 N}{\kappa(\phi + \mu)(\kappa + B)} \\ 0 \end{bmatrix} \geq 0. \tag{21}$$

Thus, condition 2 holds as well.

Summarizing these results, we obtain the theorem below.

Theorem 5. *When $\mathcal{R}_0 < 1$, the disease-free equilibrium of the system (1) - (4) with constant controls is globally asymptotically stable.*

In addition, the following result now can be easily derived.
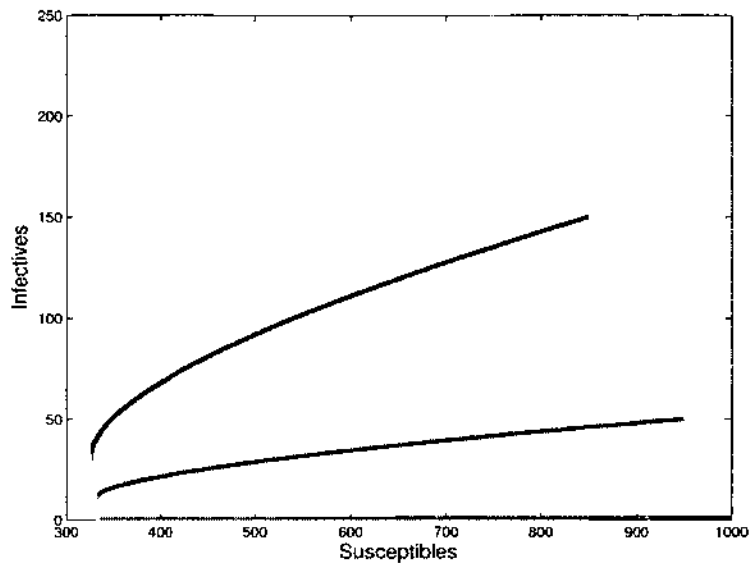
Figure 1. The phase portrait of I vs. S for the system (1) - (4) with parameters set such that $\mathcal{R}_0 \approx 0.8$. The curves correspond to six different initial conditions with $I(0) = 1$, 50, 100, 150, 200, and 250. All of the curves converge to the disease-free equilibrium where $S_0 = \mu N/(\phi + \mu) \approx 333.3$ and $I_0 = 0$.

Theorem 6. *When $\mathcal{R}_0 > 1$, the system (1) - (4) with constant controls is uniformly persistent; i.e., there exists a constant $d > 0$ such that*

$$\liminf_{t \to \infty} \{S(t),\ I(t),\ B(t)\} > d.$$

Proof. Based on Theorem 3, the disease-free equilibrium is unstable when $\mathcal{R}_0 > 1$. Since the disease-free equilibrium is unique and located on the boundary of the domain Γ, this implies the uniform persistence (Theorem 4.3 in [22]). $\square$

Numerical evidence of the global stability of the disease-free equilibrium when $\mathcal{R}_0 < 1$ is provided in Figure 1. We set the total population as $N = 1,000$ and the model parameters in such a way that $\mathcal{R}_0 \approx 0.8$. We then choose different initial conditions $I(0) = 1$, 50, 100, 150, 200, and 250, conduct a numerical simulation for each, and plot the solution curves for the phase plane portrait of I vs. S in Figure 1. We observe that all of these curves converge to the disease-free equilibrium (8). We also observe the same pattern for various other initial conditions (though not shown here).

2.2 EXISTENCE AND UNIQUENESS OF THE ENDEMIC EQUILIBRIUM

Now that we have completely described the dynamics at the disease-free equilibrium, by Theorems 3, 5 and 6, we turn to the analysis of the endemic equilibrium. As discussed before, when the effects of the controls are not strong enough to reduce $\mathcal{R}_0$ below 1, the disease-free equilibrium becomes unstable and the disease will persist. Below we will study the endemic equilibrium when $\mathcal{R}_0 > 1$, which is related to the long-term behavior of cholera dynamics.

Let $X^* = (S^*, V^*, I^*, B^*)$ denote the endemic equilibrium of the system (1) - (4). The endemic equilibrium can be deduced by solving the following system of equations,

$$
\begin{cases}
\mu N - (1 - \rho)\left[\beta_e \frac{B^*}{\kappa + B^*} + \beta_h I^*\right] S^* - (\phi + \mu)S^* = 0, \\
\phi S^* - \sigma(1 - \rho)\left[\beta_e \frac{B^*}{\kappa + B^*} + \beta_h I^*\right] V^* - \mu V^* = 0, \\
(1 - \rho)\left[\beta_e \frac{B^*}{\kappa + B^*} + \beta_h I^*\right](S^* + \sigma V^*) - (\tau + \gamma + \mu)I^* = 0, \\
\xi I^* - (\delta + \nu)B^* = 0.
\end{cases}
$$

For convenience, let us denote

$$
E = (1 - \rho)\beta_e, \qquad H = (1 - \rho)\beta_h, \qquad T = \tau + \gamma + \mu. \tag{22}
$$

Thus, we obtain

$$
S^* = \frac{\mu N}{E\frac{\xi I^*}{\kappa(\delta + \nu) + \xi I^*} + HI^* + (\phi + \mu)}, \tag{23}
$$

$$
V^* = \frac{\mu \phi N}{\left[\sigma E\frac{\xi I^*}{\kappa(\delta + \nu) + \xi I^*} + \sigma HI^* + \mu\right]\left[E\frac{\xi I^*}{\kappa(\delta + \nu) + \xi I^*} + HI^* + (\phi + \mu)\right]}, \tag{24}
$$

$$
I^* = \frac{\frac{E\xi I^*}{\kappa(\delta + \nu) + \xi I^*}(S^* + \sigma V^*)}{T - H(S^* + \sigma V^*)}, \tag{25}
$$

$$
B^* = \frac{\xi I^*}{\delta + \nu}. \tag{26}
$$

To proceed, we treat S and V as (implicit) functions of I, as suggested by equations (23) and (24). Also, let

$$
g(I) = S(I) + \sigma V(I), \qquad g_1(I) = \frac{E\xi I}{\kappa(\delta + \nu) + \xi I} + HI + (\phi + \mu),
$$

and

$$
g_2(I) = \sigma\left[\frac{E\xi I}{\kappa(\delta + \nu) + \xi I} + HI\right] + \mu.
$$

Therefore, from equations (23)-(26), we have that at an equilibrium,

$$S(I) \;=\; \frac{\mu N}{g_1(I)} \,, \tag{27}$$

$$V(I) \;=\; \frac{\mu \phi N}{g_1(I) g_2(I)} \,, \tag{28}$$

$$I \;=\; \frac{\frac{E\xi I}{\kappa(\delta+\nu)+\xi I} g(I)}{T - Hg(I)} \,, \tag{29}$$

$$B(I) \;=\; \frac{\xi I}{\delta + \nu} \,. \tag{30}$$

From equation (29) and $I \neq 0$, it follows that for an endemic equilibrium to exist we must have,

$$\frac{T - Hg(I)}{g(I)} = \frac{E\xi}{\kappa(\delta+\nu) + \xi I} \tag{31}$$

for some $I = I^* > 0$.

Now, let us denote $f_1(I) = \frac{T - Hg(I)}{g(I)} = \frac{T}{g(I)} - H$ and $f_2(I) = \frac{E\xi}{\kappa(\delta+\nu)+\xi I}$. Clearly both f_1 and f_2 are differentiable functions for $I \geq 0$. It is easy to see that

$$f_2'(I) = -\frac{E\xi^2}{[\kappa(\delta+\nu)+\xi I]^2} < 0,$$

whereas

$$f_1'(I) = \frac{-Tg'(I)}{[g'(I)]^2}.$$

Since $g(I) = \frac{\mu N}{g_1(I)} + \frac{\sigma\mu\phi N}{g_1(I)g_2(I)}$, the sign of $f_1'(I)$ is determined by the sign of $g_1'(I)$ and $g_2'(I)$. For $I \geq 0$, it is obvious that $g_1(I) > 0$ and $g_2(I) > 0$. Also, we see that

$$g_1'(I) = \frac{\kappa(\delta+\nu)E\xi}{[\kappa(\delta+\nu)+\xi I]^2} + H > 0,$$

and $g_2'(I) = \sigma g_1'(I) > 0$. Thus,

$$g'(I) = -\frac{\mu N g_1'(I)}{[g_1(I)]^2} - \frac{\sigma\mu\phi N [g_1'(I)g_2(I) + g_1(I)g_2'(I)]}{[g_1(I)g_2(I)]^2} < 0,$$

which yields $f_1'(I) > 0$.

Hence, on $[0, \infty]$, $f_1(I)$ is an increasing curve and $f_2(I)$ is a decreasing one. We can compare their vertical intercepts to determine if the two curves intersect and thus, if a positive endemic equilibrium exists. We have that $f_2(0) = \frac{E\xi}{\kappa(\delta+\nu)}$, and $f_1(0) = \frac{T}{S(0)+\sigma V(0)} - H = \frac{T(\mu+\phi)}{N(\mu+\sigma\phi)} - H$. Using equation (15), we can easily observe that if $\mathcal{R}_0 > 1$, then $f_1(0) < f_2(0)$, and there is a unique endemic equilibrium $I = I^*$; if $\mathcal{R}_0 \leq 1$, then $f_1(0) \geq f_2(0)$, and there is no endemic equilibrium. Therefore, we can establish the following theorem.

Theorem 7. *When $\mathcal{R}_0 > 1$, there exists a unique endemic equilibrium of the system (1) - (4) with constant controls.*

2.3 BIFURCATION ANALYSIS

Let us now investigate the bifurcation of the system (1) - (4) at the bifurcation point $\mathcal{R}_0 = 1$. We pick β_h as the bifurcation parameter. Our analysis makes use of the following bifurcation theorem based on the center manifold theory, originally stated in [12].

Theorem 8. *Consider a general system of ODEs with a real parameter β:*

$$\frac{dx}{dt} = f(x, \beta); \qquad f : \mathbb{R}^n \times \mathbb{R} \to \mathbb{R}^n, \quad \text{and} \quad f \in C^2(\mathbb{R}^n \times \mathbb{R}). \qquad (32)$$

Assume $x = X_0$ is an equilibrium of system (32) for all β. Also, assume

(A1) $A = D_x f(X_0, \beta^*) = \left(\frac{\partial f_i}{\partial x_j}(X_0, \beta^*) \right)$ is the linearization matrix of system (32) at the equilibrium $x = X_0$ with β evaluated at β^*. Zero is a simple eigenvalue of A and all other eigenvalues of A have negative real parts.

(A2) Matrix A has a right eigenvector w and a left eigenvector v corresponding to the zero eigenvalue.

Let f_k be the kth component of f and,

$$a = \sum_{k,i,j=1}^{4} v_k w_i w_j \frac{\partial^2 f_k}{\partial x_i \partial x_j}(X_0, \beta^*), \qquad (33)$$

$$b = \sum_{k,i=1}^{3} v_k w_i \frac{\partial^2 f_k}{\partial x_i \partial \beta}(X_0, \beta^*). \qquad (34)$$

The local dynamics of the system (32) around $x = X_0$ are totally determined by a and b.

(i) $a > 0$, $b > 0$. When $\beta - \beta^* < 0$ with $|\beta - \beta^*| << 1$, $x = X_0$ is locally asymptotically stable, and there exists a positive unstable equilibrium; when $0 < \beta - \beta^* << 1$, $x = X_0$ is unstable and there exists a negative and locally asymptotically stable equilibrium;

(ii) $a < 0$, $b < 0$. When $\beta - \beta^* < 0$ with $|\beta - \beta^*| << 1$, $x = X_0$ is unstable; when $0 < \beta - \beta^* << 1$, $x = X_0$ is locally asymptotically stable, and there exists a positive unstable equilibrium;

(iii) $a > 0$, $b < 0$. When $\beta - \beta^* < 0$ with $|\beta - \beta^*| << 1$, $x = X_0$ is unstable, and there exists a locally asymptotically stable negative equilibrium; when $0 < \beta - \beta^* << 1$, $x = X_0$ is stable, and a positive unstable equilibrium appears;

(iv) $a < 0$, $b > 0$. When $\beta - \beta^*$ changes from negative to positive, $x = X_0$ changes its stability from stable to unstable. Correspondingly a negative unstable equilibrium becomes positive and locally asymptotically stable.

Let us consider $\mathcal{R}_0$ as a function of β_h such that

$$\mathcal{R}_0(\beta_h) = \frac{(\kappa(\delta + \nu)(1 - \rho)\beta_h + \xi E)(\mu + \sigma\phi)}{T\kappa(\delta + \nu)(\phi + \mu)} N .$$

Setting $\mathcal{R}_0$ equal to 1 and solving for $\beta_h = \beta_h^*$ gives

$$\beta_h^* = \frac{1}{\kappa(\delta + \nu)(1 - \rho)} \left[\frac{T\kappa(\delta + \nu)(\phi + \mu)}{(\mu + \sigma\phi)N} - \xi E \right] .$$

We consider the disease-free equilibrium (8) and $\mathcal{R}_0 = 1$ in terms of the parameter β_h^*, and we have the following Jacobian,

$$J(X_0, \beta_h^*) = \begin{bmatrix} -(\phi + \mu) & 0 & -\frac{\mu(1-\rho)\beta_h^* N}{\phi+\mu} & -\frac{\mu E N}{\kappa(\phi+\mu)} \\ \phi & -\mu & -\frac{\sigma\phi(1-\rho)\beta_h^* N}{\phi+\mu} & -\frac{\sigma\phi E N}{\kappa(\phi+\mu)} \\ 0 & 0 & \frac{(1-\rho)\beta_h^*(\mu+\sigma\phi)N}{\phi+\mu} - T & \frac{E(\mu+\sigma\phi)N}{\kappa(\phi+\mu)} \\ 0 & 0 & \xi & -(\delta + \nu) \end{bmatrix} .$$

Denote $w = (w_1, w_2, w_3, w_4)^T$, a right eigenvector such that

$$\begin{cases} -(\phi + \mu)w_1 - \frac{\mu(1-\rho)\beta_h^* N}{\phi+\mu}w_3 - \frac{\mu E N}{\kappa(\phi+\mu)}w_4 = 0 , \\ \phi w_1 - \mu w_2 - \frac{\sigma\phi(1-\rho)\beta_h^* N}{\phi+\mu}w_3 - \frac{\sigma\phi E N}{\kappa(\phi+\mu)}w_4 = 0 , \\ \left(\frac{(1-\rho)\beta_h^*(\mu+\sigma\phi)N}{\phi+\mu} - T \right) w_3 + \frac{E(\mu+\sigma\phi)N}{\kappa(\phi+\mu)}w_4 = 0 , \\ \xi w_3 - (\delta + \nu)w_4 = 0 . \end{cases}$$

Solving this system of equations gives

$$w = \left(-\frac{\mu T}{(\phi + \mu)(\mu + \sigma\phi)}, -\frac{\phi T}{\mu + \sigma\phi} \left(\frac{1}{\phi + \mu} + \frac{\sigma}{\mu} \right), 1, \frac{\xi}{\delta + \nu} \right)^T . \tag{35}$$

Now, denote $v = (v_1, v_2, v_3, v_4)$, a left eigenvector such that

$$
\begin{cases}
-(\phi + \mu)v_1 + \phi v_2 = 0 \ , \\[4pt]
-\mu v_2 = 0 \ , \\[4pt]
-\dfrac{\mu(1-\rho)\beta_h^* N}{\phi+\mu}v_1 - \dfrac{\sigma\phi(1-\rho)\beta_h^* N}{\phi+\mu}v_2 + \left(\dfrac{(1-\rho)\beta_h^*(\mu+\sigma\phi)N}{\phi+\mu} - T\right)v_3 + \xi v_4 = 0 \ , \\[4pt]
-\dfrac{\mu EN}{\kappa(\phi+\mu)}v_1 - \dfrac{\sigma\phi EN}{\kappa(\phi-\mu)}v_2 + \dfrac{E(\mu+\sigma\phi)N}{\kappa(\phi+\mu)}v_3 - (\delta+\nu)v_4 = 0 \ ,
\end{cases}
$$

and

$$
v_4\left(\frac{\kappa(\delta+\nu)(\phi+\mu)}{E(\mu+\sigma\phi)N} + \frac{\xi}{\delta+\nu}\right) = 1 \ .
$$

Solving this system of equations gives

$$
v = \left(0, 0, \frac{\kappa(\delta+\nu)^2(\phi+\mu)}{\kappa(\delta+\nu)^2(\phi+\mu) + \xi E(\mu+\sigma\phi)N}, \frac{E(\mu+\sigma\phi)N(\delta+\nu)}{\kappa(\delta+\nu)^2(\phi+\mu) + \xi E(\mu+\sigma\phi)N}\right).
$$

(36)

Note that we have $v \cdot w = 1$, $J \cdot w = 0$ and $v \cdot J = 0$.

From equations (33)-(34), and considering only the nonzero derivatives for the terms $\frac{\partial^2 f_k}{\partial x_i \partial x_j}(X_0, \beta_h^*)$ and $\frac{\partial^2 f_k}{\partial x_i \partial \beta_h}(X_0, \beta_h^*)$, it follows that

$$
\begin{aligned}
a = {} & 2v_1 w_1 w_3 \frac{\partial^2 f_1}{\partial S \partial I}(X_0, \beta_h^*) + 2v_1 w_1 w_4 \frac{\partial^2 f_1}{\partial S \partial B}(X_0, \beta_h^*) \\
& + 2v_2 w_2 w_3 \frac{\partial^2 f_2}{\partial V \partial I}(X_0, \beta_h^*) + 2v_2 w_2 w_4 \frac{\partial^2 f_2}{\partial V \partial B}(X_0, \beta_h^*) \\
& + 2v_3 w_1 w_3 \frac{\partial^2 f_3}{\partial S \partial I}(X_0, \beta_h^*) + 2v_3 w_1 w_4 \frac{\partial^2 f_3}{\partial S \partial B}(X_0, \beta_h^*) \\
& + 2v_3 w_2 w_3 \frac{\partial^2 f_3}{\partial V \partial I}(X_0, \beta_h^*) + 2v_3 w_2 w_4 \frac{\partial^2 f_3}{\partial V \partial B}(X_0, \beta_h^*)
\end{aligned}
$$

(37)

and

$$
b = 2v_1 w_3 \frac{\partial^2 f_1}{\partial I \partial \beta_h}(X_0, \beta_h^*) + 2v_2 w_3 \frac{\partial^2 f_2}{\partial I \partial \beta_h}(X_0, \beta_h^*) + 2v_3 w_3 \frac{\partial^2 f_3}{\partial I \partial \beta_h}(X_0, \beta_h^*).
$$

(38)

With our definitions of v and w and some algebra, we obtain

$$
\begin{aligned}
a & = \frac{-2\kappa(\delta+\nu)^2(\phi+\mu)}{\kappa(\delta+\nu)^2(\phi+\mu) + \xi E(\mu+\sigma\phi)N}\left[\frac{T^2}{(\mu+\sigma\phi)^2 N}\left(\mu + \sigma\phi + \frac{\sigma^2\phi(\phi+\mu)}{\mu}\right)\right] \ , \\
b & = \frac{2\kappa(\delta+\nu)^2(\mu+\sigma\phi)(1-\rho)N}{\kappa(\delta+nu)^2(\phi+\mu) + \xi E(\mu+\sigma\phi)N} \ .
\end{aligned}
$$

Clearly, $a < 0$ and $b > 0$. Hence, based on Theorem 8, the following result holds.

Theorem 9. *The system (1) - (4) with constant controls exhibits a forward bifurcation at $\mathcal{R}_0 = 1$.*
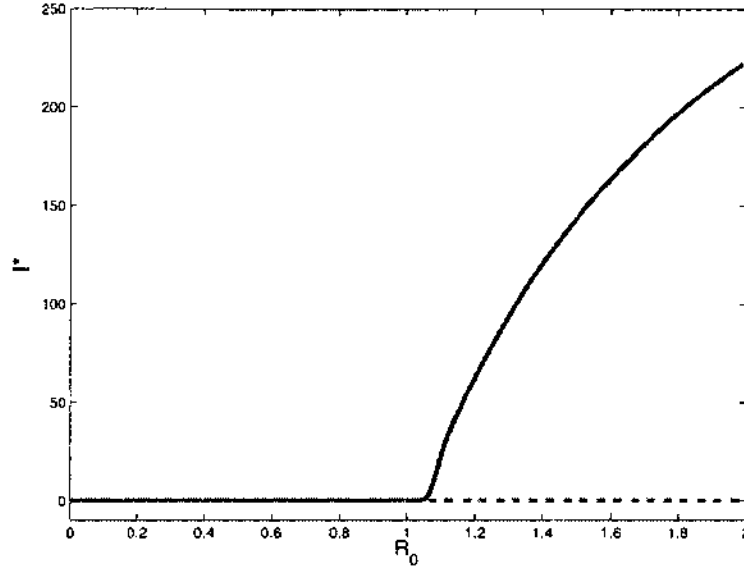
Figure 2. A bifurcation diagram of I^* vs. $\mathcal{R}_0$ which shows a forward transcritical bifurcation at $\mathcal{R}_0 = 1$. Red solid line represents the stable disease-free equilibrium (when $0 < \mathcal{R}_0 < 1$) and red dashed line represents the unstable disease-free equilibrium (when $\mathcal{R}_0 > 1$); blue solid line represents the positive stable endemic equilibrium (when $\mathcal{R}_0 > 1$). The negative unstable endemic equilibrium (when $0 < \mathcal{R}_0 < 1$) is biologically non-feasible and not shown here.

A typical bifurcation diagram of I^* vs. $\mathcal{R}_0$ near the bifurcation point $\mathcal{R}_0 = 1$ is presented in Figure 2, which is generated numerically by varying the bifurcation parameter β_h. The diagram clearly shows a forward transcritical bifurcation at $\mathcal{R}_0 = 1$.

Theorem 9 precludes the possibility of backward bifurcation for the cholera model (1) - (4). This reinforces our observation from the disease-free equilibrium analysis that reducing the basic reproductive number below one by using control measures would be sufficient to eradicate the disease.

2.4 ENDEMIC STABILITY ANALYSIS

We have presented Theorem 9 that describes the local dynamics of the system (1) - (4) near the bifurcation point $\mathcal{R}_0 = 1$. Furthermore, we can establish the following theorem regarding the stability of the endemic equilibrium.

Theorem 10. *When $\mathcal{R}_0 > 1$, the unique endemic equilibrium of the system (1) - (4)*

with constant controls is both locally and globally asymptotically stable.

The proof of the local asymptotic stability follows from direct algebraic calculation. For simplicity, set

$$P = \frac{EB^*}{\kappa + B^*} + HI^* \quad \text{and} \quad Q = \frac{E\kappa}{(\kappa + B^*)^2} . \tag{39}$$

The Jacobian evaluated at the endemic equilibrium is,

$$J(X^*) = \begin{bmatrix} -P - (\phi + \mu) & 0 & -HS^* & -QS^* \\ \phi & -\sigma P - \mu & -\sigma HV^* & -\sigma QV^* \\ P & \sigma P & H(S^* + \sigma V^*) - T & Q(S^* + \sigma V^*) \\ 0 & 0 & \xi & -(\delta + \nu) \end{bmatrix}, \tag{40}$$

giving the following characteristic polynomial,

$$\det(\lambda I - J(X^*)) = a_0\lambda^4 + a_1\lambda^3 + a_2\lambda^2 + a_3\lambda + a_4 \tag{41}$$

where

$$\begin{cases}
a_0 &= 1, \\
a_1 &= P + \phi + \mu + \sigma P + \mu + \delta + \nu + T - H(S^* + \sigma V^*) , \\
a_2 &= (P + \phi + \mu)(\sigma P + \mu + \delta + \nu + T - H(S^* + \sigma V^*)) \\
&\quad + (\delta + \nu)(T - H(S^* + \sigma V^*)) - \xi Q(S^* + \sigma V^*) \\
&\quad + (\sigma P + \mu)(\delta + \nu + T - H(S^* + \sigma V^*)) + \sigma^2 PHV^* + PHS^* , \\
a_3 &= (P + \phi + \mu)[(\sigma P + \mu)(\delta + \nu + T - H(S^* + \sigma V^*)) \\
&\quad + (\delta + \nu)(T - H(S^* + \sigma V^*)) - \xi Q(S^* + \sigma V^*) + \sigma^2 PHV^*] \\
&\quad + (\sigma P + \mu)[(\delta + \nu)(T - H(S^* + \sigma V^*)) - \xi Q(S^* + \sigma V^*)] \\
&\quad + \sigma P((\delta + \nu)\sigma HV^* + \sigma \xi QV^*) + \sigma \phi PHS^* + P((\sigma P + \mu)HS^* \\
&\quad + HS^*(\delta + \nu) + \xi QS^*) , \\
a_4 &= (P + \phi + \mu)[(\sigma P + \mu)[(\delta + \nu)(T - H(S^* + \sigma V^*)) - \xi Q(S^* + \sigma V^*)] \\
&\quad + \sigma P((\delta + \nu)\sigma HV^* + \sigma \xi QV^*)] + \sigma \phi P(HS^*(\delta + \nu) + \xi QS^*) \\
&\quad + P[(\sigma P + \mu)(HS^*(\delta + \nu) + \xi QS^*)] .
\end{cases}$$

Based on the Routh-Hurwitz stability criterion, the necessary and sufficient conditions for the stability of a quartic polynomial are

$$a_i > 0 \quad (0 \le i \le 4); \qquad a_1 a_2 - a_0 a_3 > 0; \qquad a_3(a_1 a_2 - a_0 a_3) > a_1^2 a_4 . \tag{42}$$

Clearly, $a_0 > 0$ is satisfied. From equation (25) and the fact that $S^*, V^*, I^* > 0$, it follows that

$$T - H(S^* + \sigma V^*) = \frac{\xi E(\kappa(\delta + \nu) + \xi I^*)}{(\kappa(\delta + \nu) + \xi I^*)^2}(S^* + \sigma V^*) > 0. \tag{43}$$

Note that $\xi Q = \frac{\xi E \kappa (\delta + \nu)^2}{(\kappa(\delta + \nu) + \xi I^*)^2}$, and thus

$$(\delta + \nu)(T - H(S^* + \sigma V^*)) > \xi Q(S^* + \sigma V^*). \tag{44}$$

The inequalities (43) and (44) are both necessary and sufficient to show that $a_i > 0$ for $1 \le i \le 4$. Next we show $a_1 a_2 - a_0 a_3 > 0$. Consider the following,

$$(P + \phi + \mu + \sigma P + \mu + \delta + \nu)a_2 - a_3 =$$
$$(1 - \sigma)PHS^* + (P + \phi + \mu)^2(\sigma P + \mu + \delta + \nu + T - H(S^* + \sigma V^*))$$
$$+ (P + \phi + \mu)(\sigma P + \mu)(\delta + \nu + T - H(S^* + \sigma V^*)) + (P + \mu)PHS^*$$
$$+ (\sigma P + \mu)^2(P + \phi + \mu) + (\sigma P + \mu)^2(\delta + \nu + T - H(S^* + \sigma V^*))$$
$$+ (\sigma P + \mu)\sigma^2 PHV^* + (\delta + \nu)P(\sigma P + \mu + \delta + \nu)$$
$$+ (\delta + \nu)(\phi + \mu)(\sigma P + \mu + \delta + \nu + T - H(S^* + \sigma V^*))$$
$$+ [(\delta + \nu)^2(T - H(S^* + \sigma V^*)) - (\delta + \nu)\xi Q(S^* + \sigma V^*)]$$
$$+ (\delta + \nu)^2 \sigma P + (\delta + \nu)\mu(\delta + \nu + T - H(S^* + \sigma V^*))$$
$$+ [(\delta + \nu)P(T - H(S^* + \sigma V^*)) - P\xi QS^*]$$
$$+ [(\delta + \nu)\sigma P(T - H(S^* + \sigma V^*)) - \sigma^2 P\xi QV^*].$$

Using condition (44), we have that

$$\begin{cases} (\delta + \nu)^2(T - H(S^* + \sigma V^*)) & > & (\delta + \nu)\xi Q(S^* + \sigma V^*), \\ (\delta + \nu)P(T - H(S^* + \sigma V^*)) & > & P\xi QS^*, \\ (\delta + \nu)\sigma P(T - H(S^* + \sigma V^*)) & > & \sigma^2 P\xi QV^*. \end{cases}$$

Thus, $(P + \phi + \mu + \sigma P + \mu + \delta + \nu)a_2 > a_3$ holds. From condition (43), we see that $a_1 > P + \phi + \mu + \sigma P + \mu + \delta + \nu$. Hence, $a_1 a_2 > a_3$. The last inequality in (42) can be proved with similar algebraic manipulation. Thus, the endemic equilibrium is locally stable. Disease will remain in the population if the initial sizes of the sub-populations contain a sufficient number of infected individuals and pathogen concentration; i.e., the initial conditions are sufficiently close to the endemic equilibrium, the solution of the system will converge to the endemic equilibrium.

2.5 GLOBAL ASYMPTOTIC STABILITY

The global asymptotic stability of the endemic equilibrium, however, is more challenging and requires significantly more work. The main reason for this difficulty is that the model (1) - (4) is a four-dimensional dynamical system, for which very few analytical theories and techniques can be applied. We establish the global endemic stability of our model by using the geometric approach originally proposed by Li and Muldowney [40,41], and extended in [24,67].

First let us present the main result of the geometric approach based on the second additive compound matrix. For a 4×4 matrix $A = [a_{ij}]$, the second additive compound matrix is defined as

$$A^{[2]} = \begin{pmatrix} a_{11} + a_{22} & a_{23} & a_{24} & -a_{13} & -a_{14} & 0 \\ a_{32} & a_{11} + a_{33} & a_{34} & a_{12} & 0 & -a_{14} \\ a_{42} & a_{43} & a_{11} + a_{44} & 0 & a_{12} & a_{13} \\ -a_{31} & a_{21} & 0 & a_{22} + a_{33} & a_{34} & -a_{24} \\ -a_{41} & 0 & a_{21} & a_{43} & a_{22} + a_{44} & a_{23} \\ 0 & -a_{41} & a_{31} & -a_{42} & a_{32} & a_{33} + a_{44} \end{pmatrix}.$$

Now consider the dynamical system

$$\frac{dX}{dt} = F(X) \tag{45}$$

where $F : \Gamma \mapsto \mathbb{R}^n$ is a C^1 function and where $\Gamma \subset \mathbb{R}^n$ is a simply connected open set. Let $X(t, X_0)$ denote the solution of equation (45) with the initial condition $X(0) = X_0$. We assume:

(H1) There exists a compact absorbing set $K \subset \Gamma$;

(H2) The system (45) has a unique equilibrium point X^* in Γ.

Moreover, let $X \mapsto W(X)$ be a $\binom{n}{2} \times \binom{n}{2}$ matrix-valued C^1 function in Γ. Set

$$P = W_F W^{-1} + W J^{[2]} W^{-1}, \tag{46}$$

where W_F is the derivative of W (entry-wise) along the direction of F, and $J^{[2]}$ is the second additive compound matrix of the Jacobian $J(X) = DF(X)$. Let $m(P)$ be the Lozinskiĭ measure of P with respect to a matrix norm [16], i.e.,

$$m(P) = \lim_{h \to 0^+} \frac{|I + hP| - 1}{h}. \tag{47}$$

For a norm $|| \cdot ||$ on $\mathbb{R}^n$, it is established in [24] that the Lozinskiĭ measure of P associated with $|| \cdot ||$ can be evaluated as

$$m(P) = \inf \left\{ c \, \Big| \, D_+ ||Z|| \leq c||Z|| \text{ for all solutions of } Z' = PZ \right\} \tag{48}$$

where D_+ denotes the right-hand total derivative with respect to t. The following result is implicitly stated in [24].

Theorem 11. *Assume that Γ is simply connected and the assumptions* **(H1)** *and* **(H2)** *hold. Then the unique equilibrium X^* of* (45) *is globally asymptotically stable in Γ if $m(P) < 0$.*

Based on Theorem 7, our system (1) - (4) has a unique endemic equilibrium when $\mathcal{R}_0 > 1$. Meanwhile, the uniform persistence (see Theorem 6) and the boundedness of the domain Γ imply that the system has a compact absorbing subset of Γ [9]. Hence, the assumptions **(H1)** and **(H2)** hold for the system (1) - (4). Below we verify the condition $m(P) < 0$.

The second additive compound matrix associated with the Jacobian of the system (1) - (4) is,

$$J^{[2]} = \begin{bmatrix} j_{11} & -\sigma HV & -\sigma QV & HS & QS & 0 \\ \sigma(\frac{EB}{\kappa+B} + HI) & j_{22} & Q(S+\sigma V) & 0 & 0 & QS \\ 0 & \xi & j_{33} & 0 & 0 & -HS \\ -(\frac{EB}{\kappa+B} + HI) & \phi & 0 & j_{44} & Q(S+\sigma V) & \sigma QV \\ 0 & 0 & \phi & \xi & j_{55} & -\sigma HV \\ 0 & 0 & \frac{EB}{\kappa+B} + HI & 0 & \sigma(\frac{EB}{\kappa+B} + HI) & j_{66} \end{bmatrix}$$

where

$$Q = \frac{E\kappa}{(\kappa + B)^2},$$

$$j_{11} = -(1+\sigma)\left(\frac{EB}{\kappa+B} + HI\right) - 2\mu - \phi,$$

$$j_{22} = -\left(\frac{EB}{\kappa+B} + HI\right) - \phi - \mu + H(S+\sigma V) - T,$$

$$j_{33} = -\left(\frac{EB}{\kappa+B} + HI\right) - \phi - \mu - \delta - \nu,$$

$$j_{44} = -\sigma\left(\frac{EB}{\kappa+B} + HI\right) - \mu + H(S+\sigma V) - T,$$

$$j_{55} = -\sigma\left(\frac{EB}{\kappa+B} + HI\right) - \mu - \delta - \nu,$$

$$j_{66} = H(S+\sigma V) - T - \delta - \nu.$$

Set

$$
W = \begin{bmatrix}
\frac{1}{I} & 0 & 0 & 0 & 0 & 0 \\
0 & \frac{1}{I} & 0 & 0 & 0 & 0 \\
0 & 0 & 0 & \frac{1}{I} & 0 & 0 \\
0 & 0 & \frac{1}{B} & 0 & 0 & 0 \\
0 & 0 & 0 & 0 & \frac{1}{B} & 0 \\
0 & 0 & 0 & 0 & 0 & \frac{1}{B}
\end{bmatrix}.
$$

Note that

$$
W_F = \begin{bmatrix}
\frac{-1}{I^2}\frac{dI}{dt} & 0 & 0 & 0 & 0 & 0 \\
0 & \frac{-1}{I^2}\frac{dI}{dt} & 0 & 0 & 0 & 0 \\
0 & 0 & 0 & \frac{-1}{I^2}\frac{dI}{dt} & 0 & 0 \\
0 & 0 & \frac{-1}{B^2}\frac{dB}{dt} & 0 & 0 & 0 \\
0 & 0 & 0 & 0 & \frac{-1}{B^2}\frac{dB}{dt} & 0 \\
0 & 0 & 0 & 0 & 0 & \frac{-1}{B^2}\frac{dB}{dt}
\end{bmatrix}.
$$

Thus, we have

$$
WJ^{[2]}W^{-1} = \begin{bmatrix}
j_{11} & -\sigma HV & HS & -\sigma QV\frac{B}{I} & QS\frac{B}{I} & 0 \\
\sigma(\frac{EB}{\kappa+B}+HI) & j_{22} & 0 & Q(S+\sigma V)\frac{B}{I} & 0 & QS\frac{B}{I} \\
-(\frac{EB}{\kappa+B}+HI) & \phi & j_{44} & 0 & Q(S+\sigma V)\frac{B}{I} & \sigma QV\frac{B}{I} \\
0 & \xi\frac{I}{B} & 0 & j_{33} & 0 & -HS \\
0 & 0 & \xi\frac{I}{B} & \phi & j_{55} & -\sigma HV \\
0 & 0 & 0 & \frac{EB}{\kappa+B}+HI & \sigma(\frac{EB}{\kappa+B}+HI) & j_{66}
\end{bmatrix},
$$

and

$$
W_FW^{-1} = \begin{bmatrix}
\frac{-1}{I}\frac{dI}{dt} & 0 & 0 & 0 & 0 & 0 \\
0 & \frac{-1}{I}\frac{dI}{dt} & 0 & 0 & 0 & 0 \\
0 & 0 & \frac{-1}{I}\frac{dI}{dt} & 0 & 0 & 0 \\
0 & 0 & 0 & \frac{-1}{B}\frac{dB}{dt} & 0 & 0 \\
0 & 0 & 0 & 0 & \frac{-1}{B}\frac{dB}{dt} & 0 \\
0 & 0 & 0 & 0 & 0 & \frac{-1}{B}\frac{dB}{dt}
\end{bmatrix}.
$$

Hence,

$$P = W_F W^{-1} + W J^{[2]} W^{-1}$$

$$= \begin{bmatrix} g_{11} & -\sigma HV & HS & -\sigma QV\frac{B}{I} & QS\frac{B}{I} & 0 \\ \sigma(\frac{EB}{\kappa+B}+HI) & g_{22} & 0 & Q(S+\sigma V)\frac{B}{I} & 0 & QS\frac{B}{I} \\ -(\frac{EB}{\kappa+B}+HI) & \phi & g_{33} & 0 & Q(S+\sigma V)\frac{B}{I} & \sigma QV\frac{B}{I} \\ 0 & \xi\frac{I}{B} & 0 & g_{44} & 0 & -HS \\ 0 & 0 & \xi\frac{I}{B} & \phi & g_{55} & -\sigma HV \\ 0 & 0 & 0 & \frac{EB}{\kappa+B}+HI & \sigma(\frac{EB}{\kappa+B}+HI) & g_{66} \end{bmatrix}$$

where

$$g_{11} = \frac{-E(S+\sigma V)}{\kappa+B}\frac{B}{I} - (1+\sigma)\left(\frac{EB}{\kappa+B}+HI\right) + T - H(S+\sigma V) - 2\mu - \phi\,,$$

$$g_{22} = \frac{-E(S+\sigma V)}{\kappa+B}\frac{B}{I} - \left(\frac{EB}{\kappa+B}+HI\right) - \phi - \mu\,,$$

$$g_{33} = \frac{-E(S+\sigma V)}{\kappa+B}\frac{B}{I} - \sigma\left(\frac{EB}{\kappa+B}+HI\right) - \mu\,,$$

$$g_{44} = -\xi\frac{I}{B} - \left(\frac{EB}{\kappa+B}+HI\right) - \phi - \mu\,,$$

$$g_{55} = -\xi\frac{I}{B} - \sigma\left(\frac{EB}{\kappa+B}+HI\right) - \mu\,,$$

$$g_{66} = H(S+\sigma V) - T - \xi\frac{I}{B}\,.$$

To proceed, we need to define a norm on $\mathbb{R}^6$. Here we use the one introduced in [24],

$$\|z\| = \max\{U_1, U_2\}\,,$$

where $x \in \mathbb{R}^6$, with components z_i, $1 \le i \le 6$. Also, define

$$U_1(z_1, z_2, z_3) = \begin{cases} \max\{|z_1|, |z_2|+|z_3|\}, & \text{if } \operatorname{sgn}(z_1) = \operatorname{sgn}(z_2) = \operatorname{sgn}(z_3) \\ \max\{|z_2|, |z_1|+|z_3|\}, & \text{if } \operatorname{sgn}(z_1) = \operatorname{sgn}(z_2) = -\operatorname{sgn}(z_3) \\ \max\{|z_1|, |z_2|, |z_3|\}, & \text{if } \operatorname{sgn}(z_1) = -\operatorname{sgn}(z_2) = \operatorname{sgn}(z_3) \\ \max\{|z_1|+|z_3|, |z_2|+|z_3|\}, & \text{if } -\operatorname{sgn}(z_1) = \operatorname{sgn}(z_2) = \operatorname{sgn}(z_3) \end{cases}$$

and

$$U_2(z_4, z_5, z_6) = \begin{cases} |z_4|+|z_5|+|z_6|, & \text{if } \operatorname{sgn}(z_4) = \operatorname{sgn}(z_5) = \operatorname{sgn}(z_6) \\ \max\{|z_4|+|z_5|, |z_4|+|z_6|\}, & \text{if } \operatorname{sgn}(z_4) = \operatorname{sgn}(z_5) = -\operatorname{sgn}(z_6) \\ \max\{|z_5|, |z_4|+|z_6|\}, & \text{if } \operatorname{sgn}(z_4) = -\operatorname{sgn}(z_5) = \operatorname{sgn}(z_6) \\ \max\{|z_4|+|z_6|, |z_5|+|z_6|\}, & \text{if } -\operatorname{sgn}(z_4) = \operatorname{sgn}(z_5) = \operatorname{sgn}(z_6). \end{cases}$$

Consequently, there are 8 different cases for $\|z\|$. We discuss each case separately as follows:

Case 1: $U_1(z) > U_2(z)$ and $z_1, z_2, z_3 > 0$. Then $\|z\| = \max\{|z_1|, |z_2| + |z_3|\}$.

(i) $|z_1| > |z_2| + |z_3|$

Then $\|z\| = |z_1| = z_1$ and $U_2(z) < |z_1|$. Taking the right-hand derivative we obtain,

$$
\begin{aligned}
D_+\|z\| &= z_1' \\
&= g_{11}z_1 + g_{12}z_2 + g_{13}z_3 + g_{14}z_4 + g_{15}z_5 + g_{16}z_6 \\
&= \left(\frac{-E(S+\sigma V)}{\kappa+B}\frac{B}{I} - (1+\sigma)\left(\frac{EB}{\kappa+B} + HI\right) + T - H(S+\sigma V) - 2\mu - \phi\right)z_1 \\
&\quad -\sigma HVz_2 + HSz_3 - \sigma QV\frac{B}{I}z_4 + QS\frac{B}{I}z_5 \\
&\leq \left(\frac{-E(S+\sigma V)}{\kappa+B}\frac{B}{I} - (1+\sigma)\left(\frac{EB}{\kappa+B} + HI\right) + T - H(S+\sigma V) - 2\mu - \phi\right)|z_1| \\
&\quad +HS(|z_2| + |z_3|) + Q(S+\sigma V)\frac{B}{I}(|z_4| + |z_5|) \\
&\leq \left(\frac{-EB(S+\sigma V)}{(\kappa+B)^2}\frac{B}{I} - (1+\sigma)\left(\frac{EB}{\kappa+B} + HI\right) + T - \sigma HV - 2\mu - \phi\right)|z_1|
\end{aligned}
$$

which yields

$$D_+\|z\| \leq (T - 2\mu - \phi)\|z\|. \tag{49}$$

(ii) $|z_1| < |z_2| + |z_3|$

Then $\|z\| = |z_2| + |z_3|$ and $U_2(z) < |z_2| + |z_3|$. Taking the right-hand derivative we obtain,

$$
\begin{aligned}
D_+\|z\| &= z_2' + z_3' \\
&= (g_{21} + g_{31})z_1 + (g_{22} + g_{32})z_2 + (g_{23} + g_{33})z_3 + (g_{24} + g_{34})z_4 \\
&\quad +(g_{25} + g_{35})z_5 + (g_{26} + g_{36})z_6 \\
&= -(1-\sigma)\left(\frac{EB}{\kappa+B} + HI\right)z_1 + \left(\frac{-E(S+\sigma V)}{\kappa+B}\frac{B}{I} - \left(\frac{EB}{\kappa+B} + HI\right) - \mu\right)z_2 \\
&\quad + \left(\frac{-E(S+\sigma V)}{\kappa+B}\frac{B}{I} - \sigma\left(\frac{EB}{\kappa+B} + HI\right) - \mu\right)z_3 \\
&\quad +Q(S+\sigma V)\frac{B}{I}(z_4 + z_5 + z_6) \\
&\leq -(1-\sigma)\left(\frac{EB}{\kappa+B} + HI\right)|z_1| \\
&\quad + \left(\frac{-E(S+\sigma V)}{\kappa+B}\frac{B}{I} - \sigma\left(\frac{EB}{\kappa+B} + HI\right) - \mu\right)(|z_2| + |z_3|) \\
&\quad -(1-\sigma)\left(\frac{EB}{\kappa+B} + HI\right)|z_2| + Q(S+\sigma V)\frac{B}{I}|z_4 + z_5 + z_6| \\
&\leq \left(\frac{-EB(S+\sigma V)}{(\kappa+B)^2}\frac{B}{I} - \left(\frac{EB}{\kappa+B} + HI\right) - \mu\right)(|z_2| + |z_3|)
\end{aligned}
$$

Hence,

$$D_+\|z\| \leq -\mu\|z\|. \tag{50}$$

Case 2: $U_1(z) > U_2(z)$ and $z_3 < 0 < z_1, z_2$. Then $\|z\| = \max\{|z_2|, |z_1| + |z_3|\}$.

(i) $|z_2| > |z_1| + |z_3|$

Then $\|z\| = |z_2| = z_2$ and $U_2(z) < |z_2|$. Taking the right-hand derivative we obtain,

$$
\begin{aligned}
D_+\|z\| &= z_2' \\
&= g_{21}z_1 + g_{22}z_2 + g_{23}z_3 + g_{24}z_4 + g_{25}z_5 + g_{26}z_6 \\
&= \sigma\left(\tfrac{EB}{\kappa+B} + HI\right)z_1 + \left(\tfrac{-E(S+\sigma V)}{\kappa+B}\tfrac{B}{I} - \left(\tfrac{EB}{\kappa+B} + HI\right) - \phi - \mu\right)z_2 \\
&\quad + Q(S+\sigma V)\tfrac{B}{I}z_4 + QS\tfrac{B}{I}z_6 \\
&\leq \sigma\left(\tfrac{EB}{\kappa+B} + HI\right)|z_1| + \left(\tfrac{-E(S+\sigma V)}{\kappa+B}\tfrac{B}{I} - \left(\tfrac{EB}{\kappa+B} + HI\right) - \phi - \mu\right)|z_2| \\
&\quad + Q(S+\sigma V)\tfrac{B}{I}(|z_4| + |z_6|) \\
&\leq \left(\tfrac{-EB(S+\sigma V)}{(\kappa+B)^2}\tfrac{B}{I} - (1-\sigma)\left(\tfrac{EB}{\kappa+B} + HI\right) - \phi - \mu\right)|z_2|
\end{aligned}
$$

Hence,

$$D_+\|z\| \leq -\mu\|z\|. \tag{51}$$

(ii) $|z_2| < |z_1| + |z_3|$

Then $\|z\| = |z_1| + |z_3| = z_1 - z_3$ and $U_2(z) < |z_1| + |z_3|$. Taking the right-hand derivative we obtain,

$$
\begin{aligned}
D_+\|z\| &= z_1' - z_3' \\
&= (g_{11} - g_{31})z_1 + (g_{12} - g_{32})z_2 + (g_{13} - g_{33})z_3 + (g_{14} - g_{34})z_4 \\
&\quad + (g_{15} - g_{35})z_5 + (g_{16} - g_{36})z_6 \\
&= \left(\tfrac{-E(S+\sigma V)}{\kappa+B}\tfrac{B}{I} - \sigma\left(\tfrac{EB}{\kappa+B} + HI\right) + T - H(S+\sigma V) - 2\mu - \phi\right)z_1 \\
&\quad - (\sigma HV + \phi)z_2 + \left(HS + \tfrac{E(S+\sigma V)}{\kappa+B}\tfrac{B}{I} + \sigma\left(\tfrac{EB}{\kappa+B} + HI\right) + \mu\right)z_3 \\
&\quad - \sigma QV\tfrac{B}{I}(z_4 + z_5 + z_6) \\
&\leq \left(\tfrac{-E(S+\sigma V)}{\kappa+B}\tfrac{B}{I} - \sigma\left(\tfrac{EB}{\kappa+B} + HI\right) + T - H(S+\sigma V) - 2\mu - \phi\right)|z_1| \\
&\quad - (\sigma HV + \phi)|z_2| - \left(HS + \tfrac{E(S+\sigma V)}{\kappa+B}\tfrac{B}{I} + \sigma\left(\tfrac{EB}{\kappa+B} + HI\right) + \mu\right)|z_3| \\
&\quad + Q(S+\sigma V)\tfrac{B}{I}|z_4 + z_5 + z_6| \\
&\leq \left(\tfrac{-EB(S+\sigma V)}{(\kappa+B)^2}\tfrac{B}{I} - \sigma\left(\tfrac{EB}{\kappa+B} + HI\right) - HS - \mu\right)(|z_1| + |z_3|) \\
&\quad + (T - \sigma HV - \mu - \phi)|z_1| \\
&\leq \max\{-\mu, T - 2\mu - \phi\}(|z_1| + |z_3|)
\end{aligned}
$$

Hence,

$$D_+\|z\| \leq \max\{-\mu, T - 2\mu - \phi\}\|z\|. \tag{52}$$

Case 3: $U_1(z) > U_2(z)$ and $z_2 < 0 < z_1, z_3$. Then $\|z\| = \max\{|z_1|, |z_2|, |z_3|\}$.

(i) $|z_1| > |z_2|, |z_3|$

Then $\|z\| = |z_1| = z_1$ and $U_2(z) < |z_1|$. Taking the right-hand derivative we obtain,

$$
\begin{aligned}
D_+\|z\| &= z_1' \\
&= g_{11}z_1 + g_{12}z_2 + g_{13}z_3 + g_{14}z_4 + g_{15}z_5 + g_{16}z_6 \\
&= \left(\frac{-E(S+\sigma V)}{\kappa+B}\frac{B}{I} - (1+\sigma)\left(\frac{EB}{\kappa+B} + HI\right) + T - H(S+\sigma V) - 2\mu - \phi\right)z_1 \\
&\quad -\sigma HVz_2 + HSz_3 - \sigma QV\frac{B}{I}z_4 + QS\frac{B}{I}z_5 \\
&\leq \left(\frac{-E(S+\sigma V)}{\kappa+B}\frac{B}{I} - (1+\sigma)\left(\frac{EB}{\kappa+B} + HI\right) + T - H(S+\sigma V) - 2\mu - \phi\right)|z_1| \\
&\quad +\sigma HV|z_2| + HS|z_3| + Q(S+\sigma V)\frac{B}{I}(|z_4| + |z_5|) \\
&\leq \left(\frac{-EB(S+\sigma V)}{(\kappa+B)^2}\frac{B}{I} - (1+\sigma)\left(\frac{EB}{\kappa+B} + HI\right) + T - 2\mu - \phi\right)|z_1|
\end{aligned}
$$

Hence,

$$D_+\|z\| \leq (T - 2\mu - \phi)\|z\|. \tag{53}$$

(ii) $|z_2| > |z_1|, |z_3|$

Then $\|z\| = |z_2| = -z_2$ and $U_2(z) < |z_2|$. Taking the right-hand derivative we obtain,

$$
\begin{aligned}
D_+\|z\| &= -z_2' \\
&= -g_{21}z_1 - g_{22}z_2 - g_{23}z_3 - g_{24}z_4 - g_{25}z_5 - g_{26}z_6 \\
&= -\sigma\left(\frac{EB}{\kappa+B} + HI\right)z_1 - \left(\frac{-E(S+\sigma V)}{\kappa+B}\frac{B}{I} - \left(\frac{EB}{\kappa+B} + HI\right) - \phi - \mu\right)z_2 \\
&\quad -Q(S+\sigma V)\frac{B}{I}z_4 - QS\frac{B}{I}z_6 \\
&\leq -\sigma\left(\frac{EB}{\kappa+B} + HI\right)|z_1| + \left(\frac{-E(S+\sigma V)}{\kappa+B}\frac{B}{I} - \left(\frac{EB}{\kappa+B} + HI\right) - \phi - \mu\right)|z_2| \\
&\quad +Q(S+\sigma V)\frac{B}{I}(|z_4| + |z_6|) \\
&\leq \left(\frac{-EB(S+\sigma V)}{(\kappa+B)^2}\frac{B}{I} - \left(\frac{EB}{\kappa+B} + HI\right) - \phi - \mu\right)|z_2|
\end{aligned}
$$

Hence,

$$D_+\|z\| \leq -\mu\|z\|. \tag{54}$$

(iii) $|z_3| > |z_1|, |z_2|$

Then $\|z\| = |z_3| = z_3$ and $U_2(z) < |z_3|$. Taking the right-hand derivative we

obtain,

$$
\begin{aligned}
D_+\|z\| &= z_3' \\
&= g_{31}z_1 + g_{32}z_2 + g_{33}z_3 + g_{34}z_4 + g_{35}z_5 + g_{36}z_6 \\
&= -\left(\frac{EB}{\kappa+B} + HI\right)z_1 + \phi z_2 + \left(\frac{-E(S+\sigma V)}{\kappa+B}\frac{B}{I} - \sigma\left(\frac{EB}{\kappa+B} + HI\right) - \mu\right)z_3 \\
&\quad + Q(S+\sigma V)\frac{B}{I}z_5 + \sigma QV\frac{B}{I}z_6 \\
&\leq -\left(\frac{EB}{\kappa+B} + HI\right)|z_1| - \phi|z_2| + \left(\frac{-E(S+\sigma V)}{\kappa+B}\frac{B}{I} - \sigma\left(\frac{EB}{\kappa+B} + HI\right) - \mu\right)|z_3| \\
&\quad + Q(S+\sigma V)\frac{B}{I}(|z_5| + |z_6|) \\
&\leq \left(\frac{-EB(S+\sigma V)}{(\kappa+B)^2}\frac{B}{I} - \sigma\left(\frac{EB}{\kappa+B} + HI\right) - \mu\right)|z_3|
\end{aligned}
$$

Hence,

$$
D_+\|z\| \leq -\mu\|z\|. \tag{55}
$$

Case 4: $U_1(z) > U_2(z)$ and $z_1 < 0 < z_2, z_3$. Then $\|z\| = \max\{|z_1| + |z_3|, |z_2| + |z_3|\}$.

(i) $|z_1| > |z_2|$

Then $\|z\| = |z_1| + |z_3| = -z_1 + z_3$ and $U_2(z) < |z_1| + |z_3|$. Taking the right-hand derivative we obtain,

$$
\begin{aligned}
D_+\|z\| &= -z_1' + z_3' \\
&= (g_{31} - g_{11})z_1 + (g_{32} - g_{12})z_2 + (g_{33} - g_{13})z_3 + (g_{34} - g_{14})z_4 \\
&\quad + (g_{35} - g_{15})z_5 + (g_{36} - g_{16})z_6 \\
&= \left(\frac{E(S+\sigma V)}{\kappa+B}\frac{B}{I} + \sigma\left(\frac{\sigma EB}{\kappa+B} + HI\right) - T + H(S+\sigma V) + 2\mu + \phi\right)z_1 \\
&\quad + (\sigma HV + \phi)z_2 + \left(\frac{-E(S+\sigma V)}{\kappa+B}\frac{B}{I} - \sigma\left(\frac{EB}{\kappa+B} + HI\right) - HS - \mu\right)z_3 \\
&\quad + \sigma QV\frac{B}{I}(z_4 + z_5 + z_6) \\
&\leq -\left(\frac{E(S+\sigma V)}{\kappa+B}\frac{B}{I} + \sigma\left(\frac{\sigma EB}{\kappa+B} + HI\right) - T + H(S+\sigma V) + 2\mu + \phi\right)|z_1| \\
&\quad + (\sigma HV + \phi)|z_2| + \left(\frac{-E(S+\sigma V)}{\kappa+B}\frac{B}{I} - \sigma\left(\frac{EB}{\kappa+B} + HI\right) - HS - \mu\right)|z_3| \\
&\quad + Q(S+\sigma V)\frac{B}{I}|z_4 + z_5 + z_6| \\
&\leq \left(\frac{-EB(S+\sigma V)}{(\kappa+B)^2}\frac{B}{I} - \sigma\left(\frac{EB}{\kappa+B} + HI\right) - HS - \mu\right)(|z_1| + |z_3|) \\
&\quad + (T - \sigma HV - \mu - \phi)|z_1| + (\sigma HV + \phi)|z_2| \\
&\leq \left(\frac{-EB(S+\sigma V)}{(\kappa+B)^2}\frac{B}{I} - \sigma\left(\frac{EB}{\kappa+B} + HI\right) - HS - \mu\right)(|z_1| + |z_3|) \\
&\quad + (T - \mu)|z_1| \\
&\leq \left(\frac{-EB(S+\sigma V)}{(\kappa+B)^2}\frac{B}{I} - \sigma\left(\frac{EB}{\kappa+B} + HI\right) + T - HS - 2\mu\right)(|z_1| + |z_3|)
\end{aligned}
$$

Hence,

$$
D_+\|z\| \leq (T - 2\mu)\|z\|. \tag{56}
$$

(ii) $|z_1| < |z_2|$

Then $\|z\| = |z_2| + |z_3| = z_2 + z_3$ and $U_2(z) < |z_2| + |z_3|$. Taking the right-hand derivative we obtain,

$$
\begin{aligned}
D_+\|z\| &= z_2' + z_3' \\
&= (g_{21} + g_{31})z_1 + (g_{22} + g_{32})z_2 + (g_{23} + g_{33})z_3 + (g_{24} + g_{34})z_4 \\
&\quad + (g_{25} + g_{35})z_5 + (g_{26} + g_{36})z_6 \\
&= -(1-\sigma)\left(\frac{EB}{\kappa+B} + HI\right)z_1 + \left(\frac{-E(S+\sigma V)}{\kappa+B}\frac{B}{I} - \left(\frac{EB}{\kappa+B} + HI\right) - \mu\right)z_2 \\
&\quad + \left(\frac{-E(S+\sigma V)}{\kappa+B}\frac{B}{I} - \sigma\left(\frac{EB}{\kappa+B} + HI\right) - \mu\right)z_3 \\
&\quad + Q(S+\sigma V)\frac{B}{I}(z_4 + z_5 + z_6) \\
&\leq (1-\sigma)\left(\frac{EB}{\kappa+B} + HI\right)|z_1| + \left(\frac{-E(S+\sigma V)}{\kappa+B}\frac{B}{I} - \left(\frac{EB}{\kappa+B} + HI\right) - \mu\right)|z_2| \\
&\quad + \left(\frac{-E(S+\sigma V)}{\kappa+B}\frac{B}{I} - \sigma\left(\frac{EB}{\kappa+B} + HI\right) - \mu\right)|z_3| \\
&\quad + Q(S+\sigma V)\frac{B}{I}|z_4 + z_5 + z_6| \\
&\leq (1-\sigma)\left(\frac{EB}{\kappa+B} + HI\right)(|z_1| - |z_2|) \\
&\quad + \left(\frac{-EB(S+\sigma V)}{(\kappa+B)^2}\frac{B}{I} - \sigma\left(\frac{EB}{\kappa+B} + HI\right) - \mu\right)(|z_2| + |z_3|) \\
&\leq \left(\frac{-EB(S+\sigma V)}{(\kappa+B)^2}\frac{B}{I} - \sigma\left(\frac{EB}{\kappa+B} + HI\right) - \mu\right)(|z_2| + |z_3|)
\end{aligned}
$$

Hence,

$$D_+\|z\| \leq -\mu\|z\|. \tag{57}$$

Case 5: $U_2(z) > U_1(z)$ and $z_4, z_5, z_6 > 0$.

Then $\|z\| = |z_4| + |z_5| + |z_6| = z_4 + z_5 + z_6$ and $U_1(z) < |z_4| + |z_5| + |z_6|$. Taking the right-hand derivative we obtain,

$$
\begin{aligned}
D_+\|z\| &= z_4' + z_5' + z_6' \\
&= (g_{41} + g_{51} + g_{61})z_1 + (g_{42} + g_{52} + g_{62})z_2 + (g_{43} + g_{53} + g_{63})z_3 \\
&\quad + (g_{44} + g_{54} + g_{64})z_4 + (g_{45} + g_{55} + g_{65})z_5 + (g_{46} + g_{56} + g_{66})z_6 \\
&= \xi\frac{I}{B}(z_2 + z_3) + (-\xi\frac{I}{B} - \mu)z_4 + (-\xi\frac{I}{B} - \mu)z_5 + (-T - \xi\frac{I}{B})z_6 \\
&\leq \xi\frac{I}{B}|z_2 + z_3| + (-\xi\frac{I}{B} - \mu)(|z_4| + |z_5|) + (-T - \xi\frac{I}{B})|z_6| \\
&\leq -\mu(|z_4| + |z_5|) - T|z_6| \\
&\leq -\mu(|z_4| + |z_5| + |z_6|)
\end{aligned}
$$

Hence,

$$D_+\|z\| \leq -\mu\|z\|. \tag{58}$$

Case 6: $U_2(z) > U_1(z)$ and $z_6 < 0 < z_4, z_5$. Then $\|z\| = \max\{|z_4| + |z_5|, |z_4| + |z_6|\}$.

(i) $|z_5| > |z_6|$

Then $\|z\| = |z_4| + |z_5| = z_4 + z_5$ and $U_1(z) < |z_4| + |z_5|$. Taking the right-hand derivative to obtain,

$$
\begin{aligned}
D_+\|z\| &= z_4' + z_5' \\
&= (g_{41} + g_{51})z_1 + (g_{42} + g_{52})z_2 + (g_{43} + g_{53})z_3 + (g_{44} + g_{54})z_4 \\
&\quad + (g_{45} + g_{55})z_5 + (g_{46} + g_{56})z_6 \\
&= \xi\frac{I}{B}(z_2 + z_3) + \left(-\xi\frac{I}{B} - \left(\frac{EB}{\kappa+B} + HI\right) - \mu\right)z_4 \\
&\quad + \left(-\xi\frac{I}{B} - \sigma\left(\frac{EB}{\kappa+B} + HI\right) - \mu\right)z_5 - H(S + \sigma V)z_6 \\
&\le \xi\frac{I}{B}|z_2 + z_3| + \left(-\xi\frac{I}{B} - \sigma\left(\frac{EB}{\kappa+B} + HI\right) - \mu\right)(|z_4| + |z_5|) \\
&\quad - (1 - \sigma)\left(\frac{EB}{\kappa+B} + HI\right)|z_4| + H(S + \sigma V)|z_6| \\
&\le \left(-\sigma\left(\frac{EB}{\kappa+B} + HI\right) + H(S + \sigma V) - \mu\right)(|z_4| + |z_5|)
\end{aligned}
$$

Noting that $\sigma \le 1$ and $S + \sigma V \le N$, we thus have

$$
\begin{aligned}
D_+\|z\| &\le (H(S + \sigma V) - \mu)\|z\| \\
&\le (HN - \mu)\|z\|.
\end{aligned}
\tag{59}
$$

(ii) $|z_5| < |z_6|$

Then $\|z\| = |z_4| + |z_6| = z_4 - z_6$ and $U_1(z) < |z_4| + |z_6|$. Taking the right-hand derivative we obtain,

$$
\begin{aligned}
D_+\|z\| &= z_4' - z_6' \\
&= (g_{41} - g_{61})z_1 + (g_{42} - g_{62})z_2 + (g_{43} - g_{63})z_3 + (g_{44} - g_{64})z_4 \\
&\quad + (g_{45} - g_{65})z_5 + (g_{46} - g_{66})z_6 \\
&= \xi\frac{I}{B}z_2 + \left(-\xi\frac{I}{B} - 2\left(\frac{EB}{\kappa+B} + HI\right) - \phi - \mu\right)z_4 - \sigma\left(\frac{EB}{\kappa+b} + HI\right)z_5 \\
&\quad - (HS + H(S + \sigma V) - T - \xi\frac{I}{B})z_6 \\
&\le \xi\frac{I}{B}|z_2| + \left(-\xi\frac{I}{B} - 2\left(\frac{EB}{\kappa+B} + HI\right) - \phi - \mu\right)|z_4| - \sigma\left(\frac{EB}{\kappa+b} + HI\right)|z_5| \\
&\quad + (HS + H(S + \sigma V) - T - \xi\frac{I}{B})|z_6| \\
&\le \left(-2\left(\frac{EB}{\kappa+B} + HI\right) - \phi - \mu\right)|z_4| - \sigma\left(\frac{EB}{\kappa+b} + HI\right)|z_5| \\
&\quad + (HS + H(S + \sigma V) - T)|z_6| \\
&\le \max\{-\mu, HS + H(S + \sigma V) - T\}(|z_4| + |z_6|)
\end{aligned}
$$

Hence,

$$
\begin{aligned}
D_+\|z\| &\le \max\{-\mu, HS + H(S + \sigma V) - T\}\|z\| \\
&\le \max\{-\mu, 2HN - T\}\|z\|.
\end{aligned}
\tag{60}
$$

Case 7: $U_2(z) > U_1(z)$ and $z_5 < 0 < z_4, z_6$. Then $\|z\| = \max\{|z_5|, |z_4| + |z_6|\}$.

(i) $|z_5| > |z_4| + |z_6|$

Then $\|z\| = |z_5| = -z_5$ and $U_1(z) < |z_5|$. Taking the right-hand derivative we obtain,

$$
\begin{aligned}
D_+\|z\| &= -z_5' \\
&= -g_{51}z_1 - g_{52}z_2 - g_{53}z_3 - g_{54}z_4 - g_{55}z_5 - g_{56}z_6 \\
&= -\xi\frac{I}{B}z_3 - \phi z_4 - \left(-\xi\frac{I}{B} - \sigma\left(\frac{EB}{\kappa+B} + HI\right) - \mu\right)z_5 + \sigma HVz_6 \\
&\le \xi\frac{I}{B}|z_3| - \phi|z_4| + \left(-\xi\frac{I}{B} - \sigma\left(\frac{EB}{\kappa+B} + HI\right) - \mu\right)|z_5| + \sigma HV|z_6| \\
&\le \sigma HV(|z_4| + |z_6|) + \left(-\sigma\left(\frac{EB}{\kappa+B} + HI\right) - \mu\right)|z_5| \\
&\le \left(-\sigma\left(\frac{EB}{\kappa+B} + HI\right) + \sigma HV - \mu\right)|z_5|
\end{aligned}
$$

Hence,

$$
\begin{aligned}
D_+\|z\| &\le (\sigma HV - \mu)\|z\| \\
&\le (HN - \mu)\|z\|.
\end{aligned}
\tag{61}
$$

(ii) $|z_5| < |z_4| + |z_6|$

Then $\|z\| = |z_4| + |z_6| = z_4 + z_6$ and $U_1(z) < |z_4| + |z_6|$. Taking the right-hand derivative we obtain,

$$
\begin{aligned}
D_+\|z\| &= z_4' + z_6' \\
&= (g_{41} + g_{61})z_1 + (g_{42} + g_{62})z_2 + (g_{43} + g_{63})z_3 + (g_{44} + g_{64})z_4 \\
&\quad + (g_{45} + g_{65})z_5 + (g_{46} + g_{66})z_6 \\
&= \xi\frac{I}{B}z_2 + (-\xi\frac{I}{B} - \phi - \mu)z_4 + \sigma\left(\frac{EB}{\kappa+B} + HI\right)z_5 + (\sigma HV - T - \xi\frac{I}{B})z_6 \\
&\le \xi\frac{I}{B}|z_2| + (-\xi\frac{I}{B} - \phi - \mu)|z_4| - \sigma\left(\frac{EB}{\kappa+B} + HI\right)|z_5| \\
&\quad + (\sigma HV - T - \xi\frac{I}{B})|z_6| \\
&\le (-\phi - \mu)|z_4| - \sigma\left(\frac{EB}{\kappa+B} + HI\right)|z_5| + (\sigma HV - T)|z_6| \\
&\le \max\{-\mu, \sigma HV - T\}(|z_4| + |z_6|)
\end{aligned}
$$

Hence,

$$
\begin{aligned}
D_+\|z\| &\le \max\{-\mu, \sigma HV - T\}\|z\| \\
&\le \max\{-\mu, HN - T\}\|z\|.
\end{aligned}
\tag{62}
$$

Case 8: $U_2(z) > U_1(z)$ and $z_4 < 0 < z_5, z_6$. Then $\|z\| = \max\{|z_4| + |z_6|, |z_5| + |z_6|\}$.

(i) $|z_4| > |z_5|$

Then $\|z\| = |z_4| + |z_6| = -z_4 + z_6$ and $U_1(z) < |z_4| + |z_6|$. Taking the right-hand derivative we obtain,

$$
\begin{aligned}
D_+\|z\| &= -z_4' + z_6' \\
&= (g_{61} - g_{41})z_1 + (g_{62} - g_{42})z_2 + (g_{63} - g_{43})z_3 + (g_{64} - g_{44})z_4 \\
&\quad + (g_{65} - g_{45})z_5 + (g_{66} - g_{46})z_6 \\
&= -\xi\tfrac{I}{B}z_2 - \left(-\xi\tfrac{I}{B} - 2\left(\tfrac{EB}{\kappa+B} + HI\right) - \phi - \mu\right)z_4 + \sigma\left(\tfrac{EB}{\kappa+B} + HI\right)z_5 \\
&\quad + (HS + H(S + \sigma V) - T - \xi\tfrac{I}{B})z_6 \\
&\leq \xi\tfrac{I}{B}|z_2| + \left(-\xi\tfrac{I}{B} - 2\left(\tfrac{EB}{\kappa+B} + HI\right) - \phi - \mu\right)|z_4| + \sigma\left(\tfrac{EB}{\kappa+B} + HI\right)|z_5| \\
&\quad + (HS + H(S + \sigma V) - T - \xi\tfrac{I}{B})|z_6| \\
&\leq \left(-2\left(\tfrac{EB}{\kappa+B} + HI\right) - \phi - \mu\right)|z_4| + \sigma\left(\tfrac{EB}{\kappa+B} + HI\right)|z_5| \\
&\quad + (HS + H(S + \sigma V) - T)|z_6| \\
&\leq \left((-2 + \sigma)\left(\tfrac{EB}{\kappa-B} + HI\right) - \phi - \mu\right)|z_4| + (HS + H(S + \sigma V) - T)|z_6| \\
&\leq \max\{-\mu, HS + H(S + \sigma V) - T\}(|z_4| + |z_6|)
\end{aligned}
$$

Hence,

$$
\begin{aligned}
D_+\|z\| &\leq \max\{-\mu, HS + H(S + \sigma V) - T\}\|z\| \\
&\leq \max\{-\mu, 2HN - T\}\|z\|.
\end{aligned}
\tag{63}
$$

(ii) $|z_4| < |z_5|$

Then $\|z\| = |z_5| + |z_6| = z_5 + z_6$ and $U_1(z) < |z_5| + |z_6|$. Taking the right-hand derivative we obtain,

$$
\begin{aligned}
D_+\|z\| &= z_5' + z_6' \\
&= (g_{51} + g_{61})z_1 + (g_{52} + g_{62})z_2 + (g_{53} + g_{63})z_3 + (g_{54} + g_{64})z_4 \\
&\quad + (g_{55} + g_{65})z_5 + (g_{56} + g_{66})z_6 \\
&= \xi\tfrac{I}{B}z_3 + \left(\phi + \left(\tfrac{EB}{\kappa+B} + HI\right)\right)z_4 + (-\xi\tfrac{I}{B} - \mu)z_5 + (HS - T - \xi\tfrac{I}{B})z_6 \\
&\leq \xi\tfrac{I}{B}|z_3| - \left(\phi + \left(\tfrac{EB}{\kappa+B} + HI\right)\right)|z_4| + (-\xi\tfrac{I}{B} - \mu)|z_5| \\
&\quad + (HS - T - \xi\tfrac{I}{B})|z_6| \\
&\leq -\left(\phi + \left(\tfrac{EB}{\kappa+B} + HI\right)\right)|z_4| - \mu|z_5| + (HS - T)|z_6| \\
&\leq -\mu|z_5| + (HS - T)|z_6| \\
&\leq \max\{-\mu, HS - T\}(|z_5| + |z_6|)
\end{aligned}
$$

Hence,

$$
\begin{aligned}
D_+\|z\| &\leq \max\{-\mu, HS - T\}\|z\| \\
&\leq \max\{-\mu, HN - T\}\|z\|.
\end{aligned}
\tag{64}
$$

We now summarize our results from the analysis above. To ensure $m(P) < 0$, from Cases $1 - 5$ we need

$$T - 2\mu < 0 ; \tag{65}$$

and from Cases $6 - 8$ we need

$$HN - \mu < 0 \quad \text{and} \quad 2HN - T < 0. \tag{66}$$

Using the condition (65), the inequalities in (66) yield

$$N < \min\left\{\frac{T}{2H}, \frac{\mu}{H}\right\} = \frac{T}{2H}. \tag{67}$$

Hence, we conclude from Theorem 11 that under the conditions (65) and (67), the endemic equilibrium of the model (1) - (4) with constant controls is globally asymptotically stable when $\mathcal{R}_0 > 1$; that is, the solution of the system will converge to the endemic equilibrium independent of the initial sizes of the sub-populations.

The existence of a stable endemic equilibrium when $\mathcal{R}_0 > 1$ is demonstrated in Figure 3. We set the total population as $N = 1,000$ and the model parameters in such a way that $\mathcal{R}_0 \approx 2.0$. We again pick different initial conditions $I(0) = 1$, 50, 100, 150, 200, and 250, conduct a numerical simulation for each, and plot the phase plane portrait of I vs. S for each case in Figure 3. We observe that all of these curves converge to the endemic equilibrium over time, a pattern that also takes place for various other initial conditions.

The focus of this study is to better understand the effects of different control strategies coupled with multiple transmission pathways of cholera. The mathematical model fully captures the epidemiology and pathogenesis of the disease and comprehensively explores the usefulness of public health control responses to cholera epidemics in resource constrained settings. The model consists of three types of public health controls: vaccination, treatment, and sanitation. Comprehensive mathematical analysis of the model using both analytical and numerical approaches is carried out and presented.

The mathematical results demonstrate that despite including vaccination in a framework that has previously shown backward bifurcation [37], our model does not exhibit such a phenomenon and retains $\mathcal{R}_0$ as an epidemic threshold governing the dynamics of the model system. This model shows that the unity of $\mathcal{R}_0$ as quantitative statistic to quantify the amount of control effort required to contain epidemic cholera is not compromised. Thus even with public health interventions, cholera epidemics
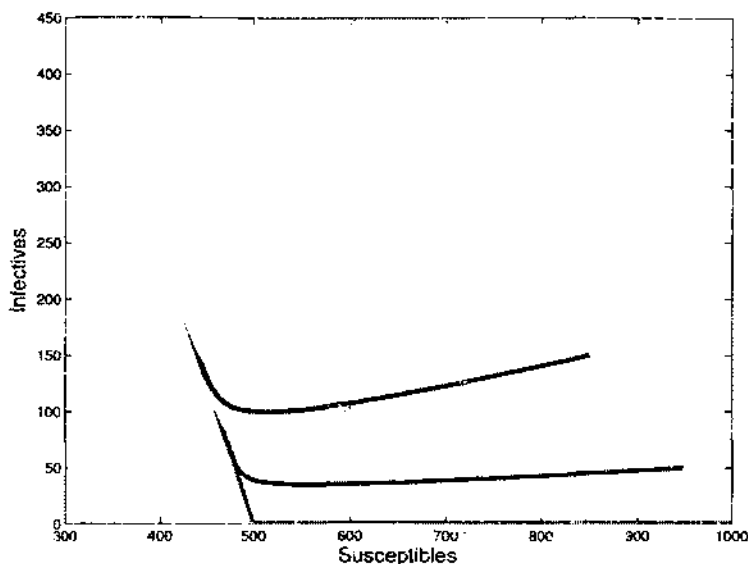
Figure 3. The phase portrait of I vs. S for the system (1) - (4) with parameters set such that $\mathcal{R}_0 \approx 2$. The curves correspond to six different initial conditions with $I(0) = 1, 50,$ 100, 150, 200, and 250. All of these curves converge to the endemic equilibrium where $S^* \approx 322.5$ and $I^* \approx 403.1$.

and endemism could still occur and the disease could persist, if the controls are not strong enough to reduce $\mathcal{R}_0$ to values below unity.

Effective control and eradication of cholera in the developing world remains a public health challenge because of the complex biological, epidemiological and environmental factors that contribute to the dynamics of the disease. The recognition of cholera burden combined with efforts to implement efficient control measures have become critical with the growing trends in cholera incidence in developing countries, and require a comprehensive and integrated strategy to implement public health control measures. The current study can be extended by a number of ways. Our model assumes that the vaccine efficacy σ and sanitation-induced preventability ρ are constants, whereas in reality both decrease after several months, thus time-dependent. Additionally, we have assumed that all the control measures, including vaccination, can be implemented from the very beginning of disease outbreak and carried out with constant strength throughout the course. It would be worthwhile to study disease dynamics with (more realistic) time-dependent control measures. Particularly, an optimal control study [23, 32, 33, 35, 39, 50] can be employed to seek the optimal balance between the gains and costs of the control measures.

CHAPTER 3

MULTI-GROUP CHOLERA MODEL

The effects of dispersal and movement among different spatial regions are critical in cholera dynamics. Disease transmission occurs through the interaction of infectious individuals amongst susceptible communities [19] and the circulation and spread of toxigenic vibrios in the aquatic environment [54]. Human hosts, symptomatic and asymptomatic, could potentially travel between susceptible communities spreading the disease. Additionally, vibrios in contaminated water may not be isolated to a certain water source. Indeed, infected individuals may shed the bacteria in multiple water sources. Furthermore, the movement of the bacteria within the aquatic environment could affect the reservoir of *V. cholerae* and spread the disease to other regions. Therefore, it is important to study disease transmission within and between different groups, investigating the movement of infected human hosts and the pathogen from one region to another.

A heterogeneous population whose individuals are distinguishable by some factor can be divided into n homogeneous compartments [64]. In general, for epidemic models, individuals are grouped into compartments according to stage of the disease or spatial position. For example, in an SIR model, the population is divided into susceptible, infected and recovered compartments. Furthermore, in a multi-group SIR model, spatial position is considered in addition to stage of the disease when generating compartments. The total population N is divided into n distinct groups each partitioned into a susceptible compartment S, an infected compartment I, and a recovered compartment R, where the population in each group is given by $N_i = S_i + I_i + R_i$, for $i = 1, \ldots, n$. Once an infected individual enters the recovered compartment, the newly recovered individual no longer influences the dynamics of the system. Also, since $R_i = N_i - S_i - I_i$, we can ignore the recovered compartment completely from each group. The pathogen concentration in the contaminated water is denoted by B_i for each group $i = 1, \ldots, n$.

The incidence function is given in the form $\sum_{j=1}^{n} f_j(I_j, B_j)$, where susceptible

individuals can be infected either by interacting with infected individuals (human-to-human direct transmission) or by ingesting contaminated water (environment-to-human indirect transmission). The rate of change for the pathogen concentration in each group is denoted by the function $h_i(I_i, B_i)$ for $i = 1, \ldots, n$.

Based on these conditions and building on the cholera model in [65] (reproduced in Appendix A), a general multi-group model can be formulated as the following system

$$\frac{dS_i}{dt} = bN_i - \sum_{j=1}^{n} S_i f_j(I_j, B_j) - bS_i , \tag{68}$$

$$\frac{dI_i}{dt} = \sum_{j=1}^{n} S_i f_j(I_j, B_j) - (\gamma_i + b)I_i , \qquad i = 1, \ldots, n \tag{69}$$

$$\frac{dB_i}{dt} = h_i(I_i, B_i) , \tag{70}$$

where the parameter b represents the natural human birth and death rate and γ_i represents the rate of recovery from cholera in each group. We assume that $f_i(I_i, B_i)$ and $h_i(I_i, B_i)$ satisfy the following biologically sensible properties for $i = 1, \ldots, n$:

(M-1) $f_i(0,0) = h_i(0,0) = 0$.

(M-2) $f_i(I_i, B_i) \geq 0$ and f_i only vanishes at $(0,0)$.

(M-3)
$$\frac{\partial f_i}{\partial I_i}(I_i, B_i) \geq 0 , \quad \frac{\partial f_i}{\partial B_i}(I_i, B_i) \geq 0 , \quad \frac{\partial h_i}{\partial I_i}(I_i, B_i) \geq 0 , \quad \frac{\partial h_i}{\partial B_i}(I_i, B_i) \leq 0 .$$

(M-4) $f_i(I_i, B_i)$ and $h_i(I_i, B_i)$ are both concave; i.e. the matrices

$$D^2 f_i = \begin{bmatrix} \frac{\partial^2 f_i}{\partial I_i^2} & \frac{\partial^2 f_i}{\partial I_i \partial B_i} \\ \frac{\partial^2 f_i}{\partial I_i \partial B_i} & \frac{\partial^2 f_i}{\partial B_i^2} \end{bmatrix} \quad \text{and} \quad D^2 h_i = \begin{bmatrix} \frac{\partial^2 h_i}{\partial I_i^2} & \frac{\partial^2 h_i}{\partial I_i \partial B_i} \\ \frac{\partial^2 h_i}{\partial I_i \partial B_i} & \frac{\partial^2 h_i}{\partial B_i^2} \end{bmatrix}$$

are negative semidefinite everywhere.

It follows from assumption (M-1) that the model admits a unique disease-free equilibrium (DFE), denoted by

$$X_0 = (S_1^0, I_1^0, B_1^0, \ldots, S_n^0, I_n^0, B_n^0) = (N_1, 0, 0, \ldots, N_n, 0, 0) , \tag{71}$$

and assumption (M-2) guarantees a non-negative force of infection. The inequalities in (M-3) respectively state that the rate of new infection increases with rises in

infected population size or bacterial concentration, increased infected population also leads to a higher growth rate for the pathogen, and the infective vibrio cannot independently thrive in the absence of replenishment of their numbers in the inflow of contaminated sewage [15]. Finally, assumption (M-4) is based on the saturation effect. We mention that another multi-group cholera model was recently proposed in [58], yet our model is more general in both the incidence representation and the pathogen dynamics

Assumption (M-4) implies that the surfaces $h_i = h_i(I_i, B_i)$ are below their tangent planes at any points $(I_{i_0}, B_{i_0}) \geq 0$; i.e.

$$h_i(I_i, B_i) \leq h_i(I_{i_0}, B_{i_0}) + \frac{\partial h_i}{\partial I_i}(I_{i_0}, B_{i_0})(I_i - I_{i_0}) + \frac{\partial h_i}{\partial B_i}(I_{i_0}, B_{i_0})(B_i - B_{i_0}).$$

In particular, setting $(I_{i_0}, B_{i_0}) = (0, 0)$ and using assumption (M-1), equation (70) yields

$$\frac{dB_i}{dt} = h_i(I_i, B_i) \leq \frac{\partial h_i}{\partial I_i}(0, 0)I_i + \frac{\partial h_i}{\partial B_i}(0, 0)B_i \leq \frac{\partial h_i}{\partial I_i}(0, 0)N_i + \frac{\partial h_i}{\partial B_i}(0, 0)B_i \,,$$

which implies that for any initial values $B_{i_0} \leq \omega_i N_i$,

$$0 \leq B_i(t, B_{i_0}) \leq \omega_i N_i \qquad \text{with} \qquad \omega_i = -\frac{(\partial h_i/\partial I_i)(0, 0)}{(\partial h_i/\partial B_i)(0, 0)} \,.$$

Therefore, the feasible region is given by

$$\Gamma = \left\{ (S_1, I_1, B_1, \ldots, S_n, I_n, B_n) \in \mathbb{R}^{3n} \middle| 0 \leq S_i + I_i \leq N_i, 0 \leq B_i \leq \omega_i N_i, 1 \leq i \leq n \right\} \tag{72}$$

and it is positively invariant in $\mathbb{R}^{3n}$.

3.1 BASIC REPRODUCTION NUMBER

Following the next-generation matrix theory [64], the basic reproduction number, $\mathcal{R}_0$, is mathematically defined as the spectral radius of the next-generation matrix. In order to determine the next-generation matrix of our model, we first consider the compartmentalized infectious subsystem:

$$\begin{bmatrix} dI_1/dt \\ \vdots \\ dI_n/dt \\ dB_1/dt \\ \vdots \\ dB_n/dt \end{bmatrix} = \begin{bmatrix} \sum_{i=1}^n S_1 f_i(I_i, B_i) \\ \vdots \\ \sum_{i=1}^n S_n f_i(I_i, B_i) \\ 0 \\ \vdots \\ 0 \end{bmatrix} - \begin{bmatrix} (\gamma_1 + b)I_1 \\ \vdots \\ (\gamma_n + b)I_n \\ -h_1(I_1, B_1) \\ \vdots \\ -h_n(I_n, B_n) \end{bmatrix} = \mathcal{F} - \mathcal{V} . \tag{73}$$

For convenience, let

$$\frac{\partial f_i}{\partial I_i}(0,0) \equiv p_i , \qquad \frac{\partial f_i}{\partial B_i}(0,0) \equiv q_i , \qquad \frac{\partial h_i}{\partial I_i}(0,0) \equiv r_i , \qquad \frac{\partial h_i}{\partial B_i}(0,0) \equiv u_i ,$$

for $i = 1, \ldots, n$. Then, the $2n \times 2n$ Jacobian matrices evaluated at X_0, the disease-free equilibrium, are given by

$$F = D\mathcal{F}(X_0) = \begin{bmatrix} N_1 p_1 & \cdots & N_1 p_n & N_1 q_1 & \cdots & N_1 q_n \\ \vdots & \ddots & \vdots & \vdots & \ddots & \vdots \\ N_n p_1 & \cdots & N_n p_n & N_n q_1 & \cdots & N_n q_n \\ 0 & \cdots & 0 & 0 & \cdots & 0 \\ \vdots & \ddots & \vdots & \vdots & \ddots & \vdots \\ 0 & \cdots & 0 & 0 & \cdots & 0 \end{bmatrix} , \tag{74}$$

and

$$V = D\mathcal{V}(X_0) = \begin{bmatrix} \gamma_1 + b & 0 & \cdots & \cdots & \cdots & \cdots & \cdots & \cdots & \cdots & 0 \\ 0 & \gamma_2 + b & 0 & \cdots & \cdots & \cdots & \cdots & \cdots & \cdots & 0 \\ \vdots & \ddots & \ddots & \ddots & \cdots & \cdots & \cdots & \cdots & & \vdots \\ \vdots & \ddots & \ddots & \ddots & \ddots & \cdots & \cdots & \cdots & & \vdots \\ 0 & \cdots & \cdots & 0 & \gamma_n + b & 0 & \cdots & \cdots & \cdots & 0 \\ -r_1 & 0 & \cdots & \cdots & 0 & -u_1 & 0 & \cdots & \cdots & 0 \\ 0 & -r_2 & 0 & \cdots & \cdots & 0 & -u_2 & 0 & \cdots & 0 \\ \vdots & \ddots & \ddots & \ddots & \cdots & \ddots & \ddots & \ddots & \ddots & \vdots \\ \vdots & \cdots & \ddots & \ddots & \ddots & \cdots & \ddots & \ddots & \ddots & 0 \\ 0 & \cdots & \cdots & 0 & -r_n & 0 & \cdots & \cdots & 0 & -u_n \end{bmatrix} . \tag{75}$$

Hence, the next-generation matrix is defined as

$$FV^{-1} = \begin{bmatrix} C & D \\ 0 & 0 \end{bmatrix} , \tag{76}$$

where

$$C = \begin{bmatrix} \frac{N_1}{\gamma_1 + b}\left(p_1 - \frac{q_1 r_1}{u_1}\right) & \cdots & \frac{N_1}{\gamma_n + b}\left(p_n - \frac{q_n r_n}{u_n}\right) \\ \frac{N_2}{\gamma_1 + b}\left(p_1 - \frac{q_1 r_1}{u_1}\right) & \cdots & \frac{N_2}{\gamma_n + b}\left(p_n - \frac{q_n r_n}{u_n}\right) \\ \vdots & \vdots & \vdots \\ \frac{N_n}{\gamma_1 + b}\left(p_1 - \frac{q_1 r_1}{u_1}\right) & \cdots & \frac{N_n}{\gamma_n + b}\left(p_n - \frac{q_n r_n}{u_n}\right) \end{bmatrix}$$

and

$$D = \begin{bmatrix} -N_1\frac{q_1}{u_1} & \cdots & -N_1\frac{q_n}{u_n} \\ -N_2\frac{q_1}{u_1} & \cdots & -N_2\frac{q_n}{u_n} \\ \vdots & \vdots & \vdots \\ -N_n\frac{q_1}{u_1} & \cdots & -N_n\frac{q_n}{u_n} \end{bmatrix}$$

are both matrices of dimension $n \times n$.

To find the spectral radius of FV^{-1}, we proceed to determine its characteristic equation. For convenience, let

$$A_k = \frac{1}{\gamma_k + b}\left(p_k - \frac{q_k r_k}{u_k}\right).$$

Then,

$$\det(\lambda I - FV^{-1}) = \lambda^n \begin{vmatrix} \lambda - N_1 A_1 & \cdots & -N_1 A_n \\ \vdots & \ddots & \vdots \\ -N_n A_1 & \cdots & \lambda - N_n A_n \end{vmatrix}.$$

Denote

$$X_1 = \begin{bmatrix} N_1 A_1 & N_1 A_2 & \cdots & N_1 A_n \\ N_2 A_1 & N_2 A_2 & \cdots & N_2 A_n \\ \vdots & \vdots & \ddots & \vdots \\ N_n A_1 & N_n A_2 & \cdots & N_n A_n \end{bmatrix}.$$

We claim:

$$\det(\lambda I - FV^{-1}) = \lambda^{2n-1}\left(\lambda - \sum_{i=1}^{n} N_i A_i\right), \tag{77}$$

or, equivalently,

$$\det(\lambda I - X_1) = \lambda^{n-1}\left(\lambda - \sum_{i=1}^{n} N_i A_i\right).$$

Proof. We prove the claim by induction. When $n = 2$, it can be easily verified that equation (77) holds. Now, assume that equation (77) is true for n. Let us test the case $n + 1$. Then, we have

$$\det(\lambda I - FV^{-1}) = \lambda^{n+1}\det(\lambda I - X_1)$$

$$= \lambda^{n+1} \begin{vmatrix} \lambda - N_1 A_1 & \cdots & -N_1 A_n & -N_1 A_{n+1} \\ \vdots & \ddots & \vdots & \vdots \\ -N_n A_1 & \cdots & \lambda - N_n A_n & -N_n A_{n+1} \\ -N_{n+1} A_1 & \cdots & -N_{n+1} A_n & \lambda - N_{n+1} A_{n+1} \end{vmatrix}.$$

Let us split up the last column so that the determinant can be written as the sum of two determinants; i.e., let

$$
\det(\lambda I - X_1) = \begin{vmatrix} \lambda - N_1 A_1 & \cdots & -N_1 A_n & 0 \\ \vdots & \ddots & \vdots & \vdots \\ -N_n A_1 & \cdots & \lambda - N_n A_n & 0 \\ -N_{n+1} A_1 & \cdots & -N_{n+1} A_n & \lambda \end{vmatrix}
$$

$$
+ \begin{vmatrix} \lambda - N_1 A_1 & \cdots & -N_1 A_n & -N_1 A_{n+1} \\ \vdots & \ddots & \vdots & \vdots \\ -N_n A_1 & \cdots & \lambda - N_n A_n & -N_n A_{n+1} \\ -N_{n+1} A_1 & \cdots & -N_{n+1} A_n & -N_{n+1} A_{n+1} \end{vmatrix}
$$

$$
= |Y_1| + |Z_1| .
$$

From our assumption on n, it is clear that the first determinant is the following

$$
|Y_1| = \lambda \left[\lambda^{n-1} \left(\lambda - \sum_{i=1}^{n} N_i A_i \right) \right] = \lambda^n \left(\lambda - \sum_{i=1}^{n} N_i A_i \right) .
$$

For the second determinant $|Z_1|$, note that the following elementary row operation $\left(C_i \leftarrow C_i - (A_i/A_{n+1}) \cdot C_{n+1} \right)$, $i = 1, \ldots, n$, yields

$$
\begin{vmatrix} \lambda & \cdot & 0 & -N_1 A_{n+1} \\ \vdots & \ddots & \vdots & \vdots \\ 0 & \cdots & \lambda & -N_n A_{n+1} \\ 0 & \cdots & 0 & -N_{n+1} A_{n+1} \end{vmatrix} = \lambda^{n-1} \begin{vmatrix} \lambda & -N_n A_{n+1} \\ 0 & -N_{n+1} A_{n+1} \end{vmatrix} = -\lambda^n N_{n+1} A_{n+1} .
$$

Therefore,

$$
\det(\lambda I - X_1) = |Y_1| + |Z_1| = \lambda^n \left(\lambda - \sum_{i=1}^{n} N_i A_i \right) - \lambda^n N_{n+1} A_{n+1} = \lambda^n \left(\lambda - \sum_{i=1}^{n+1} N_i A_i \right) .
$$

Thus,

$$
\det(\lambda I - FV^{-1}) = \lambda^{2(n+1)-1} \left(\lambda - \sum_{i=1}^{n+1} N_i A_i \right) ,
$$

and the claim holds. $\qquad \square$

Hence, the basic reproduction number is given by

$$\mathcal{R}_0 = \rho(FV^{-1}) = \sum_{i=1}^{n} \frac{N_i}{\gamma_i + b} \left(p_i - \frac{q_i r_i}{u_i} \right)$$

$$= \sum_{i=1}^{n} \frac{N_i}{\gamma_i + b} \left\{ \frac{\partial f_i}{\partial I_i}(0,0) - \frac{\partial f_i}{\partial B_i}(0,0) \left(\frac{\partial h_i}{\partial B_i}(0,0) \right)^{-1} \frac{\partial h_i}{\partial I_i}(0,0) \right\}.$$

$$\text{(78)}$$

Note that $\frac{\partial h_i}{\partial B_i} \le 0$ from assumption (M-3). Equation (78) clearly shows that the basic reproduction number $\mathcal{R}_0$ for the entire system is the summation of individual reproduction numbers from all the n groups. Within each group, the reproduction number consists of two parts: one is the contribution from the direct (or, human-to-human) transmission $\frac{N_i}{\gamma_i + b} \frac{\partial f_i}{\partial I_i}(0,0)$; the other is the contribution from the indirect (or, environment-to-human) transmission, $\frac{N_i}{\gamma_i + b} \frac{\partial f_i}{\partial B_i}(0,0) \left(-\frac{\partial h_i}{\partial B_i}(0,0) \right)^{-1} \frac{\partial h_i}{\partial I_i}(0,0)$.

Based on the work of [64], we immediately obtain the following result regarding the local stability of the disease-free equilibrium.

Theorem 12. *Let $\mathcal{R}_0$ be defined as in equation (78), Then the disease-free equilibrium X_0 of the system (68) - (70) is locally asymptotically stable if $\mathcal{R}_0 < 1$, and unstable if $\mathcal{R}_0 > 1$.*

3.2 STABILITY ANALYSIS OF DISEASE-FREE EQUILIBRIUM

Indeed, we can establish a stronger result regarding the stability of the disease-free equilibrium. We prove global stability by constructing a Lyapunov function and utilizing LaSalle's Invariance Principle [38].

Lemma 13. *Assume (M-1) - (M-4). If $\mathcal{R}_0 \le 1$, then the disease-free equilibrium X_0 is globally asymptotically stable in Γ. Additionally, if $\mathcal{R}_0 > 1$, the system (68) - (70) is uniformly persistent.*

Proof. Let

$$\begin{bmatrix} w_1 & \cdots & w_n & w_{n+1} & \cdots & w_{2n} \end{bmatrix} = \begin{bmatrix} p_1 & \cdots & p_n & q_1 & \cdots & q_n \end{bmatrix} V^{-1}. \quad \text{(79)}$$

Since V is a nonsingular M-matrix, then $V^{-1} \ge 0$ [6], and it follows that $w_i \ge 0$ for all $i = 1, \ldots, 2n$. Also, note that

$$\sum_{i=1}^{n} N_i w_i \equiv \mathcal{R}_0. \quad \text{(80)}$$

Let us construct a Lyapunov function

$$L = w_1 I_1 + \cdots + w_n I_n + w_{n+1} B_1 + \cdots + w_{2n} B_n . \tag{81}$$

Differentiating L along the solutions of the system (68) - (70) yields the following

$$L' = w_1 \frac{dI_1}{dt} + \cdots + w_n \frac{dI_n}{dt} + w_{n+1} \frac{dB_1}{dt} + \cdots + w_{2n} \frac{dB_n}{dt}$$

$$= w_1 \left(\sum_{j=1}^{n} S_1 f_j(I_j, B_j) - (\gamma_1 + b) I_1 \right) + \cdots + w_n \left(\sum_{j=1}^{n} S_n f_j(I_j, B_j) - (\gamma_n + b) I_n \right)$$

$$+ w_{n+1} h_1(I_1, B_1) + \cdots + w_{2n} h_n(I_n, B_n) .$$

From assumption (M-4) and (M-1), it follows that

$$L' \leq w_1 \left(\sum_{j=1}^{n} N_1 \{p_j I_j + q_j B_j\} - (\gamma_1 + b) I_1 \right) + \cdots$$

$$+ w_n \left(\sum_{j=1}^{n} N_n \{p_j I_j + q_j B_j\} - (\gamma_n + b) I_n \right) + w_{n+1}(r_1 i_1 + u_1 B_1) + \cdots$$

$$+ w_{2n}(r_n I_n + u_n B_n)$$

$$= \sum_{i=1}^{n} N_i w_i \begin{bmatrix} p_1 & \cdots & p_n & q_1 & \cdot & \cdot & q_n \end{bmatrix} \begin{bmatrix} I_1 \\ \vdots \\ I_n \\ B_1 \\ \vdots \\ B_n \end{bmatrix}$$

$$- \begin{bmatrix} w_1 & \cdots & w_n & w_{n+1} & \cdots & w_{2n} \end{bmatrix} V \begin{bmatrix} I_1 \\ \vdots \\ I_n \\ B_1 \\ \vdots \\ B_n \end{bmatrix} .$$

Further, from equation (79), we obtain

$$L' \leq \sum_{i=1}^{n} N_i w_i \begin{bmatrix} p_1 & \cdots & p_n & q_1 & \cdots & q_n \end{bmatrix} \begin{bmatrix} I_1 \\ \vdots \\ I_n \\ B_1 \\ \vdots \\ B_n \end{bmatrix}$$

$$- \begin{bmatrix} p_1 & \cdots & p_n & q_1 & \cdots & q_n \end{bmatrix} \begin{bmatrix} I_1 \\ \vdots \\ I_n \\ B_1 \\ \vdots \\ B_n \end{bmatrix}.$$

That is,

$$L' \leq \left\{ \left(\sum_{i=1}^{n} N_i w_i \right) - 1 \right\} \begin{bmatrix} p_1 & \cdots & p_n & q_1 & \cdots & q_n \end{bmatrix} \begin{bmatrix} I_1 \\ \vdots \\ I_n \\ B_1 \\ \vdots \\ B_n \end{bmatrix}$$

$$= (\mathcal{R}_0 - 1) \begin{bmatrix} p_1 & \cdots & p_n & q_1 & \cdots & q_n \end{bmatrix} \begin{bmatrix} I_1 \\ \vdots \\ I_n \\ B_1 \\ \cdot \\ B_n \end{bmatrix}.$$

(82)

Now, note that $L' = 0$ if and only if either

(a) $\mathcal{R}_0 < 1$ and $I_1 = B_1 = \cdots = I_n = B_n = 0$, or

(b) $\mathcal{R}_0 = 1$ and $S_i = N_i$ for $i = 1, \ldots, n$.

Let K be the largest compact invariant subset of

$$G = \left\{ (S_1, I_1, B_1, \ldots, S_n, I_n, B_n) \in \Gamma \mid L' = 0 \right\}.$$

In Case (a), each solution in K satisfies $S_i' = bN_i - bS_i$ for $i = 1, \ldots, n$, and obviously the solution converges to $S_i = N_i$ for $i = 1, \ldots, n$. In Case (b), note that $S_i = N_i$ satisfies

$$S_i' = bN_i - \sum_{j=1}^{n} S_i f_j(I_j, B_j) - bS_i$$

which implies

$$\sum_{j=1}^{n} f_j(I_j, B_j) = 0.$$

Hence, from assumption (M-2), it is obvious that $I_1 = B_1 = \cdots = I_n = B_n = 0$. Therefore, all solutions in Γ converge to the disease-free equilibrium; that is, the largest compact invariant set where $L' = 0$ is the singleton $\{X_0\}$. By LaSalle's Invariance Principle, X_0 is globally asymptotically stable in Γ if $\mathcal{R}_0 \leq 1$.

If $\mathcal{R}_0 > 1$, then $L' > 0$ in a neighborhood of X_0 in the interior of Γ. Thus, solutions in the interior of Γ sufficiently close to X_0 move away from X_0, implying that X_0 is unstable. Consequently, the instability of X_0 (which is on the boundary of the domain Γ) implies uniform persistence of the system [22]. $\qquad\square$

3.3 EXISTENCE AND UNIQUENESS OF THE ENDEMIC EQUILIBRIUM

The dynamics of the system (68) - (70) when $\mathcal{R}_0 < 1$ have been completely described by Theorem 12 and Lemma 13. Now, we conduct an endemic analysis when $\mathcal{R}_0 > 1$. The following theorem shows the existence and uniqueness of the endemic equilibrium.

Theorem 14. *For the system* (68) *-* (70), *if* $\mathcal{R}_0 > 1$, *there exists a unique positive endemic equilibrium, and if* $\mathcal{R}_0 < 1$, *there is no positive endemic equilibrium.*

Proof. Under assumption (M-3), the equation $h_i(I_i, B_i) = 0$ implicitly defines a function $B_i = g_i(I_i)$ with $g_i'(I_i) \geq 0$, for $i = 1, \cdots, n$. In addition, differentiating $h_i(I_i, B_i) = 0$ twice with respect to I_i yields

$$\begin{bmatrix} 1, & g_i'(I_i) \end{bmatrix} \begin{bmatrix} \frac{\partial^2 h_i}{\partial I_i^2} & \frac{\partial^2 h_i}{\partial I_i \partial B_i} \\ \frac{\partial^2 h_i}{\partial I_i \partial B_i} & \frac{\partial^2 h_i}{\partial B_i^2} \end{bmatrix} \begin{bmatrix} 1 \\ g'(I_i) \end{bmatrix} + \frac{\partial h_i}{\partial B_i} g_i''(I_i) = 0.$$

Using assumption (M-4), we can readily see that $g_i''(I_i) \leq 0$, for $i = 1, \cdots, n$.

Then, setting the right-hand sides of equations (68) - (70) to zero, we obtain

$$S_k = \frac{bN_k}{b + \sum_{i=1}^{n} f_i(I_i, g_i(I_i))}, \tag{83}$$

$$I_k = \frac{bN_k}{\gamma_k + b} \left\{ \frac{\sum_{i=1}^{n} f_i(I_i, g_i(I_i))}{b + \sum_{i=1}^{n} f_i(I_i, g_i(I_i))} \right\}, \tag{84}$$

$$B_k = g_k(I_k). \tag{85}$$

In particular, from equation (84), it follows that

$$\frac{I_k}{I_1} = \frac{bN_k}{\gamma_k + b} \cdot \frac{\gamma_1 + b}{bN_1} = \frac{\gamma_1 + b}{\gamma_k + b} \cdot \frac{N_k}{N_1}, \qquad k = 1, \ldots, n,$$

implying that

$$I_k = \frac{\gamma_1 + b}{\gamma_k + b} \cdot \frac{N_k}{N_1} \cdot I_1 \equiv c_k \cdot I_1, \qquad k = 1, \ldots, n. \tag{86}$$

Note that $c_k > 0$ and thus $I_1 > 0$ implies that $I_k > 0$ for all $k = 1, \ldots, n$. Also, it is clear that $c_1 \equiv 1$.

Let us define the following

$$H(I_1) \equiv I_1 = \frac{bN_1}{\gamma_1 + b} \left\{ \frac{\sum_{i=1}^{n} f_i(c_i I_1, g_i(c_i I_1))}{b + \sum_{i=1}^{n} f_i(c_i I_1, g_i(c_i I_1))} \right\}. \tag{87}$$

Note that $H(0) = 0$ and $H(I_1) \geq 0$ for all $I_k \geq 0$ with $k = 1, \ldots, n$. Denote

$$P_i(I_1) \equiv f_i(c_i I_1, g_i(c_i I_1)) \quad i = 1, \ldots, n.$$

Then we have,

$$H(I_1) = \frac{bN_1}{\gamma_1 + b} \left\{ \frac{P_1(I_1) + P_2(I_1) + \cdots + P_n(I_1)}{b + P_1(I_1) + P_2(I_1) + \cdots + P_n(I_1)} \right\}, \tag{88}$$

and taking the derivative we find that

$$H'(I_1) = \frac{bN_1}{\gamma_1 + b} \left\{ \frac{b(P_1'(I_1) + P_2'(I_1) + \cdots + P_n'(I_1))}{(b + P_1(I_1) + P_2(I_1) + \cdots P_n(I_1))^2} \right\} \tag{89}$$

where

$$P_k'(I_1) = c_k \left\{ \frac{\partial f_k}{\partial I_k}(c_k I_1, g_k(c_k I_1)) + \frac{\partial f_k}{\partial B_k}(c_k I_1, g_k(c_k I_1)) \cdot g_k'(c_k I_1) \right\} \geq 0. \tag{90}$$

for $k = 1, \ldots, n$. Therefore, $H'(I_1) \geq 0$ for $I_1 \geq 0$. In particular, note that

$$
\begin{aligned}
H'(0) &= \frac{N_1}{\gamma_1 + b}(P_1'(0) + P_2'(0) + \cdots + P_n'(0)) \\
&= \frac{N_1}{\gamma_1 + b}\left\{\sum_{k=1}^{n} c_k\left(\frac{\partial f_k}{\partial I_k}(0,0) + \frac{\partial f_k}{\partial B_k}(0,0)\cdot g_k'(0)\right)\right\} \\
&= \frac{N_1}{\gamma_1 + b}\left\{\sum_{k=1}^{n} \frac{\gamma_1 + b}{\gamma_k + b}\cdot\frac{N_k}{N_1}\left(\frac{\partial f_k}{\partial I_k}(0,0) + \frac{\partial f_k}{\partial B_k}(0,0)\cdot g_k'(0)\right)\right\} \\
&= \frac{N_1}{\gamma_1 + b}\left\{\frac{\partial f_1}{\partial I_1}(0,0) + \frac{\partial f_1}{\partial B_1}(0,0)\cdot g_1'(0)\right\} \\
&\quad + \frac{N_1}{\gamma_1 + b}\left(\frac{\gamma_1 + b}{\gamma_2 + b}\cdot\frac{N_2}{N_1}\right)\left\{\frac{\partial f_2}{\partial I_2}(0,0) + \frac{\partial f_2}{\partial B_2}(0,0)\cdot g_2'(0)\right\} \\
&\quad + \cdots + \frac{N_1}{\gamma_1 + b}\left(\frac{\gamma_1 + b}{\gamma_n + b}\cdot\frac{N_n}{N_1}\right)\left\{\frac{\partial f_n}{\partial I_n}(0,0) + \frac{\partial f_n}{\partial B_n}(0,0)\cdot g_n'(0)\right\} \\
&= \frac{N_1}{\gamma_1 + b}\left\{\frac{\partial f_1}{\partial I_1}(0,0) + \frac{\partial f_1}{\partial B_1}(0,0)\cdot g_1'(0)\right\} \\
&\quad + \frac{N_2}{\gamma_2 + b}\left\{\frac{\partial f_2}{\partial I_2}(0,0) + \frac{\partial f_2}{\partial B_2}(0,0)\cdot g_2'(0)\right\} \\
&\quad + \cdots + \frac{N_n}{\gamma_n + b}\left\{\frac{\partial f_n}{\partial I_n}(0,0) + \frac{\partial f_n}{\partial B_n}(0,0)\cdot g_n'(0)\right\} \\
&= \sum_{k=1}^{n}\frac{N_k}{\gamma_k + b}\left\{\frac{\partial f_k}{\partial I_k}(0,0) + \frac{\partial f_k}{\partial B_k}(0,0)\cdot g_k'(0)\right\} \\
&= \mathcal{R}_0.
\end{aligned}
\tag{91}
$$

Next, we have

$$
H''(I_1) = \frac{b^2 N_1}{\gamma_1 + b}\left\{\frac{\sum_{i=1}^{n} P_i''(I_1)(b + \sum_{i=1}^{n} P_i(I_1)) - 2(\sum_{i=1}^{n} P_i'(I_1))^2}{(b + \sum_{i=1}^{n} P_i(I_1))^3}\right\}
\tag{92}
$$

where

$$
\begin{aligned}
P_k''(I_1) &= c_k^2\left\{\frac{\partial^2 f_k}{\partial I_k^2}(c_k I_1, g_k(c_k I_1)) + 2\cdot g_k'(c_k I_1)\cdot\frac{\partial^2 f_k}{\partial I_k \partial B_k}(c_k I_1, g_k(c_k I_1))\right. \\
&\quad \left. + (g_k'(c_k I_1))^2\cdot\frac{\partial^2 f_k}{\partial B_k^2}(c_k I_1, g_k(c_k I_1)) + \frac{\partial f_k}{\partial B_k}(c_k I_1, g_k(c_k I_1))\cdot g_k''(c_k I_1)\right\} \\
&= c_k^2\begin{bmatrix} 1 & g_k'(c_k I_1) \end{bmatrix}\begin{bmatrix} \frac{\partial^2 f_k}{\partial I_k^2}(c_k I_1, g_k(c_k I_1)) & \frac{\partial^2 f_k}{\partial I_k \partial B_k}(c_k I_1, g_k(c_k I_1)) \\ \frac{\partial^2 f_k}{\partial I_k \partial B_k}(c_k I_1, g_k(c_k I_1)) & \frac{\partial^2 f_k}{\partial B_k^2}(c_k I_1, g_k(c_k I_1)) \end{bmatrix}\begin{bmatrix} 1 \\ g_k'(c_k I_1) \end{bmatrix} \\
&\quad + c_k^2\cdot\frac{\partial f_k}{\partial B_k}\cdot g_k''(c_k I_1)
\end{aligned}
\tag{93}
$$

for $k = 1, \ldots n$. From assumption (M-4) and the fact $g_k''(I_k) \leq 0$, it follows that $P_k''(I_1) \leq 0$ for $k = 1, \ldots, n$. And therefore, $H''(I_1) \leq 0$ for $I_1 \geq 0$. That is, the function $H(I_1)$ is increasing and concave on $(0, \infty)$ with $H'(0) = R_0$. If $H'(0) = \mathcal{R}_0 > 1$, there is a unique positive fixed point I_1^* for $H(I_1)$, and thus, from equation (86), unique positive fixed points $I_2^*, \ldots, I_n^*$. Furthermore, with $I_k > 0$ for $k = 1, \ldots, n$ and equations (83) and (85), it follows that there exists a unique endemic equilibrium denoted by

$$X^* = (S_1^*, I_1^*, B_1^*, \ldots, S_n^*, I_n^*, B_n^*). \tag{94}$$

In contrast, if $H'(0) = \mathcal{R}_0 < 1$, there is no positive fixed point for $H(I_1)$ and thus no endemic equilibrium. $\qquad\square$

3.4 GLOBAL STABILITY OF THE ENDEMIC EQUILIBRIUM

We proceed to show the global asymptotic stability of the endemic equilibrium. By Theorem 14, the endemic equilibrium $X^* = (S_1^*, I_1^*, B_1^*, \ldots, S_n^*, I_n^*, B_n^*)$ exists and is unique when $\mathcal{R}_0 > 1$. Note that $S_1^*, I_1^*, B_1^*, \ldots, S_n^*, I_n^*, B_n^*$ are positive and satisfy the following equilibrium equations:

$$bN_k = \sum_{j=1}^{n} S_k^* f_j(I_j^*, B_j^*) + bS_k^*, \tag{95}$$

$$(\gamma_k + b) = \sum_{j=1}^{n} S_k^* f_j(I_j^*, B_j^*) \cdot \frac{1}{I_k^*}, \tag{96}$$

$$h_k(I_k^*, B_k^*) = 0, \tag{97}$$

for $k = 1, \ldots, n$.

To study the endemic global dynamics, we introduce another assumption here. We assume that the solutions to the system (68) - (70) implicitly define a function $B_j = B_j(I_j)$ with $B_j'(I_j) \geq 0$ and $B_j''(I_j) \leq 0$, for $j = 1, \cdots, n$. Biologically, this means that the bacterial concentration in the aquatic environment will increase with the rise of the infected human population, but the rate of the increase will slow down when the infected population is high due to saturation. Let us denote

$$Q_j(I_j) = f_j(I_j, B_j(I_j)), \qquad j = 1, \cdots, n.$$

Then we have

$$Q_j'(I_j) = \frac{\partial f_j}{\partial I_j} + \frac{\partial f_j}{\partial B_j} B_j'(I_j) \geq 0, \tag{98}$$

and·

$$Q_j''(I_j) = \begin{bmatrix} 1, & B_j'(I_j) \end{bmatrix} \begin{bmatrix} \frac{\partial^2 f_j}{\partial I_j^2} & \frac{\partial^2 f_j}{\partial I_j \partial B_j} \\ \frac{\partial^2 f_j}{\partial I_j \partial B_j} & \frac{\partial^2 f_j}{\partial B_j^2} \end{bmatrix} \begin{bmatrix} 1 \\ B_j'(I_j) \end{bmatrix} + \frac{\partial f_j}{\partial B_j} B_j''(I_j) \leq 0, \quad (99)$$

where the inequalities follow assumptions (M-3) and (M-4). Using equations (98) and (99), we obtain that $Q_j(I_j)$ is monotonically non-decreasing and $\frac{Q_j(I_j)}{I_j}$ is monotonically non-increasing with respect to I_j. It is then easy to observe that

$$\left(\frac{Q_j(I_j)}{Q_j(I_j^*)} - 1 \right) \left(1 - \frac{Q_j(I_j^*)/I_j^*}{Q_j(I_j)/I_j} \right) \leq 0.$$

In other words,

$$\left(\frac{f_j(I_j, B_j)}{f_j(I_j^*, B_j^*)} - 1 \right) \left(1 - \frac{f_j(I_j^*, B_j^*)}{f_j(I_j, B_j)} \cdot \frac{I_j}{I_j^*} \right) \leq 0. \quad (100)$$

We now establish the following result.

Theorem 15. *Assume (M-1) - (M-4). If $\mathcal{R}_0 > 1$, then the unique endemic equilibrium X^* is globally asymptotically stable in the interior of Γ.*

Proof. We will use an approach similar to that described in [58]. In particular, we will construct a Lyapunov function and determine the appropriate coefficients by graph theory. For completeness, we list some related definitions and results from graph theory in Appendix B.

Let

$$D_k = S_k - S_k^* - S_k^* \ln \frac{S_k}{S_k^*} + I_k - I_k^* - I_k^* \ln \frac{I_k}{I_k^*} + B_k - B_k^* - B_k^* \ln \frac{B_k}{B_k^*}, \quad (101)$$

for $k = 1, \ldots, n$. Differentiating and using the equilibrium equations (95) - (97)

yields

$$D'_k = \left(\frac{S_k - S^*_k}{S_k}\right) S'_k + \left(\frac{I_k - I^*_k}{I_k}\right) I'_k + \left(\frac{B_k - B^*_k}{B_k}\right) B'_k$$

$$= \left(1 - \frac{S^*_k}{S_k}\right) \left[\sum_{j=1}^{n} S^*_k f_j(I^*_j, B^*_j) + bS^*_k - \sum_{j=1}^{n} S_k f_j(I_j, B_j) - bS_k\right]$$

$$+ \left(1 - \frac{I^*_k}{I_k}\right) \left[\sum_{j=1}^{n} S_k f_j(I_j, B_j) - \sum_{j=1}^{n} S^*_k f_j(I^*_j, B^*_j) \cdot \frac{I_k}{I^*_k}\right]$$

$$+ \left(1 - \frac{B^*_k}{B_k}\right) h_k(I_k, B_k)$$

$$= \sum_{j=1}^{n} S^*_k f_j(I^*_j, B^*_j) \left[1 - \frac{S^*_k}{S_k} - \frac{S_k f_j(I_j, B_j)}{S^*_k f_j(I^*_j, B^*_j)} + \frac{f_j(I_j, B_j)}{f_j(I^*_j, B^*_j)}\right]$$

$$+ \left(1 - \frac{S^*_k}{S_k}\right) b(S^*_k - S_k)$$

$$+ \sum_{j=1}^{n} S^*_k f_j(I^*_j, B^*_j) \left[\frac{S_k f_j(I_j, B_j)}{S^*_k f_j(I^*_j, B^*_j)} - \frac{I_k}{I^*_k} - \frac{S_k f_j(I_j, B_j)}{S^*_k f_j(I^*_j, B^*_j)} \cdot \frac{I^*_k}{I_k} + 1\right]$$

$$+ \left(1 - \frac{B^*_k}{B_k}\right) \left[\frac{h_k(I^*_k, B_k) - h_k(I^*_k, B^*_k)}{h_k(I^*_k, B_k)}\right] h_k(I_k, B_k)$$

$$= \sum_{j=1}^{n} S^*_k f_j(I^*_j, B^*_j) \left[2 - \frac{S^*_k}{S_k} + \frac{f_j(I_j, B_j)}{f_j(I^*_j, B^*_j)} - \frac{I_k}{I^*_k} - \frac{S_k f_j(I_j, B_j)}{S^*_k f_j(I^*_j, B^*_j)} \cdot \frac{I^*_k}{I_k}\right]$$

$$+ \left(1 - \frac{S^*_k}{S_k}\right) b(S^*_k - S_k) + \left(1 - \frac{B^*_k}{B_k}\right) [h_k(I^*_k, B_k) - h_k(I^*_k, B^*_k)] \left(\frac{h_k(I_k, B_k)}{h_k(I^*_k, B_k)}\right)$$

Let $a_{kj} = S^*_k f_j(I^*_j, B^*_j)$ and

$$F_{kj}(S_k, I_k, B_k, I_j, B_j) = 2 - \frac{S^*_k}{S_k} + \frac{f_j(I_j, B_j)}{f_j(I^*_j, B^*_j)} - \frac{I_k}{I^*_k} - \frac{S_k f_j(I_j, B_j)}{S^*_k f_j(I^*_j, B^*_j)} \cdot \frac{I^*_k}{I_k}. \tag{102}$$

It is clear that

$$\left(1 - \frac{S^*_k}{S_k}\right) (S^*_k - S_k) \le 0.$$

Meanwhile, we have

$$[h_k(I^*_k, B_k) - h_k(I^*_k, B^*_k)] (B_k - B^*_k) < 0$$

which immediately follows from the last inequality of assumption (M-2). If we further assume that $h_k(I_k, B_k)$ and $h_k(I^*_k, B_k)$ have the same sign, then we obtain

$$D'_k \le \sum_{j=1} a_{kj} F_{kj}(S_k, I_k, B_k, I_j, B_j). \tag{103}$$

Let $\Phi(x) \equiv 1 - x + \ln x$ for $x \in (0, \infty)$. Note that $\Phi(x) \leq 0$ with $\Phi(x) = 0$ if and only if $x = 1$. Using the inequality (100), it follows that

$$
\begin{aligned}
F_{kj}(S_k, I_k, B_k, I_j, B_j) &= \Phi\left(\frac{S_k^*}{S_k}\right) - \frac{I_k}{I_k^*} + \Phi\left(\frac{S_k f_j(I_j, B_j)}{S_k^* f_j(I_j^*, B_j^*)} \cdot \frac{I_k^*}{I_k}\right) - \ln\frac{I_k^*}{I_k} \\
&\quad + \left(\frac{f_j(I_j, B_j)}{f_j(I_j^*, B_j^*)} - 1\right)\left(1 - \frac{f_j(I_j^*, B_j^*)}{f_j(I_j, B_j)} \cdot \frac{I_j}{I_j^*}\right) + \frac{I_j}{I_j^*} \\
&\quad + \Phi\left(\frac{f_j(I_j^*, B_j^*)}{f_j(I_j, B_j)} \cdot \frac{I_j}{I_j^*}\right) - \ln\frac{I_j}{I_j^*} \\
&= \Phi\left(\frac{S_k^*}{S_k}\right) + \Phi\left(\frac{S_k f_j(I_j, B_j)}{S_k^* f_j(I_j^*, B_j^*)} \cdot \frac{I_k^*}{I_k}\right) + \Phi\left(\frac{f_j(I_j^*, B_j^*)}{f_j(I_j, B_j)} \cdot \frac{I_j}{I_j^*}\right) \\
&\quad + \left(\frac{f_j(I_j, B_j)}{f_j(I_j^*, B_j^*)} - 1\right)\left(1 - \frac{f_j(I_j^*, B_j^*)}{f_j(I_j, B_j)} \cdot \frac{I_j}{I_j^*}\right) \\
&\quad - \frac{I_k}{I_k^*} + \ln\frac{I_k}{I_k^*} + \frac{I_j}{I_j^*} - \ln\frac{I_j}{I_j^*} \\
&= G_k(I_k) - G_j(I_j) \\
&\quad + \Phi\left(\frac{S_k^*}{S_k}\right) + \Phi\left(\frac{S_k f_j(I_j, B_j)}{S_k^* f_j(I_j^*, B_j^*)} \cdot \frac{I_k^*}{I_k}\right) + \Phi\left(\frac{f_j(I_j^*, B_j^*)}{f_j(I_j, B_j)} \cdot \frac{I_j}{I_j^*}\right) \\
&\quad + \left(\frac{f_j(I_j, B_j)}{f_j(I_j^*, B_j^*)} - 1\right)\left(1 - \frac{f_j(I_j^*, B_j^*)}{f_j(I_j, B_j)} \cdot \frac{I_j}{I_j^*}\right) \\
&\leq G_k(I_k) - G_j(I_j)
\end{aligned}
$$
(104)

where

$$
G_k(I_k) = -\frac{I_k}{I_k^*} + \ln\frac{I_k}{I_k^*} \, .
\tag{105}
$$

Note that

$$
D_k' = \sum_{j=1} a_{kj} F_{kj}(S_k, I_k, B_k, I_j, B_j) \quad \text{and} \quad F_{kj}(S_k, I_k, B_k, I_j, B_j) = G_k(I_k) - G_j(I_j)
$$

if and only if

$$
\left(1 - \frac{S_k^*}{S_k}\right)(S_k^* - S_k) = 0 \, ,
\tag{106}
$$

$$
\left(1 - \frac{B_k^*}{B_k}\right) h_k(I_k, B_k) = 0 \, ,
\tag{107}
$$

$$
\left(\frac{f_j(I_j, B_j)}{f_j(I_j^*, B_j^*)} - 1\right)\left(1 - \frac{f_j(I_j^*, B_j^*)}{f_j(I_j, B_j)} \cdot \frac{I_j}{I_j^*}\right) = 0 \, .
\tag{108}
$$

Let $A = [a_{kj}]$ and c_k be as given in Proposition 3.1 [58] for the weighted digraph $(\mathcal{G}, A)$ (also defined in Appendix B). For $k = 1, \ldots, n$,

$$d^-(k) = d^+(k) = n - 1.$$

Then, for $n > 2$,

$$\begin{aligned}
D' = \sum_{k=1}^{n} c_k D_k' &\leq \sum_{k=1}^{n} \sum_{j=1}^{n} c_k a_{kj} F_{kj} \\
&\leq \sum_{k=1}^{n} \sum_{j=1}^{n} c_k a_{kj} [G_k(I_k) - G_j(I_j)] \\
&= \sum_{k=1}^{n} \sum_{j=1}^{n} c_k a_{kj} \left(-\frac{I_k}{I_k^*} + \ln \frac{I_k}{I_k^*} + \frac{I_j}{I_j^*} - \ln \frac{I_j}{I_j^*} \right) \\
&= 0 \, .
\end{aligned}$$

Hence, D is a Lyapunov function.

Now, suppose $n = 2$. Since $d^-(k) = n - 1 = 1$ for $k = 1, 2$, by Theorem 3.3 of [58],

$$c_k a_{kj} = \sum_{i=1}^{2} c_j a_{ji} \, ; \qquad \text{that is, } c_k = \sum_{i=1}^{2} c_j a_{ji}/a_{kj} \, .$$

Then,

$$\begin{aligned}
D' \leq \sum_{k=1}^{2} \sum_{j=1}^{2} c_k a_{kj} F_{kj} &= \sum_{k=1}^{2} \sum_{j=1}^{2} \sum_{i=1}^{2} c_j a_{ji} F_{kj} \\
&\leq \sum_{k=1}^{2} \sum_{j=1}^{2} \sum_{i=1}^{2} c_j a_{ji} \left(-\frac{I_k}{I_k^*} + \ln \frac{I_k}{I_k^*} + \frac{I_j}{I_j^*} - \ln \frac{I_j}{I_j^*} \right) \\
&= 0 \, .
\end{aligned}$$

Therefore, D is a Lyapunov function for $n = 2$ as well.

Thus, $D' \leq 0$ for all $(S_1, I_1, B_1, \ldots, S_n, I_n, B_n)$ in the interior of Γ. Furthermore, $D' = 0$ implies that for some constant $\lambda > 0$,

$$S_1 = S_1^*, \quad \ldots, \quad S_n = S_n^* \, ,$$

$$I_1 = \lambda I_1^*, \quad \ldots, \quad I_n = \lambda I_n^* \, ,$$

$$B_1 = B_1^*, \quad \ldots, \quad B_n = B_n^* \, ,$$

using conditions (106) - (108), the properties of $\Phi(x)$ and strong connectivity of the weighted graph $(\mathcal{G}, A)$. Now, substituting these relations into the equation $dS_k/dt +$

dI_k/dt gives

$$0 = bN_k - bS_k^* - (\gamma_k + b)\lambda I_k^*$$

From our equilibrium equations (95) - (97), we clearly see that this holds only if $\lambda = 1$; that is, only at the endemic equilibrium X^*. Therefore, the only invariant set such that $D' = 0$ is the singleton X^*. By LaSalle's Principle, X^* is globally asymptotically stable in the interior of Γ. $\qquad\square$

3.5 EXAMPLE AND NUMERICAL SIMULATIONS

In this section, we will conduct numerical simulations to verify some of our analytical results. For simplicity, we consider only two groups; i.e., $n = 2$. Meanwhile, we use bilinear incidence for both the direct and indirect transmission pathways (see [62]), and we express $h_i(I_i, B_i)$ as a linear function for each group.

Our two-group cholera model thus takes the form below:

$$\frac{dS_1}{dt} = \mu_1 N_1 - (\lambda_{11}S_1B_1 + \lambda_{12}S_1B_2) - (\beta_{11}S_1I_1 + \beta_{12}S_1I_2) - \mu_1S_1, \quad (109)$$

$$\frac{dI_1}{dt} = (\lambda_{11}S_1B_1 + \lambda_{12}S_1B_2) + (\beta_{11}S_1I_1 + \beta_{12}S_1I_2) - (\mu_1 + \gamma_1)I_1, \quad (110)$$

$$\frac{dB_1}{dt} = \xi_1 I_1 - \delta_1 B_1, \quad (111)$$

$$\frac{dS_2}{dt} = \mu_2 N_2 - (\lambda_{21}S_2B_1 + \lambda_{22}S_2B_2) - (\beta_{21}S_2I_1 + \beta_{22}S_2I_2) - \mu_2S_2, \quad (112)$$

$$\frac{dI_2}{dt} = (\lambda_{21}S_2B_1 + \lambda_{22}S_2B_2) + (\beta_{21}S_2I_1 + \beta_{22}S_2I_2) - (\mu_2 + \gamma_2)I_2, \quad (113)$$

$$\frac{dB_2}{dt} = \xi_2 I_2 - \delta_2 B_2. \quad (114)$$

The parameter λ_{ij} $(i,j = 1,2)$ represents the transmission rate from vibrios in group j to susceptibles in group i, and β_{ij} $(i,j = 1,2)$ represents the transmission rate from infectives in group j to susceptibles in group i. Definitions and values for other parameters are provided in Table 1.

We have run the numerical simulation for this two-group model with various parameter values and initial conditions, and the results are consistent with our analytical predictions: when $\mathcal{R}_0 < 1$, the disease dies out; when $\mathcal{R}_0 > 1$, the disease persists and all solutions converge to the endemic equilibrium X^*. In particular, using the parameter values given in Table 1 (with $\mathcal{R}_0 > 1$), we display a typical set of results in Figures 4 and 5, where we plot the phase portraits for I_1 vs. S_1 and I_2 vs. S_2 separately with three different initial conditions and zoom in the results. We

Table 1. Parameter values for the two-group cholera model

Parameter	Symbol	Value	Source
Total population in each group	N_1, N_2	5,000	-
Natural human birth and death rate in each group	μ_1, μ_2	$(43.5\,\mathrm{yr})^{-1}$	[47]
Rate of recovery from cholera in each group	γ_1, γ_2	$(5\,\mathrm{day})^{-1}$	[15, 28]
Rate of human contribution to *V. cholerae* in each group	ξ_1, ξ_2	10 cells/ml-day	[15, 28]
Death rate of vibrios in the environment in each group	δ_1, δ_2	$(30\,\mathrm{day})^{-1}$	[15, 28]
Ingestion rate from environment to humans in each group	$\lambda_{11}, \lambda_{22}$	0.0001/day	[62]
Ingestion rate through human-human interaction in each group	β_{11}, β_{22}	0.00011/day	[47]
Cross transmission rate from vibrios in group 2 to susceptibles in group 1	β_{12}	0.0005/day	-
Cross transmission rate from vibrios in group 1 to susceptibles in group 2	β_{21}	0.0001/day	-
Cross transmission rate from infectives in group 2 to susceptibles in group 1	λ_{12}	0.00008/day	-
Cross transmission rate from infectives in group 1 to susceptibles in group 2	λ_{21}	0.00001/day	-

Figure 4. I_1 vs. S_1. Phase portrait (zoomed-in) for the two-group cholera model with different initial conditions, and $\mathcal{R}_0 > 1$. All of the curves converge to the endemic equilibrium with $I_1^* \approx 1.572$, $S_1^* \approx 3.664$.

observe that all three curves approach the endemic equilibrium over time, indicating the global asymptotic stability of the endemic equilibrium.

We have proposed a general multi-group model describing cholera dynamics that involve spatial heterogeneity and dispersal. Both direct (or, human-to-human) and indirect (or, environment-to-human) transmission pathways are incorporated into the model in a most general manner, and the pathogen dynamics are also represented by a general function. Under biologically feasible assumptions, the basic reproduction number $\mathcal{R}_0$, given in equation (78), remains a sharp threshold for cholera dynamics in multiple groups. If $\mathcal{R}_0 < 1$, the disease will completely die out whereas if $\mathcal{R}_0 > 1$, the disease will persist. Additionally, when $\mathcal{R}_0 > 1$, there exists a unique positive endemic equilibrium that is globally asymptotically stable. The analytical predictions are verified by our numerical simulation results for a two-group cholera model.
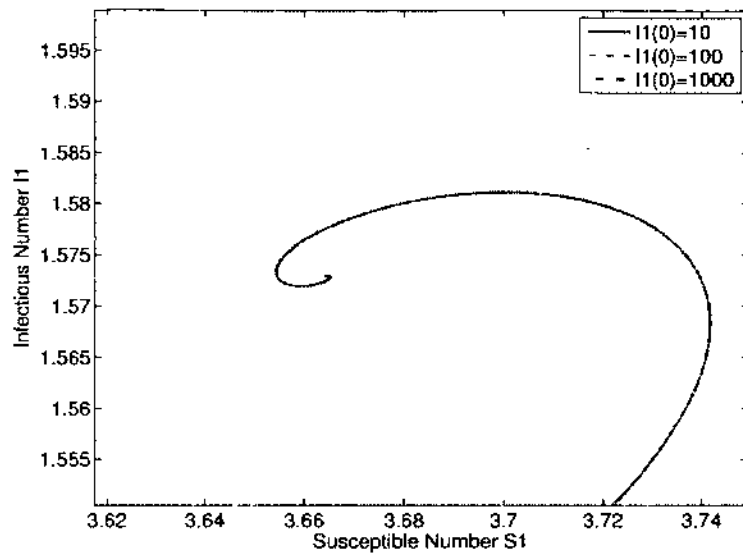
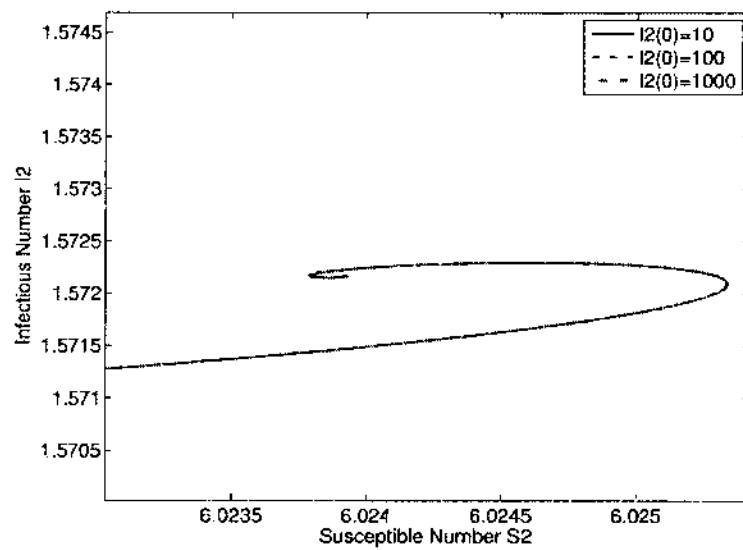Figure 5. I_2 vs. S_2. Phase portrait (zoomed-in) for the two-group cholera model with different initial conditions, and $\mathcal{R}_0 > 1$. All of the curves converge to the endemic equilibrium with $I_2^* \approx 1.572$, $S_2^* \approx 6.024$.

CHAPTER 4

PERIODIC CHOLERA MODEL

Environmental and climatic factors play an important role in cholera epidemics. In particular, in developing countries where endemicity is established, cholera tends to settle into a seasonal pattern [60]. Runoff from monsoons and floods during the wet seasons can wash sewage into the local rivers and drinking water, causing a bloom of *V. cholerae* in the aquatic environment. Thus, environmental influences, such as monsoons, floods, droughts, and water temperature changes, due to the alternating dry and wet seasons, can disrupt the toxigenic vibrio concentration in the aquatic environment, as well as their survival and epidemic spread [15,60]. That is, seasonal variations could cause epidemics and lead to a heterogeneous environment for disease transmission in the time domain.

Building on the cholera model in [65] (reproduced in Appendix A), we construct the following non-autonomous dynamical system to describe cholera dynamics in a time-periodic environment,

$$\frac{dS}{dt} = bN - Sf(t, I, B) - bS, \tag{115}$$

$$\frac{dI}{dt} = Sf(t, I, B) - (\gamma + b)I, \tag{116}$$

$$\frac{dR}{dt} = \gamma I - bR, \tag{117}$$

$$\frac{dB}{dt} = h(t, I, B), \tag{118}$$

where S, I, R and B denote the susceptible population, infected population, recovered population and the concentration of vibrios in the contaminated water, respectively. For simplicity, we assume B to be scalar. The total population $N = S + I + R$ is assumed to be a constant for all $t \geq 0$. The parameter b represents the natural human birth and death rate, and γ represents the rate of recovery from cholera. In this generalized model, the incidence function, $f(t, I, B)$, which determines the rate of new infection and the function $h(t, I, B)$, which describes the rate of change for the pathogen in the environment, are both periodic in time with a common period ω. That is,

$$f(t + \omega, I, B) = f(t, I, B) \qquad \text{and} \qquad h(t + \omega, I, B) = h(t, I, B).$$

To make biological sense, we extend assumptions (M1) - (M4) from Chapter 3 to incorporate time; that is, we assume that the periodic functions f and h satisfy the following conditions for all $t \geq 0$:

(P-1) $f(t,0,0) = h(t,0,0) = 0$.

(P-2) $f(t,I,B) \geq 0$.

(P-3) $\frac{\partial f}{\partial I}(t,I,B) \geq 0$, $\frac{\partial f}{\partial B}(t,I,B) \geq 0$, $\frac{\partial h}{\partial I}(t,I,B) \geq 0$, $\frac{\partial h}{\partial B}(t,I,B) \leq 0$.

(P-4) $f(t,I,B)$ and $h(t,I,B)$ are both concave for any $t \geq 0$; i.e. the matrices $D^2 f$ and $D^2 h$ are negative semidefinite everywhere.

Hence, from assumption (P-1), it is obvious that the model has a unique, constant disease-free equilibrium

$$X_0 = (S_0, I_0, R_0, B_0)^T = (N, 0, 0, 0)^T. \tag{119}$$

In addition, we assume that

(P-5) $f(t,0,B) > 0$ if $B > 0$; $h(t,I,0) > 0$ if $I > 0$.

The first condition in (P-5) implies that infection can start by the indirect transmission route alone; in other words, a positive bacterial concentration can lead to a positive incidence even if $I = 0$ initially. The second condition in (P-5) states that infected people will contribute to the growth of the vibrios in the environment (e.g., by shedding) even if $B = 0$ initially.

Furthermore, we introduce an additional regulation on the profiles of the incidence and pathogen functions for small I and B. We assume that

(P-6) There exists $\epsilon^* > 0$ such that when $0 < I < \epsilon^*$, $0 < B < \epsilon^*$,

$$f(t,I,B) \geq f(t,0,0) + I \cdot \frac{\partial f}{\partial I}(t,0,0) + B \cdot \frac{\partial f}{\partial B}(t,0,0)$$
$$+ \frac{1}{2}I^2 \cdot \frac{\partial^2 f}{\partial I^2}(t,0,0) + I \cdot B \cdot \frac{\partial^2 f}{\partial I \partial B}(t,0,0) + \frac{1}{2}B^2 \cdot \frac{\partial^2 f}{\partial B^2}(t,0,0),$$

and

$$h(t,I,B) \geq h(t,0,0) + I \cdot \frac{\partial h}{\partial I}(t,0,0) + B \cdot \frac{\partial h}{\partial B}(t,0,0)$$
$$+ \frac{1}{2}I^2 \cdot \frac{\partial^2 h}{\partial I^2}(t,0,0) + I \cdot B \cdot \frac{\partial^2 h}{\partial I \partial B}(t,0,0) + \frac{1}{2}B^2 \cdot \frac{\partial^2 h}{\partial B^2}(t,0,0).$$

Here we make some comments on the assumption (P-6). Based on concavity of f (assumption P-4), the surface of f is below its tangent plane every where. Meanwhile, since the matrix $D^2 f$ is negative semidefinite, we have

$$f(t,0,0) + I \cdot \frac{\partial f}{\partial I}(t,0,0) + B \cdot \frac{\partial f}{\partial B}(t,0,0) \geq f(t,0,0) + I \cdot \frac{\partial f}{\partial I}(t,0,0) + B \cdot \frac{\partial f}{\partial B}(t,0,0)$$
$$+ \frac{1}{2} I^2 \cdot \frac{\partial^2 f}{\partial I^2}(t,0,0) + I \cdot B \cdot \frac{\partial^2 f}{\partial I \partial B}(t,0,0)$$
$$+ \frac{1}{2} B^2 \cdot \frac{\partial^2 f}{\partial B^2}(t,0,0).$$

Thus, assumption (P-6) essentially states that at least in a small neighborhood of $I = B = 0$, the surface of f lies below its tangent plane and above a concave tangent paraboloid. Similar reasoning holds for h.

Finally, we mention that many well known cholera models, such as those in [15, 28, 47, 62], all satisfy the above assumptions (P-1) - (P-6), though these models are based on autonomous dynamical systems.

4.1 BASIC REPRODUCTION NUMBER

Following the standard next-generation matrix theory [64], we consider the sub-system of model (115) - (118) that is directly related to the infection:

$$\begin{bmatrix} dI/dt \\ dB/dt \end{bmatrix} = \begin{bmatrix} Sf(t,I,B) \\ 0 \end{bmatrix} - \begin{bmatrix} (\gamma+b)I \\ -h(t,I,B) \end{bmatrix} = \mathcal{F} - \mathcal{V}.$$

For this non-autonomous model, we have

$$F(t) = D\mathcal{F}(X_0) = \begin{bmatrix} N\frac{\partial f}{\partial I}(t,0,0) & N\frac{\partial f}{\partial B}(t,0,0) \\ 0 & 0 \end{bmatrix},$$

and

$$V(t) = D\mathcal{V}(X_0) = \begin{bmatrix} \gamma+b & 0 \\ -\frac{\partial h}{\partial I}(t,0,0) & -\frac{\partial h}{\partial B}(t,0,0) \end{bmatrix},$$

where X_0 is the disease-free equilibrium of the model defined in equation (119).

Generally, for a compartmental epidemiological model based on an *autonomous* system, the basic reproduction number is determined by the spectral radius of the next-generation matrix, FV^{-1} (which is independent of time). It is thus a simple matter to calculate the time-averaged reproduction number, $[\mathcal{R}_0]$, for our cholera model. Wesley and Allen [69] showed that for some epidemic models with periodic

coefficients and constant population size, the time-averaged basic reproduction number is a threshold for disease extinction. For any continuous periodic function $g(t)$ with period ω, we may define its average as

$$[g] = \frac{1}{\omega} \int_0^\omega g(t)dt.$$

Thus, keeping with this notation, we define the time-averaged matrices of $F(t)$ and $V(t)$ as the following, respectively,

$$[F] = \begin{bmatrix} N\left[\frac{\partial f}{\partial I}\right] & N\left[\frac{\partial f}{\partial B}\right] \\ 0 & 0 \end{bmatrix}, \qquad [V] = \begin{bmatrix} \gamma + b & 0 \\ -\left[\frac{\partial h}{\partial I}\right] & -\left[\frac{\partial h}{\partial B}\right] \end{bmatrix}.$$

Therefore, the time-averaged basic reproduction number, defined as the spectral radius of the next generation matrix $[F][V]^{-1}$, is given by,

$$[\mathcal{R}_0] = \rho([F][V]^{-1}) = \frac{N}{\gamma + b}\left\{\left[\frac{\partial f}{\partial I}\right] - \left[\frac{\partial f}{\partial B}\right]\left[\frac{\partial h}{\partial B}\right]^{-1}\left[\frac{\partial h}{\partial I}\right]\right\}. \tag{120}$$

Although the definition of the basic reproduction number of a general non-autonomous model system is still an open question, Wang and Zhao [66] extended the framework in [64] to include epidemiological models in periodic environments (background reproduced in Appendix C). Wang and Zhao [66] introduced the next infection operator L by

$$(L\phi)(t) = \int_0^\infty Y(t, t-s)F(t-s)\phi(t-s)ds, \tag{121}$$

where $Y(t, s)$, $t \geq s$, is the evolution operator of the linear ω-periodic system $dy/dt = -V(t)y$ and $\phi(t)$, the initial distribution of infected individuals, is ω-periodic and nonnegative. The basic reproduction number is then defined as the spectral radius of the next infection operator,

$$\mathcal{R}_0 = \rho(L). \tag{122}$$

Analytical determination of $\rho(L)$ is impossible in general. Therefore, we will numerically calculate the basic reproduction number $\mathcal{R}_0$ by explicitly determining the maximum eigenvalue λ of the next infection operator L such that $(L\phi)(t) = \lambda\phi(t)$ for all ω-periodic functions $\phi(t) \in C_\omega$. From equation (121) and the ω-periodicity of ϕ, we obtain

$$(L\phi)(t) = \int_0^\omega G(t, s)\phi(t-s)ds, \tag{123}$$

where

$$G(t,s) = \sum_{m=0}^{\infty} Y(t, t - s - m\omega) F(t - s - m\omega). \tag{124}$$

Since $Y(t,s)$, $t \geq s$, is defined as the evolution operator of a linear ω-periodic system, there exist $K > 0$ and $\alpha > 0$ such that $\|Y(t,s)\| \leq Ke^{-\alpha(t-s)}$ for all $t \geq s$ with $s \in \mathbb{R}$ [27]. Then it is clear that $\|Y(t, t - s - m\omega)F(t - s - m\omega)\| \leq K\|F(t - s - m\omega)\|e^{-\alpha(s+m\omega)}$ for all $t \in \mathbb{R}$ and $s \geq 0$. Hence, we may approximate G by a finite sum

$$G(t,s) \approx \sum_{m=0}^{M} Y(t, t - s - m\omega) F(t - s - m\omega) \tag{125}$$

for some $M > 0$ sufficiently large. We proceed to numerically integrate equation (121) with the integrand approximated by (125).

Let us partition the interval $[0, \omega]$ uniformly into n nodes labeled as $t_i = i \cdot \frac{\omega}{n}$ for $i = 0, \ldots, n - 1$. Using the trapezoidal rule, we can approximate this integral in equation (121) with second-order accuracy,

$$(L\phi)(t) \approx \frac{\omega}{n} \left(\sum_{i=1}^{n-1} G(t, t_i)\phi(t - t_i) + \frac{1}{2}G(t, t_0)\phi(t - t_0) + \frac{1}{2}G(t, t_n)\phi(t - t_n) \right).$$

Since $\phi(t)$ is ω-periodic, it is clear that $\phi(t - t_0) = \phi(t - t_n)$. For convenience, let

$$\tilde{G}(t, t_0) \equiv \frac{1}{2}\left[G(t, t_0) + G(t, t_n) \right].$$

Then,

$$(L\phi)(t) \approx \frac{\omega}{n} \left[\tilde{G}(t, t_0)\phi(t - t_0) + \sum_{i=1}^{n-1} G(t, t_i)\phi(t - t_i) \right].$$

Now $(L\phi)(t) = \lambda\phi(t)$ can be written as a matrix equation,

$$\frac{\omega}{n} \begin{bmatrix} \tilde{G}(t, t_0) & G(t, t_1) & G(t, t_2) & \cdots & G(t, t_{n-1}) \end{bmatrix} \begin{bmatrix} \phi(t - t_0) \\ \phi(t - t_1) \\ \phi(t - t_2) \\ \vdots \\ \phi(t - t_{n-1}) \end{bmatrix} = \lambda\phi(t).$$

Setting $t = t_j$ $(j = 0, \ldots, n-1)$ in the above equation yields

$$\frac{\omega}{n} \left[\tilde{G}(t_j, t_0) \quad G(t_j, t_1) \quad G(t_j, t_2) \quad \cdots \quad G(t_j, t_{n-1}) \right] \begin{bmatrix} \phi(t_j - t_0) \\ \phi(t_j - t_1) \\ \phi(t_j - t_2) \\ \vdots \\ \phi(t_j - t_{n-1}) \end{bmatrix} = \lambda\phi(t_j) .$$

(126)

Again, by the periodicity of $\phi(t)$, it follows that

$$\phi(t_j - t_0) = \phi(t_j), \qquad \phi(t_j - t_1) = \phi(t_{j-1}), \qquad \cdots$$

$$\phi(t_j - t_{j-1}) = \phi(t_1), \qquad \phi(t_j - t_j) = \phi(t_0), \qquad \phi(t_j - t_{j+1}) = \phi(t_{n-1}),$$

$$\cdots \qquad \phi(t_j - t_{n-2}) = \phi(t_{j+2}), \quad \phi(t_j - t_{n-1}) = \phi(t_{j+1}),$$

and we can rearrange the terms in equation (126) to obtain

$$\frac{\omega}{n} \left[G(t_j, t_j) \quad G(t_j, t_{j-1}) \quad \cdots \quad \tilde{G}(t_j, t_0) \quad \cdots \quad G(t_j, t_{j+2}) \quad G(t_j, t_{j+1}) \right] \begin{bmatrix} \phi(t_0) \\ \phi(t_1) \\ \vdots \\ \phi(t_j) \\ \vdots \\ \phi(t_{n-2}) \\ \phi(t_{n-1}) \end{bmatrix} = \lambda\phi(t_j) .$$

(127)

Note that this equation holds for all $j = 0, \ldots, n-1$, thus generating a matrix system. The coefficient matrix, denoted by A, is given by

$$A = \begin{bmatrix} \tilde{G}(t_0, t_0) & G(t_0, t_{n-1}) & \cdots & \cdots & \cdots & G(t_0, t_2) & G(t_0, t_1) \\ G(t_1, t_1) & \tilde{G}(t_1, t_0) & \cdots & \cdots & \cdots & G(t_1, t_3) & G(t_1, t_2) \\ \vdots & \ddots & \ddots & \ddots & \ddots & \ddots & \vdots \\ G(t_j, t_j) & G(t_j, t_{j-1}) & \cdots & \tilde{G}(t_j, t_0) & \cdots & G(t_j, t_{j+2}) & G(t_j, t_{j+1}) \\ \vdots & \ddots & \ddots & \ddots & \ddots & \ddots & \vdots \\ G(t_{n-2}, t_{n-2}) & G(t_{n-2}, t_{n-3}) & \cdots & \cdots & \cdots & \tilde{G}(t_{n-2}, t_0) & G(t_{n-2}, t_{n-1}) \\ G(t_{n-1}, t_{n-1}) & G(t_{n-1}, t_{n-2}) & \cdots & \cdots & \cdots & G(t_{n-1}, t_1) & \tilde{G}(t_{n-1}, t_0) \end{bmatrix} .$$

(128)

Therefore, equation (127) can be put into a compact form,

$$\frac{\omega}{n} A\tilde{\phi} = \lambda\tilde{\phi}$$

(129)

where A is a matrix of dimension $(nm) \times (nm)$ and $\tilde{\phi}$ is a vector of dimension $(nm) \times 1$.

Hence, to find the basic reproduction number defined by $\mathcal{R}_0 = \rho(L)$, it is equivalent to find the maximum λ such that the matrix equation (129) is valid; i.e.,

$$\mathcal{R}_0 \approx \frac{\omega}{n}\rho(A). \tag{130}$$

For the periodic cholera model (115) - (118), the evolution operator can be easily determined by solving the system of differential equations $dy/dt = -V(t)y$ with the condition $y(s) = I_{2\times 2}$; thus,

$$Y(t,s) = \begin{bmatrix} e^{-(\gamma+b)(t-s)} & 0 \\ \tilde{Y}(t,s) & e^{\int_s^t \frac{\partial h}{\partial B}(\tau,0,0)d\tau} \end{bmatrix}, \tag{131}$$

where

$$\tilde{Y}(t,s) = \left\{ \int_s^t e^{-\int \frac{\partial h}{\partial B}(\tau,0,0)d\tau} \frac{\partial h}{\partial I}(\tau,0,0)e^{-(\gamma+b)(\tau-s)}d\tau \right\} \Big/ e^{-\int \frac{\partial h}{\partial B}(t,0,0)dt}. \tag{132}$$

The next infection operator can be numerically evaluated by

$$(L\phi)(t) = \int_0^\infty Y(t,t-s)F(t-s)\phi(t-s)ds = \int_0^\omega G(t,s)\phi(t-s)ds, \tag{133}$$

where

$$G(t,s) \approx \sum_{k=0}^M Y(t,t-s-k\omega)F(t-s-k\omega)$$

$$\approx N \sum_{k=0}^M \begin{bmatrix} \frac{\partial f}{\partial I}(t-s-k\omega,0,0)e^{-(\gamma+b)(s+k\omega)} & \frac{\partial f}{\partial B}(t-s-k\omega,0,0)e^{-(\gamma-b)(s+k\omega)} \\ \frac{\partial f}{\partial I}(t-s-k\omega,0,0)\tilde{Y}(t,t-s-k\omega) & \frac{\partial f}{\partial B}(t-s-k\omega,0,0)\tilde{Y}(t,t-s-k\omega) \end{bmatrix} \tag{134}$$

for some $M > 0$ sufficiently large.

From the work of [64], we immediately obtain the following result regarding the local stability of the disease-free equilibrium.

Theorem 16. *Let $\mathcal{R}_0$ be defined as equation (122). The disease-free equilibrium of the system (115) - (118) is locally asymptotically stable if $\mathcal{R}_0 < 1$, and unstable if $\mathcal{R}_0 > 1$.*

4.2 DISEASE EXTINCTION

We proceed to investigate the global stability of the disease-free equilibrium for our cholera model, which will also provide a condition for the extinction of the disease. Consider the matrix function $F(t) - V(t)$,

$$F(t) - V(t) = \begin{bmatrix} N\frac{\partial f}{\partial I}(t,0,0) - (\gamma + b) & N\frac{\partial f}{\partial B}(t,0,0) \\ \\ \frac{\partial h}{\partial I}(t,0,0) & \frac{\partial h}{\partial B}(t,0,0) \end{bmatrix}. \tag{135}$$

It can be easily shown that the above matrix function is continuous, cooperative, irreducible and ω-periodic. Let $\Phi_{(F-V)(\cdot)}(t)$ be the fundamental solution matrix of the linear ordinary differential system

$$x' = [F(t) - V(t)]x, \tag{136}$$

and $\rho(\Phi_{(F-V)(\cdot)}(\omega))$ be the spectral radius of $\Phi_{(F-V)(\cdot)}(\omega)$.

From Lemma 2.1 in [71], we immediately obtain the following result,

Lemma 17. *Let* $\mu = \frac{1}{\omega}\ln\rho(\Phi_{(F-V)(\cdot)}(\omega))$. *Then there exists a positive ω-periodic function $v(t)$ such that $e^{\mu t}v(t)$ is a solution to equation* (136).

Now let us consider equations (116) and (118) from our cholera model. It can be easily obtained, using assumption (P-4), that

$$\frac{dI}{dt} = Sf(t,I,B) - (\gamma + b)I \leq N\left[I\frac{\partial f}{\partial I}(t,0,0) + B\frac{\partial f}{\partial B}(t,0,0)\right] - (\gamma + b)I,$$

and

$$\frac{dB}{dt} = h(t,I,B) \leq I\frac{\partial h}{\partial I}(t,0,0) + B\frac{\partial h}{\partial B}(t,0,0).$$

That is,

$$\frac{d}{dt}\begin{bmatrix} I \\ B \end{bmatrix} \leq [F(t) - V(t)]\begin{bmatrix} I \\ B \end{bmatrix}. \tag{137}$$

Meanwhile, based on Lemma 17, there exists $v(t)$ such that

$$x(t) = (\bar{I}(t), \bar{B}(t)) = e^{\mu t}v(t) \tag{138}$$

is a solution to equation (136), with $\mu = \frac{1}{\omega}\ln\rho(\Phi_{(F-V)(\cdot)}(\omega))$. It follows from equations (136) and (137) that

$$(I(t), B(t)) \leq (\bar{I}(t), \bar{B}(t)) \tag{139}$$

when t is large. Theorem 2.2 in [66] (also presented in Appendix C as Theorem 2) states that $\mathcal{R}_0 < 1$ if and only if $\rho(\Phi_{(F-V)(\cdot)}(\omega)) < 1$. Therefore, $\mu < 0$. Then, given equation (138) and inequality (139), it is clear that

$$\lim_{t\to\infty} I(t) = 0, \qquad \lim_{t\to\infty} B(t) = 0. \tag{140}$$

Next, we consider equation (117) from our model. For any $\epsilon > 0$, there exists $T > 0$ such that whenever $t > T$, it follows that

$$I < \frac{\epsilon}{\gamma} \quad \text{and} \quad \frac{dR}{dt} < \epsilon - bR.$$

And hence, $R(t) < \epsilon/b$ for $t > T$. Since $\epsilon > 0$ was arbitrary, it is clear that

$$\lim_{t\to\infty} R(t) = 0. \tag{141}$$

Finally, since population $N = S + I + R$ is a constant, we have that

$$\lim_{t\to\infty} S(t) = N. \tag{142}$$

Hence, we have established the following result.

Theorem 18. *If $\mathcal{R}_0 < 1$, then the disease-free equilibrium of the model* (115) - (118) *is globally asymptotically stable, and* $\lim_{t\to\infty} X(t) = X_0 = (N,0,0,0)^T$ *for any solution $X(t)$ of the system* (115) - (118).

Theorem 18 shows that the disease will completely die out as long as $\mathcal{R}_0 < 1$. This further implies that reducing and keeping $\mathcal{R}_0$ below the unity would be sufficient to eradicate cholera infection even in a periodic environment. Similar result was established for the autonomous system in [65]; i.e., the cholera model with time-independent f and h.

4.3 UNIFORM PERSISTENCE OF THE DISEASE

Now we consider the dynamics of the periodic model (115) - (118) when $\mathcal{R}_0 > 1$. For ease of discussion, let us omit equation (117) from the system, since the total population is fixed such that $N = S + I + R$. Define

$$X = \mathbb{R}_+^3; \qquad X_0 = \mathbb{R}_+ \times \text{Int}(\mathbb{R}_+) \times \text{Int}(\mathbb{R}_+); \qquad \partial X_0 = X\backslash X_0.$$

Let $P : X \to X$ be the Poincaré map associated with the model (115) - (118) such that $P(x_0) = u(\omega, x_0)$ for all $x_0 \in X$ where $u(t, x_0)$ denotes the unique solution of the system with $u(0, x_0) = x_0$.

Definition 19. *The solutions of the system* (115) - (118) *are said to be uniformly persistent if there exists some* $\eta > 0$ *such that*

$$\liminf_{t \to \infty} S(t) \geq \eta, \qquad \liminf_{t \to \infty} I(t) \geq \eta, \qquad \liminf_{t \to \infty} B(t) \geq \eta$$

whenever $S(0) > 0$, $I(0) > 0$, *and* $B(0) > 0$.

A more general definition of uniform persistence can be found in [72]. We now state the following theorem, the proof of which is inspired by the work of [71].

Theorem 20. *Let* $\mathcal{R}_0 > 1$ *and let (P-1) - (P-6) hold. Then the solutions of the system* (115) - (118) *are uniformly persistent, and the system admits at least one positive* ω-*periodic solution.*

Proof. Set

$$M_\partial = \left\{ (S(0), I(0), B(0)) \in \partial X_0 : P^m(S(0), I(0), B(0)) \in \partial X_0, \ \forall m \geq 0 \right\}.$$

We first show that

$$M_\partial = \{ (S, 0, 0) : S \geq 0 \}. \tag{143}$$

Clearly, $M_\partial \supseteq \{ (S, 0, 0) : S \geq 0 \}$. Consider any initial values $(S(0), I(0), B(0)) \in \partial X_0 \setminus \{ (S, 0, 0) : S \geq 0 \}$. If $I(0) = 0$ and $B(0) > 0$, then $I'(0) > 0$ by assumption (P-5). Similarly, if $B(0) = 0$ and $I(0) > 0$, then $B'(0) > 0$. Thus, it follows that $(S(t), I(t), B(t)) \notin \partial X_0$ for $0 < t \ll 1$. This implies that $M_\partial \subseteq \{ (S, 0, 0) : S \geq 0 \}$, and hence, we have (143).

Now, let us consider the fixed point $M_0 = (N, 0, 0)$ and define $W^S(M_0) = \{ x_0 : P^m(x_0) \to M_0, m \to \infty \}$. We show that

$$W^S(M_0) \bigcap X_0 = \emptyset. \tag{144}$$

Based on the continuity of solutions with respect to the initial conditions, for any $\epsilon > 0$, there exists $\delta > 0$ small enough such that for all $(S(0), I(0), B(0)) \in X_0$ with $\|(S(0), I(0), B(0)) - M_0\| \leq \delta$, we have

$$\|u(t, (S(0), I(0), B(0))) - u(t, M_0)\| < \epsilon, \qquad \forall t \in [0, \omega]. \tag{145}$$

We claim that

$$\limsup_{m \to \infty} \|P^m(S(0), I(0), B(0)) - M_0\| \geq \delta, \qquad \forall (S(0), I(0), B(0)) \in X_0. \tag{146}$$

Suppose by contradiction; that is, we suppose $\limsup_{m\to\infty} \|P^m(S(0), I(0), B(0)) - M_0\| < \delta$ for some $(S(0), I(0), B(0)) \in X_0$. Without loss of generality, we assume that $\|P^m(S(0), I(0), B(0)) - M_0\| < \delta, \forall m \geq 0$. Thus,

$$\|u(t, P^m(S(0), I(0), B(0))) - u(t, M_0)\| < \epsilon, \qquad \forall t \in [0, \omega] \text{ and } m \geq 0. \tag{147}$$

Moreover, for any $t \geq 0$, we can write $t = t' + n\omega$, where $t' \in [0, \omega)$ and n being the greatest integer less than or equal to t/ω. Then we obtain

$$\|u(t, (S(0), I(0), B(0))) - u(t, M_0)\| = \|u(t', P^m(S(0), I(0), B(0))) - u(t', M_0)\| < \epsilon \tag{148}$$

for any $t \geq 0$. Let $(S(t), I(t), B(t)) = u(t, (S(0), I(0), B(0)))$. It follows that $N - \epsilon < S(t) < N + \epsilon$, $0 < I(t) < \epsilon$ and $0 < B(t) < \epsilon$. Note again that $\epsilon < \epsilon^*$. Then, based on assumptions (P-1) and (P-6), we have

$$\frac{dI}{dt} \geq N \cdot I \cdot \frac{\partial f}{\partial I}(t, 0, 0) + N \cdot B \cdot \frac{\partial f}{\partial B}(t, 0, 0) - (\gamma + b)I$$
$$+ N \cdot \epsilon \cdot \frac{1}{2} I \cdot \frac{\partial^2 f}{\partial I^2}(t, 0, 0) + N \cdot \epsilon \cdot \frac{1}{2} B \cdot \frac{\partial^2 f}{\partial B^2}(t, 0, 0) - N \cdot \epsilon \cdot I \cdot \left| \frac{\partial^2 f}{\partial I \partial B}(t, 0, 0) \right|$$
$$- \epsilon \cdot I \cdot \frac{\partial f}{\partial I}(t, 0, 0) - \epsilon \cdot B \cdot \frac{\partial f}{\partial I}(t, 0, 0) - \epsilon \cdot \epsilon \cdot I \left| \frac{\partial^2 f}{\partial I \partial B}(t, 0, 0) \right|,$$

and

$$\frac{dB}{dt} \geq I \cdot \frac{\partial h}{\partial I}(t, 0, 0) + B \cdot \frac{\partial h}{\partial B}(t, 0, 0)$$
$$+ \epsilon \cdot \frac{1}{2} I^2 \cdot \frac{\partial^2 h}{\partial I}(t, 0, 0) + \epsilon \cdot \frac{1}{2} B \cdot \frac{\partial^2 h}{\partial B^2}(t, 0, 0) - \epsilon \cdot I \cdot \left| \frac{\partial^2 h}{\partial I \partial B}(t, 0, 0) \right|.$$

Hence, we obtain

$$\begin{bmatrix} dI/dt \\ dB/dt \end{bmatrix} \geq \begin{bmatrix} F - V - \epsilon \cdot K \end{bmatrix} \cdot \begin{bmatrix} I \\ B \end{bmatrix}, \tag{149}$$

where $F - V$ was given by equation (135) and

$$-\epsilon \cdot K = \epsilon \cdot \begin{bmatrix} \frac{1}{2} N \frac{\partial^2 f}{\partial I^2}(t, 0, 0) - \frac{\partial f}{\partial I}(t, 0, 0) - (N + \epsilon) \left| \frac{\partial^2 f}{\partial I \partial B}(t, 0, 0) \right| & \frac{1}{2} N \frac{\partial^2 f}{\partial B^2}(t, 0, 0) - \frac{\partial f}{\partial B}(t, 0, 0) \\ \frac{1}{2} \frac{\partial^2 h}{\partial I^2}(t, 0, 0) - \left| \frac{\partial^2 h}{\partial I \partial B}(t, 0, 0) \right| & \frac{1}{2} \frac{\partial^2 h}{\partial B^2}(t, 0, 0) \end{bmatrix}. \tag{150}$$

Again based on Theorem 2.2 in [66], $\mathcal{R}_0 > 1$ if and only if $\rho(\Phi_{F-V}(\omega)) > 1$. Thus, for $\epsilon > 0$ small enough we have $\rho(\Phi_{F-V-\epsilon K}(\omega)) > 1$. Using Lemma 17 and the comparison principle, we obtain

$$\lim_{t \to \infty} I(t) = \infty \quad \text{and} \quad \lim_{t \to \infty} B(t) = \infty, \tag{151}$$

which is a contradiction.

Hence, M_0 is acyclic in M_∂, and P is uniformly persistent with respect to $(X_0, \partial X_0)$, which implies the uniform persistence of the solutions to the original system. Consequently, the Poincaré map P has a fixed point $(\tilde{S}(0), \tilde{I}(0), \tilde{B}(0)) \in X_0$, and it can be easily seen that $\tilde{S}(0) \neq 0$. Thus, $(\tilde{S}(0), \tilde{I}(0), \tilde{B}(0)) \in \text{Int}(\mathbb{R}_+) \times \text{Int}(\mathbb{R}_+) \times \text{Int}(\mathbb{R}_+)$ and $(\tilde{S}(t), \tilde{I}(t), \tilde{B}(t)) = u(t, (\tilde{S}(0), \tilde{I}(0), \tilde{B}(0)))$ is a positive ω-periodic solution of the system.

$\square$

4.4 EXAMPLES AND NUMERICAL SIMULATIONS

We briefly discuss three different, and specific, cholera models in periodic environments. The models presented below are extended from work of Codeço [15], and more recently, of Mukandavire et al. [47] and Tien and Earn [62] (see Appendix A for the original models). We focus on simulating seasonal variations by incorporating periodic environment-to-human transmission rates and periodic rates of human contribution to the population of *V. cholerae* in the aquatic environment. We study the epidemic and endemic cholera dynamics of a hypothetical community with $N = 10,000$ as the (normalized) total population, and compute the basic reproduction number $\mathcal{R}_0$ for each model. Meanwhile, the time-averaged reproduction number $[\mathcal{R}_0]$ can be easily calculated for each of these models, though it has been noted that $[\mathcal{R}_0]$ may overestimate or underestimate the infection risk for a non-autonomous epidemiological system [66]. Thus, it is of our interest to compare the values of $\mathcal{R}_0$ and $[\mathcal{R}_0]$ for these models. Also, we conduct numerical simulation for each model with initial conditions $B(0) = R(0) = 0, S(0) = N$, and $I(0) = 1$; that is, one infected individual enters an entirely susceptible community. For easy comparison, we use the same parameter setting for all the three models, and these parameter values are based on the cholera data published on the recent Zimbabwe cholera outbreak [47, 70]. We present typical infection curves for both scenarios, $\mathcal{R}_0 < 1$ and $\mathcal{R}_0 > 1$, demonstrating disease extinction and disease persistence. Finally, in presenting each of these

Table 2. Incidence functions and pathogen concentration functions

Model	Incidence function $f(t, I, B)$	Pathogen concentration rate of change $h(t, I, B)$
Codeço	$a(t)\lambda(B)$	$e(t)I - \beta B$
Mukandavire et al.	$\beta_e(t)\frac{B}{\kappa+B} - \beta_h I$	$\xi(t)I - \delta B$
Tien and Earn	$b_W(t)W - b_I I$	$\alpha(t)I - \xi W$

models, we keep the same notations for variables and parameters from the original autonomous model. We will clarify the different notations among the three extended models when necessary.

4.4.1 THE MODEL OF CODEÇO

The original model in [15] is now modified as

$$\frac{dS}{dt} = n(H - S) - a(t)\lambda(B)S, \tag{152}$$

$$\frac{dI}{dt} = a(t)\lambda(B)S - rI, \tag{153}$$

$$\frac{dB}{dt} = e(t)I - \beta B, \tag{154}$$

which includes seasonal oscillations of the rate of exposure to contaminated water, $a(t)$, and the rate of human contribution to the population of the pathogen, $e(t)$, that are both periodic functions of time with a common period, $\omega = 365$ days, or 1 year:

$$a(t) = \bar{a}\left[1 + \tilde{a}\sin\left(\frac{2\pi t}{365}\right)\right], \qquad e(t) = \bar{e}\left[1 + \tilde{e}\sin\left(\frac{2\pi t}{365}\right)\right]. \tag{155}$$

The periodic contact rate $a(t)$ simulates the seasonal variations in water quality whereas the periodic per capita excretion rate simulates the seasonal variations in per capita water contamination. Here $\bar{a}$ (or $\bar{e}$) is the baseline value, or the time average, of $a(t)$ (or $e(t)$), and $\tilde{a}$ (or $\tilde{e}$) denotes the (relative) amplitude of the seasonal oscillation in $a(t)$ (or $e(t)$). To ensure both rates to be positive, we require $0 < \tilde{a} < 1$ and $0 < \tilde{e} < 1$. In this model, H is the total population, $\lambda(B) = B/(K+B)$ is the probability a susceptible person becomes infected with cholera, $\beta = mb - nb$ represents the net

death rate of vibrios, and only the environment-to-human transmission pathway is considered. The incidence is $f(t, I, B) = a(t)\lambda(B)$ and the pathogen function is $h(t, I, B) = e(t)I - \beta B$. It is easily verified that the assumptions (P-1) - (P-6) hold for the system (152) - (154).

The disease-free equilibrium is given by

$$X_0 = (S_0, I_0, B_0)^T = (H, 0, 0)^T. \tag{156}$$

From the next generation matrices

$$F(t) = \begin{bmatrix} 0 & \frac{a(t)H}{K} \\ 0 & 0 \end{bmatrix}, \qquad V(t) = \begin{bmatrix} r & 0 \\ -e(t) & \beta \end{bmatrix},$$

it follows that basic reproduction number of the time-averaged autonomous system, based on (120), is given by

$$[\mathcal{R}_0] = \frac{H}{r}\left(\frac{\bar{a}}{K}\frac{\bar{e}}{\beta}\right) = \frac{H\bar{a}\bar{e}}{Kr\beta}. \tag{157}$$

The evolution operator $Y(t, s)$ is given by

$$Y(t, s) = \begin{bmatrix} e^{-r(t-s)} & 0 \\ \tilde{Y}(t, s) & e^{-\beta(t-s)} \end{bmatrix}$$

where

$$\tilde{Y}(t, s) = e^{-r(t-s)}\bar{e}\left(\frac{1}{\beta - r} + \frac{\bar{e}}{\left(\frac{2\pi}{365}\right)^2 + (\beta - r)^2}\left[(\beta - r)\sin\left(\frac{2\pi t}{365}\right) - \frac{2\pi}{365}\cos\left(\frac{2\pi t}{365}\right)\right]\right)$$

$$- e^{-\beta(t-s)}\bar{e}\left(\frac{1}{\beta - r} + \frac{\bar{e}}{\left(\frac{2\pi}{365}\right)^2 + (\beta - r)^2}\left[(\beta - r)\sin\left(\frac{2\pi s}{365}\right) - \frac{2\pi}{365}\cos\left(\frac{2\pi s}{365}\right)\right]\right).$$

Thus,

$$G(t, s) = \sum_{k=0}^{\infty} Y(t, t - s - k\omega)F(t - s - k\omega)$$

$$\approx \frac{H\bar{a}}{K}\left(1 + \tilde{a}\sin\left(\frac{2\pi(t - s)}{365}\right)\right)\sum_{k=0}^{M}\begin{bmatrix} 0 & e^{-r(s+k\omega)} \\ 0 & \tilde{Y}(t, t - s - k\omega) \end{bmatrix}$$

for some positive integer M. To compute the basic reproduction number $\mathcal{R}_0$, the matrix A can be constructed by arranging the entries of G and the spectral radius of A can be numerically determined as described previously in Section 4.1. We have conducted numerical simulation to this model, and computed the reproductive
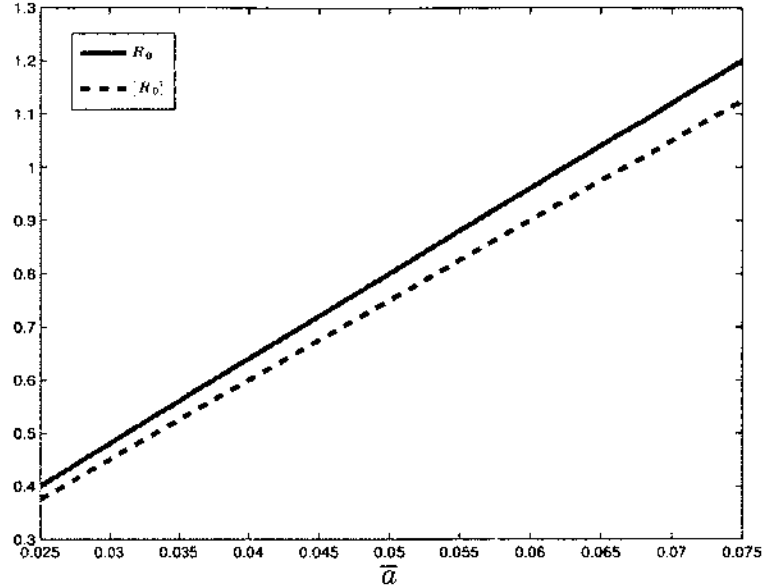
Figure 6. Plot of the periodic threshold of $\mathcal{R}_0$ for various $\bar{a}$. $\mathcal{R}_0 = 1$ when $\bar{a} \approx 0.0625$ and $[\mathcal{R}_0] = 1$ when $\bar{a} \approx 0.0667$.

numbers $\mathcal{R}_0$ and $[\mathcal{R}_0]$, for various values of $a(t)$ and $e(t)$. For illustration, we focus on the variation of $a(t)$ here. In Figures 6 and 7, we vary $\bar{a}$ and $\tilde{a}$, respectively, while keeping the values of other parameters fixed. In Figure 6, we see that $\mathcal{R}_0 = 1$ when $\bar{a} \approx 0.0625$ and $[\mathcal{R}_0] = 1$ when $\bar{a} \approx 0.0667$. It is clear that the time-averaged basic reproduction number underestimates the infection risk. Meanwhile, in Figure 7, we see that $\mathcal{R}_0 = 1$ when $\tilde{a} \approx 0.8407$ and $[\mathcal{R}_0] = 0.9$ for all $\tilde{a}$, again showing the inaccuracy of using $[\mathcal{R}_0]$ for infection prediction. In addition, Figure 8 shows a typical infection curve of this model when $\mathcal{R}_0 < 1$, where we observe the disease quickly dies out and the disease-free equilibrium is asymptotically stable. In contrast, Figure 9 is a typical infection curve of this model when $\mathcal{R}_0 > 1$, where the disease persists and there is a positive ω-periodic solution.

4.4.2 THE MODEL OF MUKANDAVIRE ET AL.

We extend the original model in [47] to a periodic environment based on the
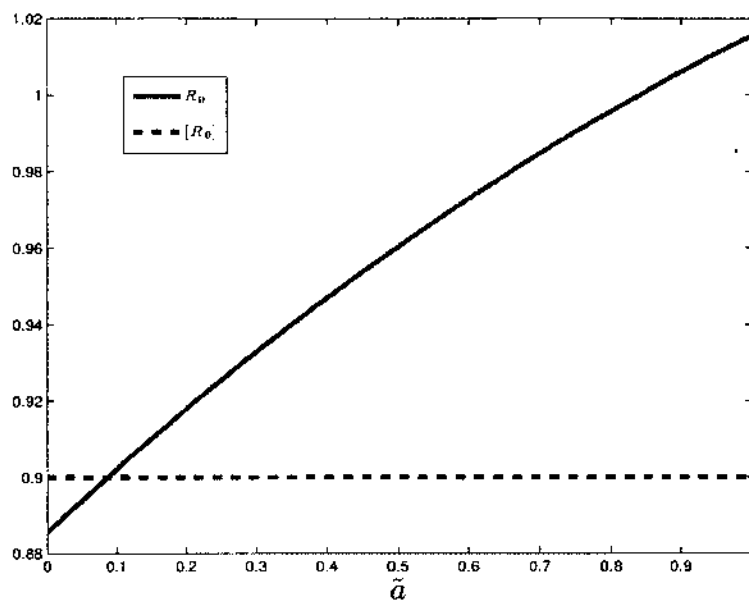
Figure 7. Plot of the periodic threshold of $\mathcal{R}_0$ for various $\tilde{a}$. $\mathcal{R}_0 = 1$ when $\tilde{a} \approx 0.8407$ and $[\mathcal{R}_0] = 0.90$ for all $\tilde{a}$.
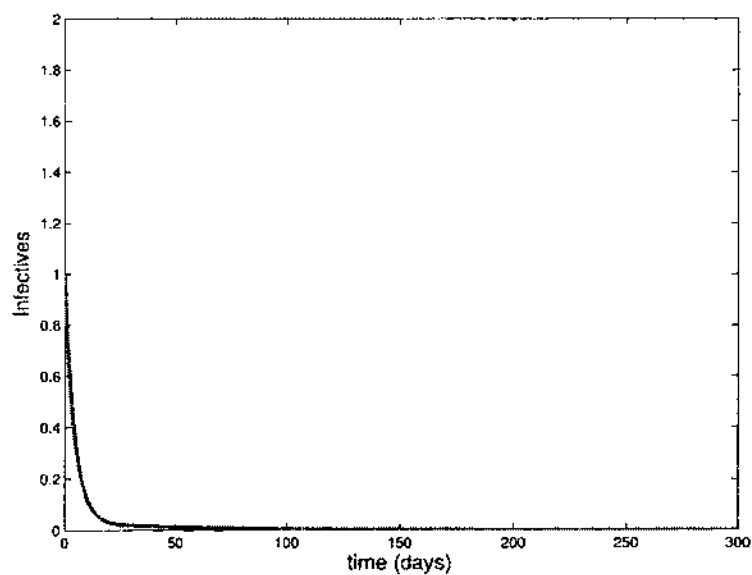

Figure 8. The model of Codeço: A typical infection curve when $\mathcal{R}_0 < 1$, with initial condition $I(0) = 1$. The solution quickly converges to the disease-free equilibrium with $I_0 = 0$.
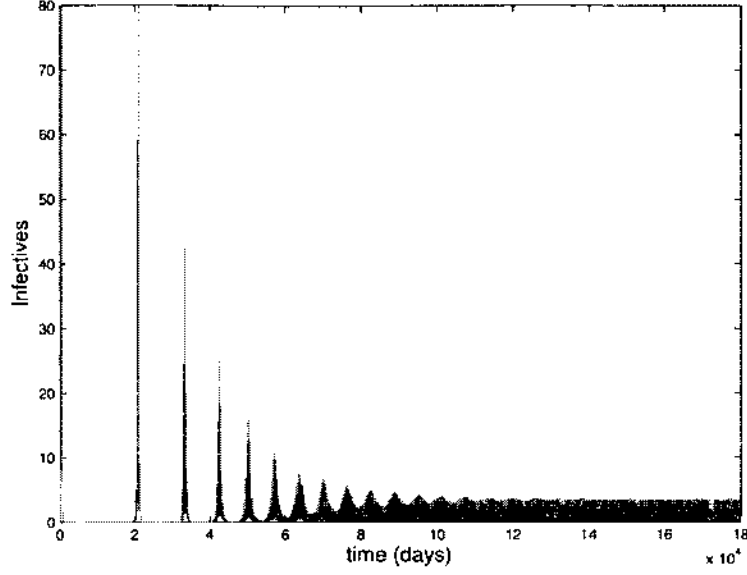
Figure 9. The model of Codeço: A typical infection curve when $\mathcal{R}_0 > 1$, with initial condition $I(0) = 1$. A periodic solution with $\omega = 365$ days forms after a long transient period.

following differential equations:

$$\frac{dS}{dt} = \mu N - \beta_e(t)S\frac{B}{\kappa + B} - \beta_h SI - \mu S, \tag{158}$$

$$\frac{dI}{dt} = \beta_e(t)S\frac{B}{\kappa + B} + \beta_h SI - (\gamma + \mu)I, \tag{159}$$

$$\frac{dB}{dt} = \xi(t)I - \delta B, \tag{160}$$

$$\frac{dR}{dt} = \gamma I - \mu R. \tag{161}$$

The two periodic functions are defined as

$$\beta_e(t) = \bar{\beta}_e\left[1 + \tilde{\beta}_e\sin\left(\frac{2\pi t}{365}\right)\right], \qquad \xi(t) = \bar{\xi}\left[1 + \tilde{\xi}\sin\left(\frac{2\pi t}{365}\right)\right], \tag{162}$$

where $\beta_e(t)$ is the environment-to-human transmission rate and $\xi(t)$ is the rate of contribution to V. cholerae in the aquatic environment. Though in different notations, $\beta_e(t)$ and $\xi(t)$ have the same meaning as $a(t)$ and $e(t)$ in (155). The incidence is $f(t, I, B) = \beta_e(t)\frac{B}{\kappa+B} + \beta_h I$ and the rate of change for the bacterial concentration is $h(t, I, B) = \xi(t)I - \delta B$. Both environment-to-human and human-to-human transmission pathways are included in this model; in particular, the environment-to-human

transmission factor is based on a saturating form, which is the same as that in model (152) - (154), and the human-to-human transmission mode takes a bilinear form. It is clear that the assumptions (P-1) - (P-6) hold for the system (158) - (161) as long as $0 < \bar{\beta}_e < 1$ and $0 < \tilde{\xi} < 1$.

The disease-free equilibrium is given by

$$X_0 = (S_0, I_0, B_0, R_0)^T = (N, 0, 0, 0)^T. \tag{163}$$

From the next generation matrices

$$F(t) = \begin{bmatrix} \beta_h N & \frac{\beta_e(t)N}{\kappa} \\ 0 & 0 \end{bmatrix}, \qquad V(t) = \begin{bmatrix} \gamma + \mu & 0 \\ -\xi(t) & \delta \end{bmatrix},$$

it follows that the time-averaged basic reproduction is

$$[\mathcal{R}_0] = \frac{N}{\gamma + \mu} \left(\beta_h + \frac{\bar{\beta}_e}{\kappa} \frac{\bar{\xi}}{\delta} \right) = \frac{N}{\delta\kappa(\gamma + \mu)} \left(\kappa\delta\beta_h + \bar{\xi}\bar{\beta}_e \right). \tag{164}$$

The evolution operator $Y(t,s)$ is given by

$$Y(t,s) = \begin{bmatrix} e^{-(\gamma-\mu)(t-s)} & 0 \\ \tilde{Y}(t,s) & e^{-\delta(t-s)} \end{bmatrix}$$

where

$$\begin{aligned}
\tilde{Y}(t,s) = & \; e^{-(\gamma+\mu)(t-s)}\bar{\xi}\left[\frac{1}{\delta - (\gamma + \mu)} \right. \\
& + \frac{\tilde{\xi}}{\left(\frac{2\pi}{365}\right)^2 + (\delta - (\gamma + \mu))^2} \left((\delta - (\gamma + \mu)) \sin\left(\frac{2\pi t}{365}\right) - \frac{2\pi}{365} \cos\left(\frac{2\pi t}{365}\right) \right) \right] \\
& - e^{-\delta(t-s)}\bar{\xi}\left[\frac{1}{\delta - (\gamma + \mu)} \right. \\
& + \frac{\tilde{\xi}}{\left(\frac{2\pi}{365}\right)^2 + (\delta - (\gamma + \mu))^2} \left((\delta - (\gamma + \mu)) \sin\left(\frac{2\pi s}{365}\right) - \frac{2\pi}{365} \cos\left(\frac{2\pi s}{365}\right) \right) \right].
\end{aligned}$$

Thus,

$$\begin{aligned}
G(t,s) = & \sum_{k=0}^{\infty} Y(t, t - s - k\omega)F(t - s - k\omega) \\
\approx & \; N \sum_{k=0}^{M} \begin{bmatrix} \beta_h e^{-(\gamma+\mu)(s+k\omega)} & \frac{\bar{\beta}_e}{\kappa}\left(1 + \bar{\beta}_e \sin\left(\frac{2\pi(t-s)}{365}\right)\right)e^{-(\gamma+\mu)(s+k\omega)} \\ \beta_h \tilde{Y}(t, t - s - k\omega) & \frac{\bar{\beta}_e}{\kappa}\left(1 + \bar{\beta}_e \sin\left(\frac{2\pi(t-s)}{365}\right)\right)\tilde{Y}(t, t - s - k\omega) \end{bmatrix}.
\end{aligned}$$

Using the function $G(t,s)$, the matrix A can be constructed and its spectral radius can be computed. In Figures 10 and 11, we vary $\bar{\beta}_e$ and $\bar{\beta}_e$, respectively, while
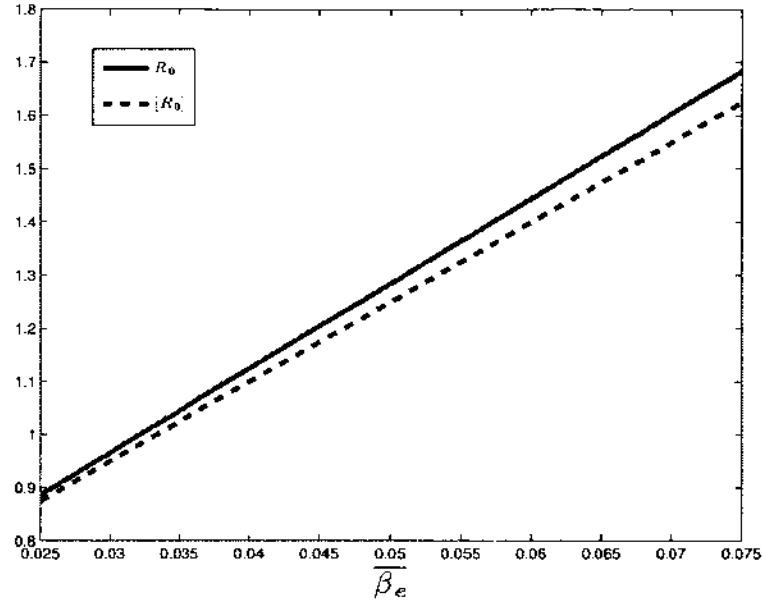
Figure 10. Plot of the periodic threshold of $\mathcal{R}_0$ for various $\bar{\beta}_e$. $\mathcal{R}_0 = 1$ when $\bar{\beta}_e \approx$ 0.0321 and $[\mathcal{R}_0] = 1$ when $\bar{\beta}_e \approx 0.0334$.

keeping other parameters fixed. In Figure 10, we again observe that the curve of $[\mathcal{R}_0]$ is below that of $\mathcal{R}_0$, and we notice that $\mathcal{R}_0 = 1$ when $\bar{\beta}_e \approx 0.0321$. In Figure 11, we see that $\mathcal{R}_0 = 1$ when $\tilde{\beta}_e \approx 0.05688$ and $[\mathcal{R}_0] = 0.9797$ for all $\tilde{\beta}_e$. Note that $\bar{\beta}_e$ and $\tilde{\beta}_e$ correspond to $\bar{a}$ and $\tilde{a}$, respectively, in (155). Comparing the result in Figure 10 to that in Figure 6, we see that a lower value of the magnitude of the indirect transmission rate ($\bar{\beta}_e \approx 0.0321$ versus $\bar{a} \approx 0.0625$) is needed to reach the threshold value $\mathcal{R}_0 = 1$ for the current model, due to the incorporation of the direct transmission mode. Similarly, we observe that the values of $[\mathcal{R}_0]$ in Figures 10 and 11 are lower than those in Figures 6 and 7 for the same value of the parameter. In addition, Figure 12 is an infection curve when $\mathcal{R}_0 < 1$, and Figure 13 is an infection curve when $\mathcal{R}_0 > 1$, for the current model. We observe similar patterns as in Figures 8 and 9. Figure 14 shows a zoomed-in picture for the periodic model of Mukandavire et al. where the periodic solution is highlighted and a period of $\omega = 365$ days (or 1 year) can be observed.

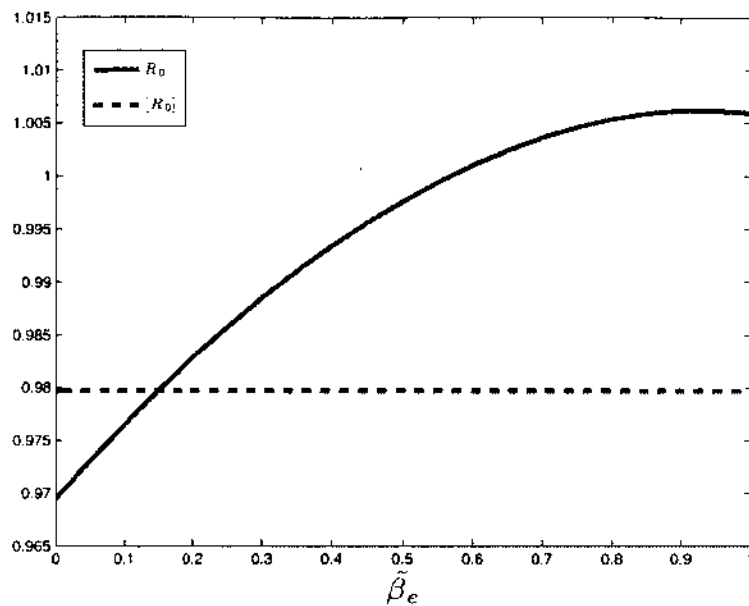Figure 11. Plot of the periodic threshold of $\mathcal{R}_0$ for various $\tilde{\beta}_e$. $\mathcal{R}_0 = 1$ when $\tilde{\beta}_e \approx$ 0.5688 and $[\mathcal{R}_0] = 0.9797$ for all $\tilde{\beta}_e$.

Figure 12. The model of Mukandavire *et al.*: A typical infection curve when $\mathcal{R}_0 < 1$, with initial condition $I(0) = 1$. The solution quickly converges to the disease-free equilibrium with $I_0 = 0$.
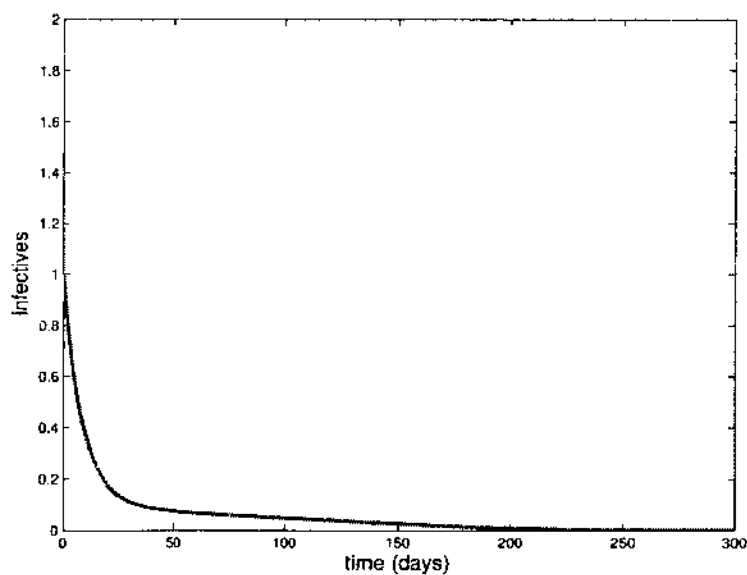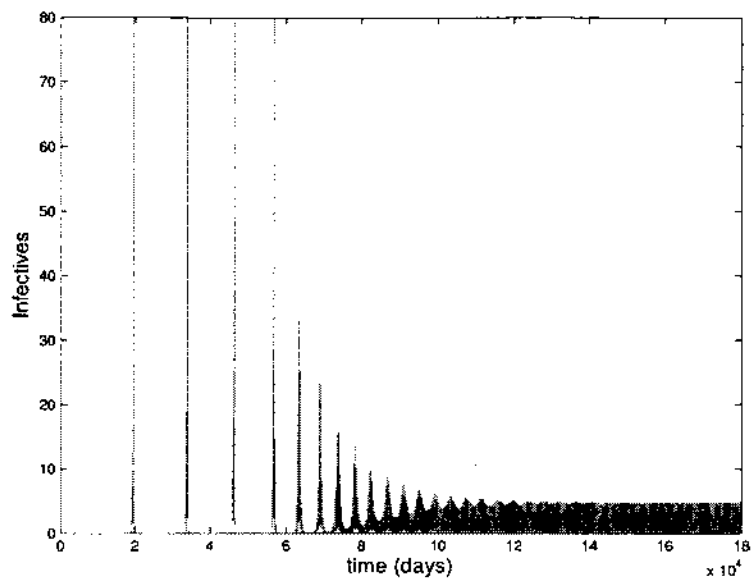
Figure 13. The model of Mukandavire *et al.*: A typical infection curve when $\mathcal{R}_0 > 1$, with initial condition $I(0) = 1$. A periodic solution with $\omega = 365$ days forms after a long transient period.
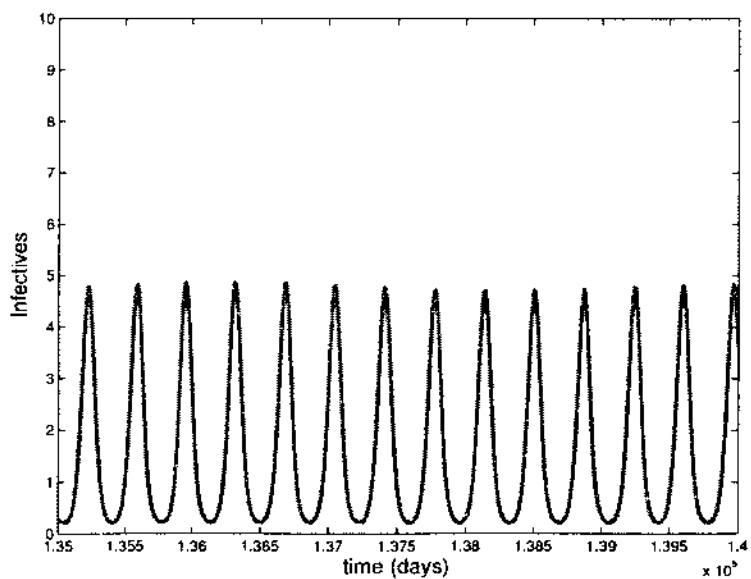

Figure 14. A typical infection curve for the model of Mukandavire *et al.* when $\mathcal{R}_0 > 1$, with initial condition $I(0) = 1$ zoomed in.

4.4.3 THE MODEL OF TIEN AND EARN

The original model in [62], where the pathogen concentration is denoted W instead of B, is extended to a periodic environment in the form of

$$\frac{dS}{dt} = \mu N - b_W(t)WS - b_I SI - \mu S, \tag{165}$$

$$\frac{dI}{dt} = b_W(t)WS + b_I SI - (\gamma + \mu)I, \tag{166}$$

$$\frac{dW}{dt} = \alpha(t)I - \xi W, \tag{167}$$

$$\frac{dR}{dt} = \gamma I - \mu R, \tag{168}$$

where

$$b_W(t) = \bar{b_W}\left[1 + \tilde{b_W}\sin\left(\frac{2\pi t}{365}\right)\right], \qquad \alpha(t) = \bar{\alpha}\left[1 + \tilde{\alpha}\sin\left(\frac{2\pi t}{365}\right)\right], \tag{169}$$

denote the water-to-person transmission rate and the shedding rate from infected individuals into the water, respectively. Here the time-periodic parameters $b_W(t)$ and $\alpha(t)$ play the same role as $a(t)$ and $e(t)$ in model (152) - (154), or $\beta_e(t)$ and $\xi(t)$ in model (158) - (160). The incidence in the current model is $f(t, I, W) = b_W(t)W + I$ and the pathogen function is $h(t, I, W) = \alpha(t)I - \xi W$. The dual-transmission pathways are included in this model by using bilinear forms, however, no saturation effect was considered. It is straightforward to verify that the assumptions (P-1) - (P-6) hold for the system (165) - (168) given that $0 < \bar{b_W} < 1$ and $0 < \tilde{\alpha} < 1$.

Clearly, the disease-free equilibrium is given by

$$X_0 = (S_0, I_0, W_0, R_0)^T = (N, 0, 0, 0)^T. \tag{170}$$

From the next generation matrices

$$F(t) = \begin{bmatrix} Nb_I & Nb_W(t) \\ 0 & 0 \end{bmatrix}, \qquad V(t) = \begin{bmatrix} \gamma + \mu & 0 \\ -\alpha(t) & \xi \end{bmatrix},$$

it follows that

$$[\mathcal{R}_0] = \frac{N}{\gamma + \mu}\left(b_I + \bar{b_W}\frac{\bar{\alpha}}{\xi}\right) = \frac{N}{\xi(\gamma + \mu)}\left(\xi b_I + \bar{\alpha}\bar{b_W}\right). \tag{171}$$

The evolution operator $Y(t, s)$ is given by

$$Y(t, s) = \begin{bmatrix} e^{-(\gamma + \mu)(t - s)} & 0 \\ \tilde{Y}(t, s) & e^{-\xi(t - s)} \end{bmatrix},$$

where

$$\bar{Y}(t,s) = e^{-(\gamma+\mu)(t-s)}\bar{\alpha}\left[\frac{1}{\xi-(\gamma+\mu)}\right.$$
$$\left.+\frac{\bar{\alpha}}{\left(\frac{2\pi}{365}\right)^2+(\xi-(\gamma+\mu))^2}\left((\xi-(\gamma+\mu))\sin\left(\frac{2\pi t}{365}\right)-\frac{2\pi}{365}\cos\left(\frac{2\pi t}{365}\right)\right)\right]$$
$$-e^{-\xi(t-s)}\bar{\alpha}\left[\frac{1}{\xi-(\gamma+\mu)}\right.$$
$$\left.+\frac{\bar{\alpha}}{\left(\frac{2\pi}{365}\right)^2+(\xi-(\gamma+\mu))^2}\left((\xi-(\gamma+\mu))\sin\left(\frac{2\pi s}{365}\right)-\frac{2\pi}{365}\cos\left(\frac{2\pi s}{365}\right)\right)\right].$$

Thus,

$$G(t,s) = \sum_{k=0}^{\infty} Y(t,t-s-k\omega)F(t-s-k\omega)$$

$$\approx N\sum_{k=0}^{M}\left[\begin{array}{cc} b_I e^{-(\gamma+\mu)(s+k\omega)} & \bar{b_W}\left(1+\tilde{b_W}\sin\left(\frac{2\pi(t-s)}{365}\right)\right)e^{-(\gamma+\mu)(s-k\omega)} \\ b_I\bar{Y}(t,t-s-k\omega) & \bar{b_W}\left(1+\tilde{b_W}\sin\left(\frac{2\pi(t-s)}{365}\right)\right)\bar{Y}(t,t-s-k\omega) \end{array}\right].$$

We have conducted similar numerical simulations as before and calculated the two reproduction numbers. In presenting the results of $\mathcal{R}_0$, we could, in principle, vary $\bar{b_W}$ while keeping other parameters fixed. However, due to the bilinear form of the indirect transmission mode employed in the current model, the meaningful values of $\bar{b_W}$ are several magnitudes smaller than those of $\bar{a}$ in equation (155), or $\bar{\beta}_c$ in equation (162), making it impossible to compare the result with the other two models. Thus, we have chosen to only present the result of $\mathcal{R}_0$ (and $[\mathcal{R}_0]$) versus $\bar{b_W}$ in Figure 15. We see that $\mathcal{R}_0 = 1$ when $\bar{b_W} \approx 0.3706$ and $[\mathcal{R}_0] = 0.9872$ for all $\bar{b_W}$. The result shows similar pattern to that in Figure 11 as both models include dual transmission pathways. Figure 16 displays an infection curve when $\mathcal{R}_0 < 1$ for the current model, and Figure 18 shows an infection curve when $\mathcal{R}_0 > 1$.

Finally, from Figures 8, 12 and 16, as expected, we see that when $\mathcal{R}_0 < 1$, the infected population I quickly decreases to zero and stays there forever (for example, see Figure 17 for the long term behavior of the periodic model of Tien and Earn), showing that the disease dies out in each model. Indeed, similar patterns were observed for various initial conditions (not shown here), an evidence that the disease-free equilibrium is globally asymptotically stable for each model. Figures 9, 13 and 18 illustrate typical infection curves for the three models when $\mathcal{R}_0 > 1$. In this case, for each model, the disease persists and after a long, transient period, the infection approaches a positive ω-periodic solution.
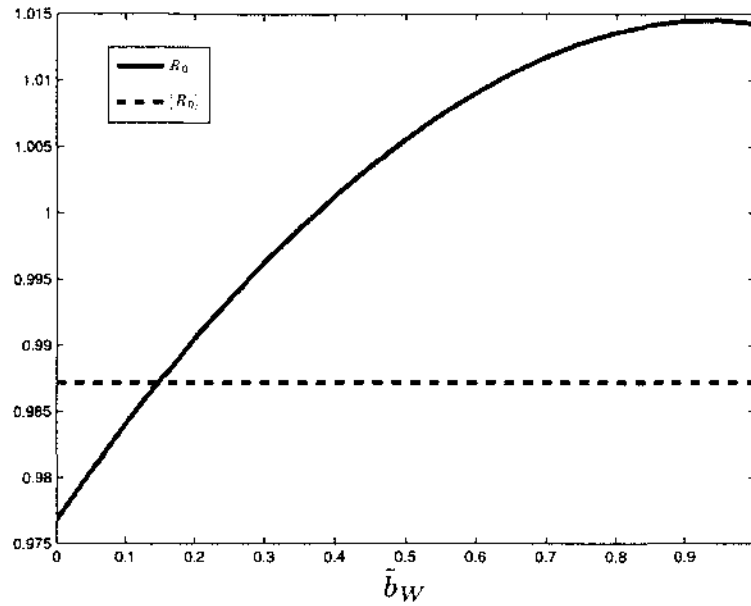
Figure 15. Plot of the periodic threshold of $\mathcal{R}_0$ for various $\tilde{b}_W$. $\mathcal{R}_0 = 1$ when $\tilde{b}_W \approx 0.3706$ and $[\mathcal{R}_0] = 0.9872$ for all $\tilde{b}_W$.
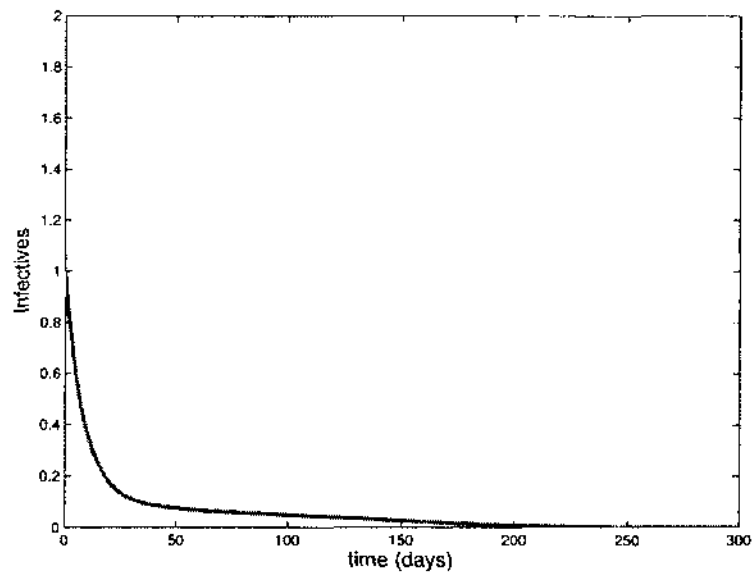
Figure 16. The model of Tien and Earn: A typical infection curve when $\mathcal{R}_0 < 1$, with initial condition $I(0) = 1$. The solution quickly converges to the disease-free equilibrium with $I_0 = 0$.
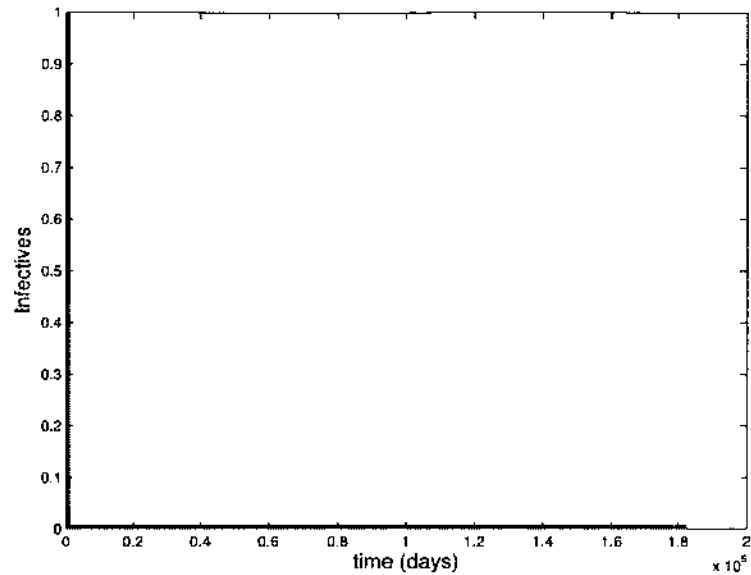
Figure 17. The model of Tien and Earn: Long-term behavior of a typical infection curve when $\mathcal{R}_0 < 1$, with initial condition $I(0) = 1$. The solution quickly converges to the disease-free equilibrium with $I_0 = 0$.
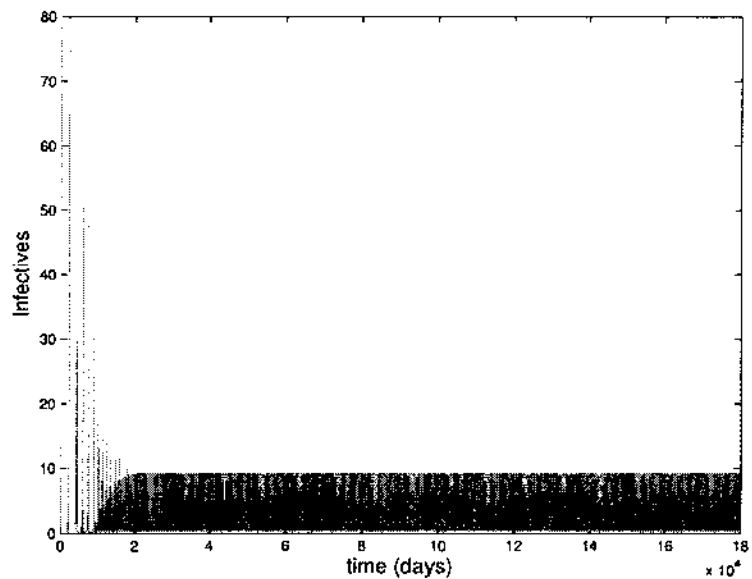
Figure 18. The model of Tien and Earn: A typical infection curve when $\mathcal{R}_0 > 1$, with initial condition $I(0) = 1$. A periodic solution with $\omega = 365$ days forms after a long transient period.

4.5 MULTI-GROUP CHOLERA MODEL WITH SEASONALITY

Finally, we extend the generalized multi-group model in Chapter 3 to a periodic environment, thus, incorporating spatial and temporal heterogeneity. Therefore, we have the following dynamical system,

$$\frac{dS_i}{dt} = bN_i - \sum_{j=1}^{n} S_i f_j(t, I_j, B_j) - bS_i , \tag{172}$$

$$\frac{dI_i}{dt} = \sum_{j=1}^{n} S_i f_j(t, I_j, B_j) - (\gamma_i + b)I_i , \qquad i = 1, \ldots, n \tag{173}$$

$$\frac{dR_i}{dt} = \gamma_i I_i - bR_i , \tag{174}$$

$$\frac{dB_i}{dt} = h_i(t, I_i, B_i) . \tag{175}$$

The functions $f_i(t, I_i, B_i)$ and $h_i(t, I_i, B_i)$ are both differentiable and periodic in time with a common period ω. Hence, we have

$$f_i(t + \omega, I_i, B_i) = f_i(t, I_i, B_i) \qquad \text{and} \qquad h_i(t + \omega, I_i, B_i) = h_i(t, I_i, B_i).$$

We assume (P-1) - (P-6) are satisfied for $i = 1, \ldots, n$ and $t \geq 0$. It is clear that the disease-free equilibrium is given by

$$X_0 = (S_1^0, I_1^0, B_1^0, \ldots, S_n^0, I_n^0, B_n^0) = (N_1, 0, 0, \ldots, N_n, 0, 0). \tag{176}$$

For convenience, let

$$\frac{\partial f_i}{\partial I_i}(t, 0, 0) \equiv p_i(t) , \qquad \frac{\partial f_i}{\partial B_i}(t, 0, 0) \equiv q_i(t) ,$$

$$\frac{\partial h_i}{\partial I_i}(t, 0, 0) \equiv r_i(t) , \qquad \frac{\partial h_i}{\partial B_i}(t, 0, 0) \equiv u_i(t) ,$$

for $i = 1, \ldots, n$. Then, the next generation matrices evaluated at the disease-free equilibrium, X_0, are given by

$$F(t) = \begin{bmatrix} N_1 p_1(t) & \cdots & N_1 p_n(t) & N_1 q_1(t) & \cdots & N_1 q_n(t) \\ \vdots & \ddots & \vdots & \vdots & \ddots & \vdots \\ N_n p_1(t) & \cdots & N_n p_n(t) & N_n q_1(t) & \cdots & N_n q_n(t) \\ 0 & \cdots & 0 & 0 & \cdots & 0 \\ \vdots & \ddots & \vdots & \vdots & \ddots & \vdots \\ 0 & \cdots & 0 & 0 & \cdots & 0 \end{bmatrix} ;$$

$$V(t) = \begin{bmatrix} \gamma_1+b & 0 & \cdots & \cdots & \cdots & \cdots & \cdots & \cdots & \cdots & 0 \\ 0 & \gamma_2+b & 0 & \cdots & \cdots & \cdots & \cdots & \cdots & \cdots & 0 \\ \vdots & \ddots & \ddots & \ddots & \cdots & \cdots & \cdots & \cdots & \cdots & \vdots \\ \vdots & \ddots & \ddots & \ddots & \ddots & \cdots & \cdots & \cdots & \cdots & \vdots \\ 0 & \cdots & \cdots & 0 & \gamma_n+b & 0 & \cdots & \cdots & \cdots & 0 \\ -r_1(t) & 0 & \cdots & \cdots & 0 & -u_1(t) & 0 & \cdots & \cdots & 0 \\ 0 & -r_2(t) & 0 & \cdots & \cdots & 0 & -u_2(t) & 0 & \cdots & 0 \\ \vdots & \ddots & \ddots & \ddots & \cdots & \ddots & \ddots & \ddots & \ddots & \vdots \\ \vdots & \cdots & \ddots & \ddots & \ddots & \cdots & \ddots & \ddots & \ddots & 0 \\ 0 & \cdots & \cdots & 0 & -r_n(t) & 0 & \cdots & \cdots & 0 & -u_n(t) \end{bmatrix}.$$

It follows that the time-averaged basic reproduction number is given by

$$[R_0] = \rho([F][V]^{-1}) = \sum_{i=1}^{n} \frac{N_i}{\gamma_i+b} \left\{ \left[\frac{\partial f_i}{\partial I_i}\right] - \left[\frac{\partial f_i}{\partial B_i}\right] \left[\frac{\partial h_i}{\partial B_i}\right]^{-1} \left[\frac{\partial h_i}{\partial I_i}\right] \right\}. \tag{177}$$

The evolution operator $Y(t,s)$ is given by

$$Y(t,s) = \begin{bmatrix} E & 0 \\ J & U \end{bmatrix},$$

where

$$E = \begin{bmatrix} e^{-(\gamma_1+b)(t-s)} & 0 & \cdots & \cdots & 0 \\ 0 & e^{-(\gamma_2+b)(t-s)} & 0 & \cdots & \vdots \\ \vdots & & \ddots & \ddots & \ddots & \vdots \\ \vdots & & \ddots & \ddots & \ddots & 0 \\ 0 & & \cdots & \cdots & 0 & e^{-(\gamma_n+b)(t-s)} \end{bmatrix},$$

$$U = \begin{bmatrix} e^{\int_s^t u_1(\tau)d\tau} & 0 & \cdots & \cdots & 0 \\ 0 & e^{\int_s^t u_2(\tau)d\tau} & 0 & \cdots & \vdots \\ \vdots & & \ddots & \ddots & \vdots \\ \cdots & & \ddots & \ddots & 0 \\ 0 & & \cdots & \cdots & 0 & e^{\int_s^t u_n(\tau)d\tau} \end{bmatrix},$$

and

$$J = \begin{bmatrix} \tilde{Y}_1(t,s) & 0 & \cdots & \cdots & 0 \\ 0 & \tilde{Y}_2(t,s) & 0 & \cdots & \vdots \\ \vdots & & \ddots & \ddots & \ddots & \vdots \\ \vdots & & \ddots & \ddots & \ddots & 0 \\ 0 & & \cdots & \cdots & 0 & \tilde{Y}_n(t,s) \end{bmatrix},$$

with

$$\bar{Y}_i(t,s) = \left\{ \int_s^t e^{-\int_s^\tau u_i(z)dz} r_i(\tau) e^{-(\gamma_i+b)(\tau-s)} d\tau \right\} \Big/ e^{-\int_s^t u_i(\tau)d\tau} .$$

Thus,

$$G(t,s) \approx \sum_{k=0}^{M} Y(t,t-s-k\omega)F(t-s-k\omega)$$

$$\approx \sum_{k=0}^{M} \begin{bmatrix} A_1 & A_2 \\ A_3 & A_4 \end{bmatrix},$$

where

$$A_1 = \begin{bmatrix} N_1 p_1(t-s-k\omega)e^{(\gamma_1-b)(s+k\omega)} & \cdots & N_1 p_n(t-s-k\omega)e^{(\gamma_1-b)(s+k\omega)} \\ \vdots & \ddots & \vdots \\ N_n p_1(t-s-k\omega)e^{(\gamma_n-b)(s+k\omega)} & \cdots & N_n p_n(t-s-k\omega)e^{(\gamma_n-b)(s+k\omega)} \end{bmatrix},$$

$$A_2 = \begin{bmatrix} N_1 q_1(t-s-k\omega)e^{(\gamma_1-b)(s+k\omega)} & \cdots & N_1 q_n(t-s-k\omega)e^{(\gamma_1-b)(s+k\omega)} \\ \vdots & \ddots & \vdots \\ N_n q_1(t-s-k\omega)e^{(\gamma_n-b)(s+k\omega)} & \cdots & N_n q_n(t-s-k\omega)e^{(\gamma_n-b)(s+k\omega)} \end{bmatrix},$$

$$A_3 = \begin{bmatrix} N_1 p_1(t-s-k\omega)\tilde{Y}_1(t,t-s-k\omega) & \cdots & N_1 p_n(t-s-k\omega)\tilde{Y}_1(t,t-s-k\omega) \\ \vdots & \ddots & \vdots \\ N_n p_1(t-s-k\omega)\tilde{Y}_n(t,t-s-k\omega) & \cdots & N_n p_n(t-s-k\omega)\tilde{Y}_n(t,t-s-k\omega) \end{bmatrix},$$

$$A_4 = \begin{bmatrix} N_1 q_1(t-s-k\omega)\tilde{Y}_1(t,t-s-k\omega) & \cdots & N_1 q_n(t-s-k\omega)\tilde{Y}_1(t,t-s-k\omega) \\ \vdots & \ddots & \vdots \\ N_n q_1(t-s-k\omega)\tilde{Y}_n(t,t-s-k\omega) & \cdots & N_n q_n(t-s-k\omega)\tilde{Y}_n(t,t-s-k\omega) \end{bmatrix}.$$

4.5.1 DISEASE EXTINCTION OF A PERIODIC MULTI-GROUP MODEL

We follow a similar argument of disease extinction as that seen in Section 4.2 for the general periodic model (115) - (118). First, consider the matrix function $F(t) - V(t)$,

$$F(t) - V(t) = \begin{bmatrix} C_1 & C_2 \\ C_3 & C_4 \end{bmatrix}, \tag{178}$$

where

$$C_1 = \begin{bmatrix} N_1p_1(t) - (\gamma_1 + b) & N_1p_2(t) & \cdots & N_1p_n(t) \\ N_2p_1(t) & N_2p_2(t) - (\gamma_2 + b) & \cdots & N_2p_n(t) \\ \vdots & \cdots & \ddots & \vdots \\ N_np_1(t) & \cdots & \cdots & N_np_n(t) - (\gamma_n + b) \end{bmatrix} ;$$

$$C_2 = \begin{bmatrix} N_1q_1(t) & \cdots & \cdots & N_1q_n(t) \\ N_2q_1(t) & \cdots & \cdots & N_2q_n(t) \\ \vdots & \cdots & \cdots & \vdots \\ N_nq_1(t) & \cdots & \cdots & N_nq_n(t) \end{bmatrix} ;$$

$$C_3 = \begin{bmatrix} r_1(t) & 0 & \cdots & 0 \\ 0 & r_2(t) & \cdots & 0 \\ \vdots & \ddots & \ddots & \vdots \\ 0 & 0 & \cdots & r_n(t) \end{bmatrix} ; \quad C_4 = \begin{bmatrix} u_1(t) & 0 & \cdots & 0 \\ 0 & u_2(t) & \cdots & \vdots \\ \vdots & \ddots & \ddots & \vdots \\ 0 & 0 & \cdots & u_n(t) \end{bmatrix} .$$

Note that $F(t) - V(t)$ is continuous, cooperative, irreducible and ω-periodic. Using assumption (P-4), it follows that

$$\frac{dI_i}{dt} = \sum_{j=1}^{n} S_i f_j(I_j, B_j) - (\gamma_i + b)I_i \leq \sum_{j=1}^{n} N_i \{I_j p_j(t) + B_j q_j(t)\} - (\gamma_i + b)I_i, \quad (179)$$

and

$$\frac{dB_i}{dt} = h_i(t, I_i, B_i) \leq I_i r_i(t) + B_i u_i(t). \quad (180)$$

Thus,

$$\frac{d}{dt} \begin{bmatrix} I_1 \\ \vdots \\ I_n \\ B_1 \\ \vdots \\ B_n \end{bmatrix} \leq [F(t) - V(t)] \begin{bmatrix} I_1 \\ \vdots \\ I_n \\ B_1 \\ \vdots \\ B_n \end{bmatrix} . \quad (181)$$

Therefore, by a similar argument presented in Section 4.2, we obtain the following result.

Theorem 21. *If $\mathcal{R}_0 < 1$, then the disease-free equilibrium of the model (172) - (175) is globally asymptotically stable, and $\lim_{t\to\infty} X(t) = X_0 = (N, 0, 0, 0)^T$ for any solution $X(t)$ of the system (172) - (175).*

4.5.2 DISEASE PERSISTENCE OF A PERIODIC MULTI-GROUP MODEL

Again, we take a similar approach to proving uniform persistence as the proof in Section 4.3. Let $\mathcal{R}_0 > 1$ and define

$$X = \mathbb{R}_+^{3n}; \qquad X_0 = \mathbb{R}_+^n \times \text{Int}(\mathbb{R}_+^n) \times \text{Int}(\mathbb{R}_+^n); \qquad \partial X_0 = X \backslash X_0.$$

Let $P : X \to X$ be the Poincaré map associated with the model (172) - (175) such that $P(x_0) = u(\omega, x_0)$ for all $x_0 \in X$, where $u(t, x_0)$ denotes the unique solution of the system with $u(0, x_0) = x_0$.

Let $S = (S_1, \ldots, S_n)$, $I = (I_1, \ldots, I_n)$, $B = (B_1, \ldots, B_n)$ and set

$$M_\partial = \{(S(0), I(0), B(0)) \in \partial X_0 : P^m(S(t), I(t), B(t)) \in \partial X_0 \; \forall m \geq 0\}.$$

Consider the fixed point $M_0 = (N, 0, 0)$ where $N = (N_1, \ldots, N_n)$. And define $W^S(M_0) = \{x_0 : P^m(x_0) \to M_0, m \to \infty\}$. We show that

$$W^S(M_0) \bigcap X_0 = \emptyset.$$

Based on the continuity of solutions with respect to the initial conditions, for any $\epsilon > 0$, there exists $\delta > 0$ small enough such that for all $(S(0), I(0), B(0)) \in X_0$ with $\|(S(0), I(0), B(0)) - M_0\| \leq \delta$, we have

$$\|u(t, (S(0), I(0), B(0))) - u(t, M_0)\| < \epsilon, \qquad \forall t \in [0, \omega].$$

We make the claim that

$$\limsup_{m \to \infty} \|P^m(S(0), I(0), B(0)) - M_0\| \geq \delta, \qquad \forall (S(0), I(0), B(0)) \in X_0.$$

Suppose by contradiction; that is, we suppose $\limsup_{m \to \infty} \|P^m(S(0), I(0), B(0)) - M_0\| < \delta$ for some $(S(0), I(0), B(0)) \in X_0$. Without loss of generality, we assume that $\|P^m(S(0), I(0), B(0)) - M_0\| < \delta, \forall m \geq 0$. Thus,

$$\|u(t, P^m(S(0), I(0), B(0))) - u(t, M_0)\| < \epsilon, \qquad \forall t \in [0, \omega] \text{ and } m \geq 0.$$

Moreover, for any $t \geq 0$, we can write $t = t' + n\omega$, where $t' \in [0, \omega)$ and n being the greatest integer less than or equal to t/ω. Then we obtain

$$\|u(t, (S(0), I(0), B(0))) - u(t, M_0)\| = \|u(t', P^m(S(0), I(0), B(0))) - u(t', M_0)\| < \epsilon$$

for any $t \geq 0$. Let $(S(t), I(t), B(t)) = u(t, (S(0), I(0), B(0)))$. It follows that $N - \epsilon < S(t) < N + \epsilon$, $0 < I(t) < \epsilon$ and $0 < B(t) < \epsilon$, and thus,

$$N_i - \epsilon < S_i(t) < N_i + \epsilon, \qquad 0 < I_i(t) < \epsilon, \qquad 0 < B_i(t) < \epsilon.$$

Again, note that $\epsilon < \epsilon^*$. Then, assuming (P-1) and (P-6), we have

$$\frac{dI_i}{dt} = \sum_{j=1}^{n} S_i f_j(t, I_j, B_j) - (\gamma_i + b)I_i$$

$$\geq \sum_{j=1}^{n} (N_i - \epsilon) \cdot f_j(t, I_j, B_j) - (\gamma_i + b)I_i$$

$$\geq \sum_{j=1}^{n} (N_i - \epsilon) \cdot \left(f_j(t, 0, 0) + I_j \cdot \frac{\partial f_j}{\partial I_j}(t, 0, 0) + B_j \cdot \frac{\partial f_j}{\partial B_j}(t, 0, 0) \right.$$

$$\left. + \frac{1}{2}I_j^2 \cdot \frac{\partial^2 f_j}{\partial I_j^2}(t, 0, 0) + I_j \cdot B_j \cdot \frac{\partial^2 f_j}{\partial I_j \partial B_j}(t, 0, 0) + \frac{1}{2}B_j^2 \cdot \frac{\partial^2 f_j}{\partial B_j^2}(t, 0, 0) \right) - (\gamma_i + b)I_i$$

$$\geq \sum_{j=1}^{n} N_i \cdot \left(I_j \cdot \frac{\partial f_j}{\partial I_j}(t, 0, 0) + B_j \cdot \frac{\partial f_j}{\partial B_j}(t, 0, 0) \right) - (\gamma_i + b)I_i$$

$$+ \sum_{j=1}^{n} N_i \cdot \left(\epsilon \cdot \frac{1}{2}I_j \cdot \frac{\partial^2 f_j}{\partial I_j^2}(t, 0, 0) + \epsilon \cdot \frac{1}{2}B_j \cdot \frac{\partial^2 f_j}{\partial B_j^2}(t, 0, 0) - \epsilon \cdot I_j \cdot \left| \frac{\partial^2 f_j}{\partial I_j \partial B_j}(t, 0, 0) \right| \right)$$

$$- \sum_{j=1}^{n} \epsilon \cdot \left(I_j \cdot \frac{\partial f_j}{\partial I_j}(t, 0, 0) + B_j \cdot \frac{\partial f_j}{\partial B_j}(t, 0, 0) - \epsilon \cdot I_j \left| \frac{\partial^2 f_j}{\partial I_j \partial B_j}(t, 0, 0) \right| \right),$$

and

$$\frac{dB_i}{dt} = h_i(t, I_i, B_i)$$

$$\geq h_i(t, 0, 0) + I_i \cdot \frac{\partial h_i}{\partial I_i}(t, 0, 0) + B_i \cdot \frac{\partial h_i}{\partial B_i}(t, 0, 0)$$

$$+ \frac{1}{2}I_i^2 \cdot \frac{\partial^2 h_i}{\partial I_i^2}(t, 0, 0) + I_i \cdot B_i \cdot \frac{\partial^2 h_i}{\partial I_i \partial B_i}(t, 0, 0) + \frac{1}{2}B_i^2 \cdot \frac{\partial^2 h_i}{\partial B_i^2}(t, 0, 0)$$

$$\geq I_i \cdot \frac{\partial h_i}{\partial I_i}(t, 0, 0) + B_i \cdot \frac{\partial h_i}{\partial B_i}(t, 0, 0)$$

$$+ \epsilon \cdot \frac{1}{2}I_i \cdot \frac{\partial^2 h_i}{\partial I_i}(t, 0, 0) + \epsilon \cdot \frac{1}{2}B_i \cdot \frac{\partial^2 h_i}{\partial B_i^2}(t, 0, 0) - \epsilon \cdot I_i \cdot \left| \frac{\partial^2 h_i}{\partial I_i \partial B_i}(t, 0, 0) \right|.$$

For further convenience, let

$$\frac{\partial^2 f_i}{\partial I_i^2}(t, 0, 0) \equiv \hat{p}_i(t), \qquad \frac{\partial^2 f_i}{\partial B_i^2}(t, 0, 0) \equiv \hat{q}_i(t), \qquad \frac{\partial^2 f_i}{\partial I_i \partial B_i}(t, 0, 0) \equiv \hat{f}_i(t),$$

$$\frac{\partial^2 h_i}{\partial I_i^2}(t, 0, 0) \equiv \hat{r}_i(t), \qquad \frac{\partial^2 h_i}{\partial B_i^2}(t, 0, 0) \equiv \hat{u}_i(t), \qquad \frac{\partial^2 h_i}{\partial I_i \partial B_i}(t, 0, 0) \equiv \hat{h}_i(t),$$

for $i = 1, \ldots, n$. Thus,

$$\frac{dI_i}{dt} \leq \sum_{j=1}^{n} N_i \cdot (I_j \cdot p_j(t) + B_j \cdot q_j(t)) - (\gamma_i + b)I_i + \sum_{j=1}^{n} N_i \cdot \left(\epsilon \cdot \frac{1}{2} I_j \cdot \hat{p}_j(t) + \epsilon \cdot \frac{1}{2} B_j \cdot \hat{q}_j(t) \right.$$

$$\left. - \epsilon \cdot I_j \cdot \left| \hat{f}_j(t) \right| \right) - \sum_{j=1}^{n} \epsilon \cdot \left(I_j \cdot p_j(t) + B_j \cdot q_j(t) - \epsilon \cdot I_j \left| \hat{f}_j(t) \right| \right),$$

and

$$\frac{dB_i}{dt} \leq I_i \cdot r_i(t) + B_i \cdot u_i(t) + \epsilon \cdot \frac{1}{2} I_i \cdot \hat{r}_i(t) + \epsilon \cdot \frac{1}{2} B_i \cdot \hat{u}_i(t) - \epsilon \cdot I_i \cdot \left| \hat{h}_i(t) \right|.$$

Hence, we obtain

$$\begin{bmatrix} dI_1/dt \\ \vdots \\ dI_n/dt \\ dB_1/dt \\ \vdots \\ dB_n/dt \end{bmatrix} \geq \begin{bmatrix} F - V - \epsilon \cdot K \end{bmatrix} \cdot \begin{bmatrix} I_1 \\ \vdots \\ I_n \\ B_1 \\ \vdots \\ B_n \end{bmatrix},$$

where $F - V$ was given by equation (178) and

$$-\epsilon \cdot K = \epsilon \cdot \begin{bmatrix} D_1 & D_2 \\ D_3 & D_4 \end{bmatrix}, \tag{182}$$

where

$$D_1 = \begin{bmatrix} \frac{1}{2} N_1 \hat{p}_1(t) - p_1(t) - (N_1 + \epsilon)|\hat{f}_1(t)| & \cdots & \frac{1}{2} N_1 \hat{p}_n(t) - p_n(t) - (N_1 + \epsilon)|\hat{f}_n(t)| \\ \vdots & \ddots & \vdots \\ \frac{1}{2} N_n \hat{p}_1(t) - p_1(t) - (N_n + \epsilon)|\hat{f}_1(t)| & \cdots & \frac{1}{2} N_n \hat{p}_n(t) - p_n(t) - (N_n + \epsilon)|\hat{f}_n(t)| \end{bmatrix};$$

$$D_2 = \begin{bmatrix} \frac{1}{2} N_1 \hat{q}_1(t) - q_1(t) & \cdots & \frac{1}{2} N_1 \hat{q}_n(t) - q_n(t) \\ \vdots & \ddots & \vdots \\ \frac{1}{2} N_n \hat{q}_1(t) - q_1(t) & \cdots & \frac{1}{2} N_n \hat{q}_n(t) - q_n(t) \end{bmatrix};$$

$$D_3 = \begin{bmatrix} \frac{1}{2} \hat{r}_1(t) - \left| \hat{h}_1(t) \right| & \cdots & 0 \\ \vdots & \ddots & \vdots \\ 0 & \cdots & \frac{1}{2} \hat{r}_n(t) - \left| \hat{h}_n(t) \right| \end{bmatrix}; \quad D_4 = \begin{bmatrix} \frac{1}{2} \hat{u}_1(t) & \cdots & 0 \\ \vdots & \ddots & \vdots \\ 0 & \cdots & \frac{1}{2} \hat{u}_n(t) \end{bmatrix}.$$

Again based on Theorem 2.2 in [66] (also presented in Appendix C as Theorem 2), $\mathcal{R}_0 > 1$ if and only if $\rho(\Phi_{F-V}(\omega)) > 1$. Thus, for $\epsilon > 0$ small enough we have $\rho(\Phi_{F-V-\epsilon K}(\omega)) > 1$. Using Lemma 17 and the comparison principle, we immediately obtain

$$\lim_{t\to\infty} I_i(t) = \infty \quad \text{and} \quad \lim_{t\to\infty} B_i(t) = \infty, \qquad i = 1,\ldots,n, \tag{183}$$

which is a contradiction.

Therefore, M_0 is acyclic in M_∂, and P is uniformly persistent with respect to $(X_0, \partial X_0)$, which implies the uniform persistence of the solutions to the original system. Consequently, the Poincaré map P has a fixed point $(\tilde{S}(0), \tilde{I}(0), \tilde{B}(0)) \in X_0$, and it can be easily seen that $\tilde{S}(0) \neq 0$. Thus, $(\tilde{S}(0), \tilde{I}(0), \tilde{B}(0)) \in \text{Int}(\mathbb{R}_+) \times \text{Int}(\mathbb{R}_+) \times \text{Int}(\mathbb{R}_+)$ and $(\tilde{S}(t), \tilde{I}(t), \tilde{B}(t)) = u(t, (\tilde{S}(0), \tilde{I}(0), \tilde{B}(0)))$ is a positive ω-periodic solution of the system. Hence, we have established the following result.

Theorem 22. *Let $\mathcal{R}_0 > 1$ and let (P-1) - (P-6) hold. Then the solutions of the system (172) - (175) are uniformly persistent, and the system admits at least one positive ω-periodic solution.*

We have presented a general non-autonomous cholera model in a periodic environment. Seasonally variational factors have been incorporated into the incidence function f and the pathogen function h. Using the next infection operator introduced in [66], we have derived and computed the basic reproduction number $\mathcal{R}_0$ of our periodic cholera model, and have conducted a careful analysis on the epidemic and endemic dynamics. Our results have established $\mathcal{R}_0$ as a sharp threshold for cholera dynamics in periodic environments; i.e., disease completely dies out if $\mathcal{R}_0 < 1$ and uniformly persists if $\mathcal{R}_0 > 1$. The general analysis is demonstrated through three specific cholera models, and numerical simulation results are consistent with analytical predictions. We have also extended the generalized multi-group model to a periodic environment. More detailed analysis of this multi-group periodic model will be completed in the near future.

The complication of cholera modeling lies in that, on top of the multiple transmission pathways that involve both environment-to-human (or, indirect) and human-to-human (or, direct) routes, disease dynamics are also subject to strong seasonal variation. Thus, many different factors, ranging from ecological, environmental, societal, and climatic, need to be considered in constructing a more accurate mathematical model. We have incorporated periodicity into the general incidence and pathogen

functions in our model, in order to represent these various seasonal oscillations in a generic manner. Although in the three specific examples presented in Section 4.4 we have focused on two periodic parameters (i e., the rates of human-environment contact and human contribution to environmental vibrios) for the purposes of demonstration and easy comparison, one can easily incorporate periodicity into other model parameters, depending on the context of the modeling. In addition, similar analysis can be conducted to other cholera models (e.g., [28]), and the framework can be extended to model other water-borne infectious diseases, such as dysentery, typhoid fever, and campylobacteriosis.

CHAPTER 5

CONCLUSIONS AND FUTURE WORK

Cholera is currently in its seventh pandemic and remains a growing public health problem in different parts of the world, with outbreaks showing complex patterns, partly explained with genetic changes in the organisms [49,55]. Despite the available knowledge on its prevention and treatment, the disease is emerging as one of the leading cause of mortality in developing countries. Successful control and eradication of the disease requires good understanding of the biological, epidemiological and environmental factors shaping these outbreaks. Infectious disease modeling helps us to understand the mechanisms influencing disease transmission dynamics. To that end, we have presented and analyzed three different cholera mathematical models: an autonomous model with added public health control measures, a general multi-group model incorporating spatial heterogeneity and a periodic model incorporating seasonal variations.

First, we modified an autonomous cholera model in a homogeneous environment to include three public health interventions (vaccination, medical treatment, and water sanitation) in an effort to better understand the effects of different control strategies. We explicitly determined the new basic reproduction number and conducted a stability analysis of the disease-free and endemic equilibria for the system with the added controls. The addition of these three control measures reduces $\mathcal{R}_0$, and hence, reduces the risk of infection. However, a cholera epidemic could still occur if the control measures are not strong enough to reduce $\mathcal{R}_0$ to below one. Consequently, $\mathcal{R}_0$ remains a significant epidemic threshold (if $\mathcal{R}_0 < 1$, then the disease will be eradicated, but if $\mathcal{R}_0 > 1$, then the disease will persist and spread) and effective control of cholera remains a critical and complex problem to solve.

Next, we proposed a general multi-group model to study the effects of spatial heterogeneity and dispersal on cholera transmission via direct and indirect pathways. This model incorporated a general formulation for the incidence and pathogen concentration in each group. By design, this framework allows for variation of the risk of infection and concentration of toxigenic vibrios in the aquatic environment between

different regions, and hence unifies many existing multi-group cholera models. Under biologically reasonable conditions, the basic reproduction number $\mathcal{R}_0$ continues to be a sharp threshold for cholera dynamics in multiple groups. In fact, the basic reproduction number $\mathcal{R}_0$ is the sum of the individual reproduction numbers from all of the n groups. The individual reproduction numbers consist of a contribution from the direct transmission and a contribution from the indirect transmission within each group, implying that the two modes of transmission can independently or jointly start an epidemic, first within the group and then potentially spread into other groups. Therefore, we now can more accurately model cholera dynamics and the implementation and effects of specific control measures in various spatial regions where infection risks are high, toxigenic vibrios are prevalent, accessibility is restricted, or provisions are not readily available or in dire need. Additionally, we conducted a stability analysis of the disease-free and endemic equilibria. We presented a two-group cholera model to verify our analysis.

Finally, we proposed a generalized cholera model in a time-periodic environment. The force of infection and pathogen concentration in the aquatic environment are considered as periodic functions to illustrate seasonal and climatic patterns. We derived the basic reproduction number using the next infection operator and established $\mathcal{R}_0$ as a sharp threshold for cholera dynamics in periodic environments; when $\mathcal{R}_0 < 1$, the disease dies out, and when $\mathcal{R}_0 > 1$, the disease persists. Further, we conducted a careful analysis on the epidemic and endemic dynamics. We validated our analysis through numerical simulation of three different cholera models with time-periodic incidence and pathogen concentration functions. Specifically, we studied periodic variations of contact rate with contaminated water and a periodic rate of human contribution to the pathogenic concentration. These factors allowed us to simulate the seasonal variations in water quality and the aquatic reservoir due to climatic occurrences such as monsoons, floods, droughts and water temperature changes. Thus, the significant contribution of this general non-autonomous cholera model in a periodic environment is that it provides a basic framework for the consideration of many different temporal environmental factors in an effort to more accurately model the complex cholera dynamics which are subject to seasonal oscillations.

Furthermore, we have extended the generalized multi-group model to a periodic setting. That is, we have constructed a model that incorporates seasonality as well

as spatial heterogeneity to more realistically describe cholera dynamics. In the future, we hope to conduct a more detailed study of this non-autonomous model with spatial heterogeneity. To that end, this research illustrates some weaknesses in the proposed generalized models. While the multi-group and periodic models provide a basic framework for autonomous and non-autonomous infectious waterborne disease models, respectively, the multi-group model omits seasonal factors which are significant in endemic regions. On the other hand, the periodic model does not consider movement and interaction between various spatial regions and their impact on cholera dynamics; i.e., the entire population being studied must exist under the same conditions in the same environment which is not realistic. Hence, a non-autonomous model that incorporates spatial heterogeneity would provide significant insight into and a better representation of the complex cholera dynamics.

In addition to a more thorough study of a multi-group periodic cholera model, we hope to have a better comprehension of the ecology of cholera vibrios and, thus, can describe the dynamics of the toxigenic vibrios in the aquatic reservoir more realistically. Since *V. cholerae* can survive for long periods of time in water, we wish to improve our understanding of this autochtonous growth of vibrios and include this behavior into a cholera model. Another attribute of *V. cholerae* is that it can assume a viable, but non-culturable form [68] which complicates the modeling and understanding of cholera dynamics. Thus, in the future, we aim to expand our knowledge and comprehension on more complex cholera epidemiological models. We are currently studying and analyzing cholera dynamics through a PDE cholera model that includes diffusion coefficients to incorporate spatial heterogeneity and a cholera model that incorporates bacterial growth and possible Allee effects.

REFERENCES

[1] S. Altizer, A. Dobson, P. Hosseini, P. Hudson, M. Pascual and P. Rohani, *Seasonality and the dynamics of infectious diseases*, Ecol. Letters 9 (2006), pp. 467-484.

[2] J.R. Andrews and S. Basu, *Transmission dynamics and control of cholera in Haiti: an epidemic model*, Lancet 377 (2011), pp. 1248-1255.

[3] Z. Bai and Y. Zhou, *Threshold dynamics of a bacillary dysentery model with seasonal fluctuations*, Disc. and Cont. Dyn. Sys. Ser. B 15 (2011), pp. 1-14.

[4] Z. Bai and Y. Zhou, *Global dynamics of an SEIRS epidemic model with periodic vaccination and seasonal contact rate*, Non. Anal.: Real World Appl. 13 (2012), pp. 1060-1068.

[5] M. Bani-Yaghoub, R. Gautam, Z. Shuai, P. van den Dreissche and R. Ivanek, *Reproduction numbers for infections with free-living pathogens growing in the environment*, J. Bio. Dyn. 6 (2012), pp. 923-940.

[6] A. Berman and R. J. Plemmons, *Nonnegative Matrices in the Mathematical Sciences*, Academic Press, New York, 1979.

[7] E. Bertuzzo, L. Mari, L. Righetto, M. Gatto, R. Casagrandi, M. Blokesch, I. Rodriguez-Iturbe and A. Rinaldo, *Prediction of the spatial evolution and effects of control measures for the unfolding Haiti cholera outbreak*, Geophysical Research Letters 38 (2011), L06403.

[8] S.M. Blower and H. Dowlatabadi, *Sensitivity and uncertainty analysis of complex models of disease transmission: an HIV model, as an example*, International Statistical Review 62 (1994), pp. 229-243.

[9] G.J. Butler and P. Waltman, *Persistence in dynamical systems*, Proceedings of the American Mathematical Society 96 (1986), pp. 425-430.

[10] V. Capasso and S.L. Paveri-Fontana, *A mathematical model for the 1973 cholera epidemic in the european mediterranean region*, Revue dépidémoligié et de santé Publiqué 27 (1979), pp. 121-132.

[11] C. Castillo-Chavez, Z. Feng and W. Huang, *On the computation of R_0 and its role on global stability*, Mathematical Approaches for Emerging and Reemerging Infectious Diseases: An Introduction, IMA Volume 125, Springer-Verlag, 2002.

[12] C. Castillo-Chavez and B. Song, *Dynamical models of tuberculosis and their applications*, Math. Biosci. and Eng. 1 (2004), pp. 361-404.

[13] D L. Chao, M.E. Halloran, and I.M. Longini, *Vaccination strategies for epidemic cholera in Haiti with implications for the developing world*, Proc. Natl. Acad. Sci. USA 108 (2011) pp. 7081-7085.

[14] Y. Cheng, J. Wang, and X. Yang, *On the global stability of a generalized cholera epidemiological model*, J. Biol. Dyn. 6 (2012), pp. 1088-1104.

[15] C.T. Codeço, *Endemic and epidemic dynamics of cholera: the role of the aquatic reservoir*, BMC Infect. Dis. 1 (2001), p. 1.

[16] W.A. Coppel, *Stability and Asymptotic Behavior of Differential Equations*, Heath Mathematical Monographs, DC Heath, Boston, 1965.

[17] G.C de Magny, R. Murtugudde, M.R.P. Sapiano, A. Nizam, C.W. Brown, A.J. Busalacchi, M. Yunus, G.B. Nair, C.F. Lanata, J. Calkins, B. Manna, K. Rajendran, M.K. Bhattacharya, A. Huq, R.B. Sack and R.R. Colwell, *Environmental signatures associated with cholera epidemics*, PNAS 105 (2008), pp. 17676-17681.

[18] O. Diekmann, J.A.P. Heesterbeek, and J.A.J. Metz, *On the definition and the computation of the basic reproduction ratio R_0 in models for infectious diseases in heterogeneous populations*, J. Math. Biol. 28 (1990), pp. 365 - 382.

[19] S.F. Dowell and C.R. Braden, *Implications of the introduction of cholera to Haiti*, Emerg. Infect. Dis. 17 (2011), pp. 1299-1300.

[20] M.C. Eisenberg, Z. Shuai, J.H. Tien and P. van den Driessche, *A cholera model in a patchy environment with water and human movement*, Math. Biosci. 246 (2013), pp. 105-112.

[21] S.M. Faruque, I.B. Naser, M.J. Islam, A.S.G Faruque, A.N. Ghosh, G.B. Nair, D.A. Sack and J.J. Mekalanos, *Seasonal epidemics of cholera inversely correlate with the prevalence of environmental cholera phages*, Proc. Nat. Acad. Sci. 102 (2005), pp. 1702-1707.

[22] H.I. Freedman, S. Ruan and M. Tang, *Uniform persistence and flows near a closed positively invariant set*, J. Dyn. Differ. Equat., 6 (1994), pp. 583-600.

[23] H.D. Gaff, E. Schaefer and S. Lenhart, *Use of optimal control model to predict treatment time for managing tick-borne disease*, J. Bio. Dyn. 5 (2011), pp. 517-530.

[24] A.B. Gumel, C.C. McCluskey and J. Watmough, *An SVEIR model assessing potential impact of an imperfect anti-SARS vaccine*, Math. Biosci. and Eng. 3 (2006), pp.: 485-512.

[25] H. Guo and M. Li, *Global dynamics of a staged progression model for infectious diseases*, Math. Bios. and Eng. 3 (2006), pp. 513-525.

[26] H. Guo, M. Li, and Z. Shuai, *Global stability of the endemic equilibrium of multi group SIR epidemic models*, Can. Appl. Math. Q. 14 (2006), pp. 259-283.

[27] J.K. Hale, *Ordinary differential equations*, Dover Publications, New York, 2009.

[28] D.M. Hartley, J.G. Morris and D.L. Smith, *Hyperinfectivity: a critical element in the ability of V. cholerae to cause epidemics?*, PLoS Medicine, 3 (2006), pp. 63-69.

[29] H.W. Hethcote, *The mathematics of infectious diseases*, SIAM Review, 42 (2000), pp. 599-653.

[30] S. Islam, S. Rheman, A.Y. Sharker, et al., *Climate change and its impact on transmission dynamics of cholera*, Climate Change Cell, DoE, MoEF; Component 4B, CDMP, MoFDM, Dhaka, 2009.

[31] R.I. Joh, H. Wang, H. Weiss and J.S. Weitz, *Dynamics of indirectly transmitted infectious diseases with immunological threshold*, Bull. Math. Bio. 71 (2009), pp. 845-862.

[32] H.R. Joshi, *Optimal control of an HIV immunology model*, Optim. Control Appl. Methods 23 (2002), pp. 199-213.

[33] E. Jung, S. Lenhart, and Z. Feng, *Optimal control of treatments in a two-strain tuberculosis model*, Discrete Contin. Dyn. Syst., Ser. B 2 (2002), pp. 473-482.

[34] A.A. King, E.L. Lonides, M. Pascual and M.J. Bouma, *Inapparent infections and cholera dynamics*, Nature 454 (2008), pp. 877-881.

[35] D. Kirschner and G.F. Webb, *A model for treatment strategy in the chemotherapy of AIDS*, Bull. Math. Bio. 58 (1996), pp. 367-390.

[36] A.M. Kramer, M.M. Lyons, F.C. Dobbs and J.M. Drake, *Bacterial colonization and extinction on marine aggregates: stochastic model of species presence and abundance*, Ecol. and Evol. 3 (2013), pp. 4300-4309.

[37] C.M. Kribs-Zaleta, J.X. Velasco-Hernandez, *A simple vaccination model with multiple endemic states*, Math. Biosci. 164 (2000), pp. 183-201.

[38] J.P. LaSalle, *The Stability of Dynamical Systems*, Regional Conference Series in Applied Mathematics, SIAM, Philadelphia, 1976.

[39] S. Lenhart and J.T. Workman, *Optimal control applied to biological models*, Chapman Hall/CRC, New York, 2007.

[40] M.Y. Li and J.S. Muldowney, *A geometric approach to global-stability problems*, SIAM J. Math. Anal. 27 (1996), pp. 1070-1083.

[41] M.Y. Li, H.L. Smith and L. Wang, *Global dynamics of an SEIR epidemic model with vertical transmission*, SIAM J. Math. Anal. 62 (2001), pp. 58-69.

[42] M. Li and Z. Shuai, *Global-stability problem for coupled systems of differential equations on networks*, J. Differ. Equat. 248 (2010), pp. 1-20.

[43] S. Liao and J. Wang, *Stability analysis and application of a mathematical cholera model*, Math. Biosci. and Eng. 8 (2011), pp. 733-752.

[44] P.R. Mason, *Zimbabwe experiences the worst epidemic of cholera in Africa*, J. Infect. Dev. Ctries. 3 (2009), pp. 148-151.

[45] D.S. Merrell, S.M. Butler, F. Qadri, N.A. Dolganov, A. Alam, M.B. Cohen, S.B. Calderwood, G.K. Schoolnik and A. Camilli, *Host-induced epidemic spread of the cholera bacterium*, Nature 417 (2002), pp. 642-645.

[46] J.G. Morris Jr., *Cholera: Modern pandemic disease of ancient lineage*, Emerg. Infect. Dis. 17 (2011), pp.(11), 2011.

[47] Z. Mukandavire, S. Liao, J. Wang, H. Gaff, D.L. Smith and J.G. Morris Jr., *Estimating the reproductive numbers for the 2008-2009 cholera outbreaks in Zimbabwe*, PNAS 108 (2011), pp. 8767-8772.

[48] S. Marino, I. Hogue, C.J. Ray and D.E. Kirschner, *A methodology for performing global uncertainty and sensitivity analysis in system biology*, Journal of Theoretical Biology 254 (2008), pp. 178-196.

[49] G.B. Nair, S.M. Faruque, N.A. Bhuiyan, M. Kamruzzaman, A.K. Siddique and D.A. Sack, *New variants of Vibrio cholerae O1 biotype El Tor with attributes of the classical biotype from hospitalized patients with acute diarrhea in Bangladesh*, J. Clin. Microbiol. 40 (2002), pp. 3296-3299.

[50] R.L.M. Neilan, E. Schaefer, H. Gaff, K.R. Fister and S. Lenhart, *Modeling optimal intervention strategies for cholera*, Bull. Math. Bio. 72 (2010), pp. 2004-2018.

[51] E.J. Nelson, J.B. Harris, J.G. Morris, S.B. Calderwood and A. Camilli, *Cholera transmission: the host, pathogen and bacteriophage dynamics*, Nature Reviews: Microbiology 7 (2009), pp. 693-702.

[52] M. Pascual, M.J. Buoma and A.P. Dobson, *Cholera and climate: revisiting the quantitative evidence*, Microbes and Infection 4 (2002), pp. 237-245.

[53] M. Pascual, L.F. Chaves, B. Cash, X. Rodo and Md. Yunus, *Predicting endemic cholera: the role of climate variability and disease dynamics*, Climate Research 36 (2008), pp. 131-140.

[54] R. Piarroux, R. Barrais, B. Faucher, R. Haus, M. Piarroux M and J. Gaudart, *Understanding the cholera epidemic, Haiti*, Emerg Infect Dis. 17 (2011), pp. 1161-1168.

[55] A. Safa, G.B. Nair, and R.Y.C. Kong, *Evolution of new variants of Vibrio cholerae O1*, Trends Microbiol. 18 (2010), pp. 46-54.

[56] S. Shin, S.N. Desai, B.K. Sah, and J.D. Clemence, *Oral vaccines against cholera*, Clin. Infect. Dis. 52 (2011), pp. 1343-1349.

[57] Z. Shuai and P. van den Driessche, *Global dynamics of cholera models with differential infectivity*, Math. Bios. 234 (2011), pp. 118 - 126.

[58] Z. Shuai and P. van den Driessche, *Global stability of infectious disease models using Lyapunov functions*, SIAM J. Appl. Math. 73 (2013), pp. 1513-1532.

[59] R. Sun and J. Shi, *Global stability of multi group epidemic model with group mixing and non- linear incidence rates*, Appl. Math. and Comp. 218 (2011), pp. 280-286.

[60] F.L. Thompson, B. Austin and J. Swings, *The Biology of Vibrios*, ASM Press, Washington, D.C., 2006.

[61] J.P. Tian and J. Wang, *Global stability for cholera epidemic models*, Math. Biosci. 232 (2011), pp. 31-41.

[62] J.H. Tien and D.J.D. Earn, *Multiple transmission pathways and disease dynamics in a waterborne pathogen model*, Bull. Math. Bio. 72 (2010), pp. 1502-1533.

[63] A.L. Tuite, J. Tien, M. Eisenberg, D.J.D. Earn, J. Ma and D.N. Fisman *Cholera epidemic in Haiti, 2010: Using a transmission model to explain spatial spread of disease and identify optimal control interventions*, Ann. Intern. Med. 154 (2011), pp. 293-302.

[64] P. van den Driessche and J. Watmough, *Reproduction numbers and sub-threshold endemic equilibria for compartmental models of disease transmission*, Math. Biosci. 180 (2002), pp. 29-48.

[65] J. Wang and S. Liao, *A generalized cholera model and epidemic-endemic analysis*, J. Biol. Dyn. 6 (2012), pp. 568-589.

[66] W. Wang and X.-Q. Zhao, *Threshold dynamics for compartmental epidemic models in periodic environments*, J. Dyn. Differ. Equat. (2008), 20: pp. 699 - 717.

[67] X. Zhou, J. Cui and Z. Zhang, *Global results for a cholera model with imperfect vaccination*, Journal of the Franklin Institute 349 (2012), pp. 770-791.

[68] I.K. Wachsmuth, P.A. Blake and Ø. Olsvik, *Vibrio cholerae and Cholera: Molecular to Global Perspectives*, ASM Press, Washington, D.C., 1994.

[69] C.L. Wesley and J.S. Allen, *The basic reproduction number in epidemic models with periodic demographics*, J. Bio. Dyn. 3 (2009), pp. 116-129.

[70] World Health Organization (WHO) web page: www.who.org.

[71] F. Zhang and X-Q. Zhao, *A periodic epidemic model in a patchy environment*, J. Math. Anal. Appl. 325 (2007), pp. 496-516.

[72] X-Q. Zhao, *Uniform persistence in processes with application to nonautonomous competitive models*, J. Math. Anal. Appl. 258 (2001), pp. 87-101.

APPENDIX A

SOME CHOLERA MODELS IN HOMOGENEOUS

SETTINGS

We briefly present four autonomous mathematical cholera models in homogeneous environments for reference.

A.1 CODEÇO'S MODEL

In 2001, Codeço [15] proposed the following mathematical cholera model:

$$\frac{dS}{dt} = n(H - S) - a\lambda(B)S, \tag{A1}$$

$$\frac{dI}{dt} = a\lambda(B)S - rI, \tag{A2}$$

$$\frac{dB}{dt} = B(nb - mb) + eI. \tag{A3}$$

In this model, H represents the total human population and n is the human birth and death rate. The incidence is given by $a\lambda(B) = a\frac{B}{B+K}$ where a is the rate of exposure to contaminated water and K is the concentration of *V. cholerae* in water that yields 50% chance of catching cholera, also known as the half saturation rate. The parameter $r = n + \gamma$ where γ is the rate at which people recover from cholera and the parameter e is the contribution of each infected person to the population of *V. cholerae* in the aquatic environment. Finally, nb and mb are the growth rate and loss rate, respectively, of *V. cholerae* in the aquatic environment.

A.2 MODEL OF MUKANDAVIRE ET AL

Mukandavire *et al.* [47] proposed the following system of differential equations

describing cholera dynamics in 2011,

$$\frac{dS}{dt} = \mu N - \beta_e S \frac{B}{\kappa + B} - \beta_h SI - \mu S, \tag{A4}$$

$$\frac{dI}{dt} = \beta_e S \frac{B}{\kappa + B} + \beta_h SI - (\gamma + \mu)I, \tag{A5}$$

$$\frac{dR}{dt} = \gamma I - \mu R, \tag{A6}$$

$$\frac{dB}{dt} = \xi I - \delta B. \tag{A7}$$

In this model, N represents the total human population and μ is the natural human birth and death rate. The incidence is given by $\beta_e \frac{B}{\kappa + B} + \beta_h I$ where β_e and β_h denote environment-to-human transmission and human-to-human transmission, respectively. Further, κ corresponds to K, γ corresponds to r, ξ corresponds to e, and δ corresponds to $mb - nb$ in the model of Codeço.

A.3 TIEN AND EARN'S MODEL

Tien and Earn [62] proposed the following compartmental ODE model in 2010,

$$\frac{dS}{dt} = \mu N - b_W WS - b_I SI - \mu S, \tag{A8}$$

$$\frac{dI}{dt} = b_W WS + b_I SI - \gamma I - \mu I, \tag{A9}$$

$$\frac{dW}{dt} = \alpha I - \xi W, \tag{A10}$$

$$\frac{dR}{dt} = \gamma I - \mu R. \tag{A11}$$

The pathogen concentration is denoted by W instead of B. Parameters b_W and b_I represent the transmission rate for water-to-person and person-to-person contact, respectively. Also, α corresponds to e, and ξ corresponds to $mb - nb$ in the model of Codeço. We note that this model is similar to that of Mukandavire et al., but no saturation effect was considered.

A.4 WANG AND LIAO'S MODEL

In 2012, Wang and Liao [65] proposed the following generalized cholera model in

a homogeneous setting:

$$\frac{dS}{dt} = bN - Sf(I, B) - bS, \tag{A12}$$

$$\frac{dI}{dt} = Sf(I, B) - (\gamma + b)I, \tag{A13}$$

$$\frac{dR}{dt} = \gamma I - bR, \tag{A14}$$

$$\frac{dB}{dt} = h(I, B) \tag{A15}$$

where $f(I, B)$ is the incidence function which determines the rate of new infection, and the function $h(I, B)$ describes the rate of change for the pathogen in the environment. In this model, b represents the human birth and death rate.

APPENDIX B

GRAPH THEORETICAL METHOD FOR

CONSTRUCTING LYAPUNOV FUNCTIONS

We briefly review the background of the graph theoretical approach in [58] to construct a Lyapunov function to assist in proving global stability of the endemic equilibrium. Let $(\mathcal{G}, A)$ be a weighted digraph where $\mathcal{G}$ has n vertices and $A = [a_{ij}] \geq 0$ is the $n \times n$ weight matrix. If the directed arc (j, i) exists, then the entry a_{ij} is equal to the weight of the arc, otherwise $a_{ij} = 0$. A digraph $\mathcal{G}$ is strongly connected if for any pair of distinct vertices i, j, there exists a directed path from i to j (and also from j to i) [58]. A weighted digraph $(\mathcal{G}, A)$ is strongly connected if and only if the weight matrix A is irreducible [6].

Let $\mathbb{T}_i$ be the set of all spanning trees of $(\mathcal{G}, A)$ that are rooted at vertex i. For $\mathcal{T} \in \mathbb{T}_i$, the weight of $\mathcal{T}$, denoted by $w(\mathcal{T})$, is the product of weights on all arcs of $\mathcal{T}$. Let

$$c_i = \sum_{\mathcal{T} \in \mathbb{T}_i} w(\mathcal{T}), \qquad i = 1, \ldots, n. \tag{B1}$$

Then $c_i \geq 0$, and for any family of functions $H_i(z)_{i=1}^n$ with $z = (z_1, \ldots, z_m)^T \in \mathbb{R}^m$, the following holds

$$\sum_{i,j=1}^n c_i a_{ij} H_i(z) = \sum_{i,j=1}^n c_i a_{ij} H_j(z).$$

In particular, if $(\mathcal{G}, A)$ is strongly connected (i.e., A is irreducible), then $c_i > 0$ for $i = 1, \ldots, n$.

Then, we have the following result for construction of Lyapunov functions for infectious disease models.

Theorem 1. *[58] Let U be an open set in $\mathbb{R}^m$. Let*

$$z_k' = f_k(z_1, z_2, \ldots, z_m), \qquad k = 1, 2, \ldots, m, \tag{B2}$$

be a differential equation system with $z = (z_1, z_2, \ldots, z_m) \in U$. Suppose that the following assumptions are satisfied:

(i) *There exist functions $D_i : U \to \mathbb{R}$, $G_{ij} : U \to \mathbb{R}$ and constants $a_{ij} \geq 0$ such that for every $1 \leq i \leq n$, $D_i' = D_i'|_{(B2)} \leq \sum_{j=1}^{n} a_{ij} G_{ij}(z)$ for $z \in U$.*

(ii) *For $A = [a_{ij}]$, each directed cycle C of $(\mathcal{G}, A)$ has $\sum_{(s,r) \in \epsilon(C)} G_{rs} \leq 0$ for $z \in U$, where $\epsilon(C)$ denotes the arc set of the directed cycle C.*

Then, the function $D(z) = \sum_{i=1}^{n} c_i D_i(z)$, with constants $c_i \geq 0$ as given in equation (B1), satisfies $D' = D'|_{(B2)} \leq 0$; that is, D is a Lyapunov function for the system (B2).

APPENDIX C

BASIC REPRODUCTION NUMBER FOR EPIDEMIC

MODELS IN PERIODIC ENVIRONMENTS

We briefly review the work in [66] below. Following the setup for autonomous epidemic models [64] (also briefly reviewed in Section 2.1), consider an epidemiological model represented by the non-autonomous system

$$\frac{dx_i}{dt} = f_i(t, x) = \mathcal{F}_i(t, x) - \mathcal{V}_i(t, x) \qquad i = 1, \ldots, n \tag{C1}$$

where $\mathcal{F}_i(t, x)$ denotes the rate of appearance of new infections in the ith compartment, and $\mathcal{V}_i(t, x)$ denotes the rate of transfer of individuals into or out of the ith compartment. Both $\mathcal{F}_i(t, x)$ and $\mathcal{V}_i(t, x)$ are ω-periodic in t for some $\omega > 0$. Let $x_1, x_2, \ldots, x_m$ denote the infected compartments, and $x_{m+1}, x_{m+2}, \ldots, x_n$ denote the uninfected compartments. Define X_S to be the set of all disease-free states:

$$X_S = \{x \geq 0 \mid x_i = 0, 1 \leq i \leq m\}.$$

In addition, assume that system (C1) has a disease-free periodic solution $x^0(t) = \left(0, \ldots, 0, x_{m+1}^0(t), \ldots, x_n^0(t)\right)^T$ and define

$$M(t) = \left(\frac{\partial f_i(t, x^0(t))}{\partial x_j}\right)_{m+1 \leq i, j \leq n}.$$

Let $\Phi_M(t)$ denote the monodromy matrix of the ω-periodic system $dz/dt = M(t)z$. It is further assumed that $x^0(t)$ is linearly asymptotically stable in the disease-free subspace X_S; i.e.,

$$\rho(\Phi_M(\omega)) < 1 \tag{C2}$$

where $\rho(\Phi_M(\omega))$ is the spectral radius of $\Phi_M(\omega)$.

It follows that

$$D_x\mathcal{F}(t, x^0(t)) = \begin{pmatrix} F(t) & 0 \\ 0 & 0 \end{pmatrix} \quad \text{and} \quad D_x\mathcal{V}(t, x^0(t)) = \begin{pmatrix} V(t) & 0 \\ J(t) & -M(t) \end{pmatrix}$$

where $F(t)$ is a non-negative matrix and $-V(t)$ is a cooperative matrix defined by

$$F(t) = \left(\frac{\partial \mathcal{F}_i(t, x^0(t))}{\partial x_j}\right)_{1 \leq i, j \leq m} \quad \text{and} \quad V(t) = \left(\frac{\partial \mathcal{V}_i(t, x^0(t))}{\partial x_j}\right)_{1 \leq i, j \leq m}$$

respectively.

Further, let $Y(t, s)$, $t \geq s$, be the evolution operator of the linear ω-periodic system

$$\frac{dy}{dt} = -V(t)y. \tag{C3}$$

Now assume that $\phi(s)$ is ω-periodic and is the initial distribution of infectious individuals. Define the linear operator $L : C_\omega \to C_\omega$ where C_ω is the ordered Banach space of all ω-periodic functions from $\mathbb{R}$ to $\mathbb{R}^m$ equipped with the maximum norm $\|.\|_\infty$ and the positive cone $C_\omega^+ = \{\phi \in C_\omega : \phi(t) \geq 0, \forall t \in \mathbb{R}\}$ by

$$(L\phi)(t) = \int_0^\infty Y(t, t - s)F(t - s)\phi(t - s)ds, \qquad \forall t \in \mathbb{R}. \tag{C4}$$

This L is referred to as the next infection operator, and the basic reproduction number is defined as the spectral radius of L, i.e.,

$$\mathcal{R}_0 = \rho(L). \tag{C5}$$

The following theorem is established to characterize $\mathcal{R}_0$.

Theorem 1. *Consider the linear ω-periodic equation*

$$\frac{dw}{dt} = \left(-V(t) + \frac{1}{\lambda}F(t)\right)w, \qquad t \in \mathbb{R}, \ w \in \mathbb{R}^n, \ \lambda \in (0, \infty).$$

Let $W(t, s, \lambda)$, $t \geq s$, $s \in \mathbb{R}$ be the evolution operator of this system on $\mathbb{R}^m$. Then the following statements are valid:

(i) If $\rho(W(\omega, 0, \lambda)) = 1$ has a positive solution λ_0, then λ_0 is an eigenvalue of L, and hence $\mathcal{R}_0 > 0$.

(ii) If $\mathcal{R}_0 > 0$, then $\lambda = \mathcal{R}_0$ is the unique solution of $\rho(W(\omega, 0, \lambda)) = 1$.

(iii) $\mathcal{R}_0 = 0$ if and only if $\rho(W(\omega, 0, \lambda)) < 1$ for all $\lambda > 0$.

On the other hand, based on the assumption (C2) and the observation

$$D_x f(t, x^0(t)) = \begin{pmatrix} F(t) - V(t) & 0 \\ -J(t) & M(t) \end{pmatrix},$$

one obtains the result below.

Theorem 2. *The following statements are valid:*

(i) $\mathcal{R}_0 = 1$ *if and only if* $\rho(\Phi_{F-V}(\omega)) = 1$.

(ii) $\mathcal{R}_0 > 1$ *if and only if* $\rho(\Phi_{F-V}(\omega)) > 1$.

(iii) $\mathcal{R}_0 < 1$ *if and only if* $\rho(\Phi_{F-V}(\omega)) < 1$.

Thus, $x^0(t)$ *is asymptotically stable if* $R_0 < 1$, *and unstable if* $\mathcal{R}_0 > 1$.

VITA

Drew Posny

Department of Computational and Applied Mathematics

Old Dominion University

Norfolk, VA 23529

EDUCATION

Ph.D. Computational and Applied Mathematics, Old Dominion University, Norfolk, VA. (2014)

M.S. Computational and Applied Mathematics, Old Dominion University, Norfolk, VA. (2012)

Graduate Certificate, Modeling and Simulation, Old Dominion University, Norfolk, VA. (2011)

B.S. Mathematics, University of North Carolina, Chapel Hill, NC. (2009)

PUBLICATIONS

D. Posny and J. Wang, *Modelling cholera in periodic environments.* J. Biological Dynamics 8, pp. 1-19, 2014.

D. Posny and J. Wang, *Computing the basic reproductive number for epidemiological models in periodic environments.* In revision.

D. Posny, J. Wang, Z. Mukandavire and C. Modnak, *Analyzing transmission dynamics of cholera with public health interventions.* Submitted, 2013.

D. Posny, C. Modnak and J. Wang, *A multigroup model for cholera dynamics and control.* Submitted, 2013.

Typeset using LaTeX.